12-2020

The Consequences of Environmental Properties and Tree Spatial Neighborhood on Post-Fire Structure of Forest in Yosemite National Park

Jelveh Tamjidi
Utah State University

THE CONSEQUENCES OF ENVIRONMENTAL PROPERTIES AND TREE SPATIAL NEIGHBORHOOD ON POST-FIRE STRUCTURE OF FOREST IN YOSEMITE NATIONAL PARK

by

Jelveh Tamjidi

A thesis submitted in partial fulfillment
of the requirements for the degree

of

MASTER OF SCIENCE

in

Ecology

Approved:

James A. Lutz, Ph.D. Major Professor	Bonnie Waring, Ph.D. Committee Member
Megan Nasto, Ph.D. Committee Member	D. Richard Cutler, Ph.D. Interim Vice Provost of Graduate Studies

UTAH STATE UNIVERSITY
Logan, Utah

2020

ABSTRACT

The Consequences of Environmental Properties and Tree Spatial Neighborhood on Post-fire Structure of Forests in Yosemite National Park

by

Jelveh Tamjidi, Master of Science

Utah State University, 2020

Major Professor: Dr. James A. Lutz
Department: Wildland Resources

One of the important questions in ecological research is to understand the underlying mechanisms shaping species distribution. Niche vs. neutral processes can explain species composition and distribution. According to the niche theory, different species have their own niche and restricted by various ecological factors. Species adaption along specific environmental condition define species distribution. Species can coexist by occupying different niche and space. In addition, neutral theory emphasizes the role of stochastic events such as dispersal-assembly in shaping community structure. Dispersal limitation plays an important role in species assemblages at local scales. The reflection of abiotic variables such as topography and edaphic characteristics can be reflected in species distribution through species-habitat associations. Quantifying the effects of habitat heterogeneity, dispersal limitation and other clustering processes on species distribution is important in understanding the mechanisms of species distributions and coexistence.

In Chapter 2, I defined habitats based on the topographic and edaphic variables in the Yosemite Forest Dynamics Plot (YFDP). Soil enzymes activities were included to the soil properties due to their key role in the ecosystem processes. The associations of demographic metrics (stem abundance, basal area increment, mortality, and recruitment) in eleven species with defined habitats were examined using the torus translation test.

Variation partitioning was used to dissociate the contribution of niche filtering and dispersal limitation. More species-habitat associations were defined by soil properties (54.5%) than topographically-defined habitat (45.4%). In addition, the relative importance of spatial and environmental factors in species assemblage were examined. My results suggest that both niche process and dispersal limitation had potential effect on species distribution but dispersal limitation played more important role in species assemblage.

In Chapter 3, I assessed the underlying mechanisms in shaping tree species spatial patterns. I examined the role of habitat heterogeneity, dispersal limitation, disturbance (fire) history, unilateral intra/interspecific interactions of adults on juveniles, and negative density dependence in shaping four dominant tree species (*Abies concolor, Pinus lambertiana, Calocedrus decurrens, and Quercus kelloggii*) spatial patterns in the YFDP. I used point processes to infer the underlying mechanisms including in governing the locations of tree species. Results displayed the joint effects of the dispersal limitation and habitat heterogeneity in forming tree species spatial patterns. Additionally, results exhibited that the species spatial patterns are partially explained by fire effect and species interactions.

(145 pages)

PUBLIC ABSTRACT

The Consequences of Environmental Properties and Tree Spatial Neighborhood on Post-fire Structure of Forests in Yosemite National Park

Jelveh Tamjidi

Separating the contribution of habitat filtering and dispersal mechanisms in forming species distribution remains a challenge in community ecology. Despite the effect of environmental variables in structuring communities, only restricted numbers of them were considered as a habitat dissimilarity.

In Chapter 2, I used topography and soil properties to define habitats within the Yosemite Forest Dynamics Plot (YFDP). The soil enzymes were added in soil samples due to their important role in releasing nutrients into the soil environment. The preference of eleven species to a specific habitat were examined. Also, the relative importance of habitat filtering and dispersal limitation were examined. I found that more species associated with habitats defined by soil properties compare to those associated with topographically defined habitat. In addition, the contribution of dispersal process was greater in explaining change in species composition.

In Chapter 3, I studied the underlying processes in shaping four abundant species spatial arrangement in YFDP. I examined the effect of habitat heterogeneity, dispersal process, fire event, interaction of adults on juveniles, and negative density dependence (as a result of increasing density) in shaping species spatial distribution. My results suggest that dominant species spatial patterns are partially explained by topographic variables, dispersal limitation, biotic interactions, and fire history.

ACKNOWLEDGMENTS

I would like to express my profound gratitude to my advisor, Dr. Jim Lutz for his continuous guidance, advice, and support during my research. I am extremely grateful to him for giving me the opportunity to be a part of his team and do my research. It was a great privilege and honor to study and work under his guidance. I would also like to thank Dr. Bonnie Waring and Dr. Megan Nasto for their precious guidance and serving on my advisory committee.

I am grateful to my parents, Sima and Ali for their supports and sacrifices for preparing me for my future. I am very much thankful to my brother, Faraz, for his continuous support and valuable advice during my life. My deepest thank belongs to my partner, Pouya, for his patience and understanding. I am thankful to my lab colleagues, Sara Germain, Tucker Furniss, Kendall Becker, and Erika Blomdahl who have been always helping me during my research.

Jelveh Tamjidi

CONTENTS

Page

ABSTRACT iii

PUBLIC ABSTRACT v

ACKNOWLEDGMENTS vi

LIST OF TABLES x

LIST OF FIGURES xii

CHAPTER

1. INTRODUCTION 1

    LITERATURE CITED 5

2. SOIL ENZYME ACTIVITY AND SOIL NUTRIENTS JOINTLY INFLUENCE POST-FIRE HABITAT MODELS IN MIXED-CONIFER FORESTS OF YOSEMITE NATIONAL PARK, USA 10

    ABSTRACT 10
    INTRODUCTION 11
    STUDY AREA 14

        Sited description 14
        Geology and soils 14
        Climate 16
        Flora 16
        Fire history 16

    METHODS 18

        Plot establishment 18
        Field sampling of trees 18
        Soil sampling 19
        Soil enzyme measurement 19
        Topographic variables and hydraulic conductivity measurements 20

    ANALYSES 22

        Habitat definition 22

Principle coordinates of neighbor matrices 23

RESULTS 24
DISCUSSION 33

Associations of different species with habitat types 33
Niche vs. dispersal limitation drive variations in abundance and basal area increment 35
The contribution of environmental and spatial variables in forming mortality numbers across species 37
The contribution of environmental and spatial variables in forming ingrowth numbers across species 37
Edaphic effects 38

CONCLUSION 40
LITERATURE CITED 41

3. THE POST-FIRE ASSEMBLY PROCESSES OF TREES SPECIES BASED ON SPATIAL ANALYSIS OF SIERRA NEVADA MIXED-CONIFER FOREST 55

ABSTRACT 55
INTRODUCTION 56
METHODS 59

Study area 59
Field methods 61
Data analysis 61

Null models and spatial point process models 61
Complete spatial randomness 62
Inhomogeneous Poisson process 62
Homogeneous Thomas process 63
Best spatial model at different scales 63
Antecedent conditions null model 64
Assessing spatial pattern 64
Conspecific negative density dependence 65

RESULTS 65

Topographic effect 66
Dispersal limitation effect 66
Best spatial model 66
Spatial patterns of Juvenile and adult trees 66
Overall changes in tree spatial pattern 70
Conspecific negative density dependence 74

DISCUSSION....75

Effect of random process, habitat heterogeneity, and dispersal limitation on the formation of the spatial patterns of abundant species....75
Biotic interactions of the four abundant species....76
Effect of disturbance on the spatial pattern of juveniles regeneration and large-diameter trees....77
Effect of Conspecific negative density dependence in regulating dominant tree species spatial pattern....79

CONCLUSION....80
LITERATURE CITED....80

4. CONCLUSION....93

LITERATURE CITED....95

APPENDICES....97

APPENDIX A: Chapter 2 Supplemental Tables and Figures....98
APPENDIX B: Chapter 3 Supplemental Tables and Figures....117
APPENDIX C: Soil Enzymes Measurements....128

LIST OF TABLES

Table Page

2.1. Total number of live stems, basal area (BA, m^2 /ha), and basal area increment (BAI, m^2 /ha) of eleven species with 25 stems (dbh ≥ 1 cm) in the Yosemite Forest Dynamics Plot (25.6 ha) from 2014 to 2019 26

2.2. Results of torus-translation test, the association of abundance in 2019 (per 400 m^2), basal area increment (per 400 $m^{2)}$ (BAI), mortality numbers (per 400 m^2), and recruitment numbers (per 400 m^2) of eleven species with greater than 25 stems with habitats, in the Yosemite Forest Dynamics Plot (25.6 ha), California 28

2.3. Results of testing the significance of contribution for each component including spatial, topographic, and soil variables in species abundance (Abundance), basal area increment (BAI), morality, and recruitment 32

A.1. Van Genuchten parameters for 12 soil texture classes and A values for a disk with a 2.25 cm radius and suction values between 0.5 cm to 6 cm 98

A.2. Correlation between environmental variables at 20 m ×20 m scale in the Yosemite Forest Dynamics Plot 99

A.3. Soil chemical properties (mean ± sd) in burned and unburned patches in the Yosemite Forest Dynamics Plot 100

A.4. Correlation among soil enzymes including URE (urease), ACP (acid phosphatase), and ALP (alkaline phosphatase) and soil chemical properties 100

A.5. Average properties (mean ± sd) for four and seven habitats at 20 m × 20 m scale in the Yosemite Forest Dynamics Plot 101

A.6. Significant spatial variables selected by forward selection ($P < 0.05$) showing adjusted cumulative square of sum of all variables, F-test (F), and p-value (P = significant variable) show in the table 103

A.7. The contribution of spatial, soil and topographic variables for each species within the Yosemite Forest Dynamics Plot with respect to stem density in each quadrat (400 m^2) in 2019 104

A.8. The contribution of spatial, soil and topographic variables for each species within the Yosemite Forest Dynamics Plot with respect to basal area increment in each quadrat (400 m^2) from 2009 to 2014 105

A.9. The contribution of spatial, soil and topographic variables for each species within the Yosemite Forest Dynamics Plot with respect to mortality in each quadrat (400 m^2) from 2014 to 2019.....106

A.10. The contribution of spatial, soil and topographic variables for each species within the Yosemite Forest Dynamics Plot with respect to recruitment in each quadrat (400 m^2) from 2014 to 2019.....112

B.1. Stem numbers of juveniles and adults in species in 2019 in the Yosemite Forest Dynamics Plot.....117

B.2. Live juveniles (1 cm ≤ dbh < 5 cm) of *Abies concolor* and *Quercus kelloggii* in 2013, 2016, and 2019 in the Yosemite Forest Dynamics Plot.....117

B.3. Relative importance of best model in most abundant species including *Abies. concolor*, *Calocedrus. decurrens*, and *Pinus. lambertiana* in 2019 in the Yosemite Forest Dynamics Plot.....118

LIST OF FIGURES

Figure Page

2.1. Location of Yosemite Forest Dynamics Plot (YFDP, 25.6 ha; 320 m ×800 m) (A) in Yosemite National Park (B), California (C) 15

2.2. Climate, water balance, and increasing climatic water deficit for the Yosemite Forest Dynamics Plot calculated using PRISM climate averages (1981 to 2019) 17

2.3. Number of abundant species (out of five) including (*Abies concolor*, *Pinus lambertiana*, *Cornus nuttallii*, *Calocedrus decurrens*, and *Quercus kelloggii*) in all 20 m × 20 m quadrats in the Yosemite Forest Dynamics Plot 18

2.4. Slope (A) and aspect (B) at the scale of 20 m × 20 m in the Yosemite Forest Dynamics Plot (25.6 ha), California, USA 25

2.5. Stem map of eleven species with ≥25 stems within the in the Yosemite Forest Dynamics Plot (25.6 ha), California, USA in 2019 27

2.6. Hydraulic conductivity between burned sites and unburned patches in the Yosemite Forest Dynamics Plot 27

2.7. Comparison of the soil enzymes of acid phosphatases (Ac), alkaline phosphatases (Al), and urease (Ure) activities between burned (B) and unburned (UB) sites 29

2.8. Topographic habitat types (A) and habitat types derived from soil properties (B) at a scale of 20 m × 20 m in the Yosemite Forest Dynamics Plot 30

2.9. Variation partitioning of 11 live species with ≥ 25 stems in the Yosemite Forest Dynamics Plot s 31

2.10. Graphs show the contribution of spatial, soil and topographic variables with respect to each species stem abundance in 2019 32

3.1. Locations of Yosemite National Park and Yosemite Forest Dynamics Plot in California (A, B) 60

3.2. Panels display the results of different point process models of *Abies concolor* in 2019 in the Yosemite Forest Dynamics Plot 67

3.3. Intensity estimation (stem/ha-1) for *Abies concolor* (A), *Calocedrus decurrens* (B), *Pinus lambertiana* (C), *Quercus kelloggii* (D) based on the slope, elevation, and aspect in 2019 in the Yosemite Forest Dynamics Plot 68

3.4. Left panels show the bivariate spatial pattern analysis to assess the interaction between juvenile (1 cm ≤ stems dbh < 5 cm dbh) around conspecific adults (individuals ≥ 20 cm dbh) in *Abies concolor* (A), *Calocedrus decurrens* (C), *Pinus lambertiana* (E), *Quercus kelloggii* (G) in 2019 in the Yosemite Forest Dynamics Plot 69

3.5. Univariate live juvenile regeneration (1 cm ≤ dbh < 5 cm) spatial pattern in 2013, 2016, and 2019 in the Yosemite Forest Dynamics Plot 71

3.6. Change in live large tree (dbh ≥ 60 cm) spatial pattern in 2013, 2016, and 2019 72

3.7. The panels (A, B, C) show the overall change in spatial pattern of three species in 2013, 2016, and 2019 73

3.8. Density dependence mortality in *Abies concolor* (A), *Calocedrus decurrens* (B), *Pinus lambertiana* (C), and *Quercus kelloggii* (D) in 2019 in the Yosemite Forest Dynamics Plot 74

A.1. Distribution and stems per hectare and distribution of the five most abundant species in the Yosemite Forest Dynamics Plot in 2019, including: *Abies concolor* (A), *Calocedrus decurrens* (B), *Pinus lambertiana* (C), *Quercus kelloggii* (D), and *Cornus nuttallii* (E) 108

A.2. Slope (A) and aspect (B) at the scale of 1 m × 1 m DEM in the Yosemite Forest Dynamics Plot (25.6 ha) in the Yosemite National Park, California, USA 109

A.3. Computation of the optimal numbers of habitats based on topographic (left panels) and soil variables (right panels) 110

A.4. The results of K-Means clustering results from topographic variables (A) and edaphic variables (B) which group data based on the minimum distance to centroids ... 111

A.5. Data flow used to quantify species-habitat association in Yosemite Forest Dynamics Plot 112

A.6. Correlation between environmental variables in each quadrat 113

A.7. Mean values of soil chemical properties in burned and unburned patches within the Yosemite Forest Dynamics Plot 114

A.8. Variation partitioning of 11 live species with ≥ 25 stems in the Yosemite Forest Dynamics Plot 115

A.9. Variation partitioning of 11 live species with ≥ 25 stems in the Yosemite Forest Dynamics Plot 116

B.1. Distribution and abundance of four most abundant species in the Yosemite Forest Dynamics Plot in 2019, including *Abies concolor* (A), *Pinus lambertiana* (B), *Calocedrus decurrens* (C), *Quercus kelloggii* (D) 119

B.2. Results of the sensitivity analysis for diameter cutoff values chosen for the grouping of adult and juvenile stems in 2019 in the Yosemite Forest Dynamics Plot....120

B.3. Results of the sensitivity analysis for diameter cutoff values chosen for the grouping of adult and juvenile stems in 2019 in the Yosemite Forest Dynamics Plot....121

B.4. Panels display the results of different point process models of *Calocedrus decurrens* in the Yosemite Forest Dynamics Plot in 2019.....122

B.5. Panels display the results of different point process models of *Pinus lambertiana* in the Yosemite Forest Dynamics Plot in 2019 123

B.6. Left panels display the distribution of juvenile (1 cm ≤ dbh < 5 cm) and conspecific adults (dbh ≥ 20 cm) in *Abies concolor* (A), *Calocedrus decurrens* (C), *Pinus lambertiana* (E), and *Quercus kelloggii* (F) in the Yosemite Forest Dynamics Plot in 2019.....124

B.7. Diameter distributions of living three species in 2013 (pre-fire), 2016 (little post-fire), and 2019 in the 25.6 ha Yosemite Forest Dynamics Plot.....125

B.8. Diameter distributions of live stems (panels in first and third rows) and dead stems (panels in second and forth rows) for species in 2013, 2016, 2019 in the 25.6 ha Yosemite Forest Dynamics Plot.....126

B.9. Diameter distributions of living (A) and dead (B) for *Abies concolor* (ABCO), *Calocedrus decurrens* (CADE), *Pinus lambertiana* (PILA), and *Quercus kelloggii* (QUKE) trees in 2019 in the 25.6 ha Yosemite Forest Dynamics Plot 127

CHAPTER 1

INTRODUCTION

Understanding the processes that shape the distribution and composition of species is a fundamental goal in community ecology. Although various mechanisms have been proposed for explaining species composition, identifying the most important determining mechanisms remains a challenge in ecology. Two distinguished mechanisms in structuring communities are often termed as niche-based theory and neutral theory (Whitfield 2002, Silvertown 2004). Niche-based theory is associated with abiotic characteristics of the environment to explain community variation. Niche theory assumes that various species have their own niche and different species coexist by occupying different resources. The adaptation of species to specific conditions determines the distribution of various species along the environmental gradients. So, Strong habitat associations of species within an environment are consistent with the predictions of niche theory (Itoh et al. 2003). Species which are associated with a habitat are relatively more abundant and dominant in that specific habitat. Environmental heterogeneity with increasing environmental gradients (such as soil nutrients, water availability, irradiance availability at ground level), resources and available niche space can affect species distribution and enable more species to coexist (Tilman and Pacala 1993, Palmer and Dixon 1990, Stein 2014). The association between habitats and species is the simplest way to show niche theory in the community.

Neutral theory is associated with spatial dynamics such as dispersal limitation. Neutral theory assumes that dispersal limitation also plays an important role in

determining species compositions and distributions at local scales (Hubbel 2001, Leibold and McPeek 2006).

Despite significant evidence confirming the importance of niche partitioning in shaping communities (Harms et al. 2001, Potts et al. 2002, De Cáceres et al. 2012), little is known about the relative importance of different environmental variables as a principle factor of habitat filtering at local scales. In some previous studies, topographic variables were used as a proxy for habitat heterogeneity at local scales (Valencia et al. 2004, Kanagaraj et al. 2011, Jucker et al. 2018), but soil properties also restrict plant species distributions. Some studies have assessed the importance of edaphic and topographic factors to increase our ability to examine the effect of niche partitioning at a wider range of environmental components (Baldeck et al. 2013, Zuleta et al. 2020). In this study, soil enzyme activities were added to edaphic variables as explanatory variables to examine the importance of other relevant and unaccounted niche parameters in shaping species composition. Soil enzymes are produced by microorganism, plants, and animals in the soil (Sherene 2017) and play a key role in mineralization of organic matter and nutrient cycling (Burns 1983, Sinsabaugh et al. 1991). Their activities depend on soil conditions (soil pH, soil depth, soil organic matter) (Bielińska et al. 2013), climatic parameters (temperature and precipitation, geographic factors (including elevation, longitude, and latitude) (Siles et al. 2016), and disturbance (Boerner et al. 2000).

Species demographic metrics including abundance (which defined by the species stems per 400 m^2), basal area increment (increase of diameter at breast height), mortality (annually compounded of mortality), and recruitment (annually compounded ingrowth) play important roles in shaping species distributions under climate change.

Understanding the association of species demographic metrics and habitats in forests is important in providing valuable information regarding the species environmental requirements.

There are opposite views about the degree to which environmental factors (topographic and soil characteristics) and dispersal limitation shape the community composition at local scale. Baldeck et al. (2013) found that environmental variables explained much more of the variation in species composition, while Punchi-Manage et al. (2014) found that dispersal limitation strongly affect species composition at local scales. Understanding the relative contribution of ecological processes in explaining species demographic metrics variations would be a good approach to predict the potential response of species to the future climatic events and can provide additional insights regarding processes that promote community assembly. With variation partitioning, the total variation in species demographic metrics would partition into proportions explained by various sets of variables including spatial and environmental variables. The fraction of species demographic metric variation explained by pure environmental variables can reveal the relative importance of niche and the proportion explained by pure spatial variation is generally result from the influence of dispersal processes and species responses to unmeasured environmental variation.

Studying spatial arrangements of tree species could reveal the potential contributions of underlying processes such as microhabitat heterogeneity (Harms et al. 2001, Queenborough et al. 2007), dispersal limitation (Valencia et al. 2004), disturbance event (Rebertus et al. 1989, Briggs and Gibson 1992, Fulé and Covington 1998), neighborhood interactions, and competition (Pillay and Ward 2012). Understanding the

underlying mechanisms in the formation of species spatial distribution can reveal important information about forest community response to perturbation and environmental change in the future.

Fire has been one of the dominant disturbances in the most forests of Western North America, and evidence from other studies showed that fire activity is increasing (Westerling et al. 2006, Dennison et al. 2014). Fire can structure species spatial aggregation by creating a patchy distribution of limiting resources through unequal consumption of litter (Neary et al. 2005, Blomdahl et al. 2019), change in light availability, and decreasing precipitation interception by the forest floor (Covington and Sackett 1984). Furthermore, species interaction including facilitation and competition can also affect the species assembly in the forest community (Long et al. 2013). Point processes were used to infer the underlying mechanisms governing the locations of tree species (Brown et al. 2016, Gelfand et al. 2010).

My research objectives are in two parts, examining the relative importance of underlying processes in structuring species composition and spatial distribution. Chapter 2 examines the relative importance of niche-assembly and neutral-assembly in explaining variation in species demographic metrics and among habitats. Environmental components (such as soil nutrients, soil enzymes, and topographic variables) and fire history were used to define habitats for the analysis. Chapter 3 investigate the potential contributions of habitat heterogeneity, dispersal limitation, fire disturbance, and neighboring interactions in the formation of dominant species spatial pattern.

Literature Cited

Baldeck, C. A., K. E. Harms, J. B. Yavitt, R. John, B. L. Turner, R. Valencia, H. Navarrete, S. J. Davies, G. B. Chuyong, and D. Kenfack. 2013. Soil resources and topography shape local tree community structure in tropical forests. Proceedings of the Royal Society B: Biological Sciences 280(1753): 20122532.

Bielińska, E. J., B. Kołodziej, and D. Sugier. 2013. Relationship between organic carbon content and the activity of selected enzymes in urban soils under different anthropogenic influence. Journal of Geochemical Exploration 129: 52-56.

Blomdahl, E. M., C. A. Kolden, A. J. Meddens, and J. A. Lutz. 2019. The importance of small fire refugia in the central Sierra Nevada, California, USA. Forest Ecology and Management 432: 1041-1052. https://doi.org/10.1016/j.foreco.2018.10.038.

Boerner, R. E., K. L. Decker, and E. K. Sutherland. 2000. Prescribed burning effects on soil enzyme activity in a southern Ohio hardwood forest: a landscape-scale analysis. Soil Biology and Biochemistry 32(7): 899-908.

Briggs, J. M., and D. J. Gibson. 1992. Effect of fire on tree spatial patterns in a tallgrass prairie landscape. Bulletin of the Torrey Botanical Club 300-307.

Brown, C., J. B. Illian, and D. F. Burslem. 2016. Success of spatial statistics in determining underlying process in simulated plant communities. Journal of Ecology 104(1): 160-172.

Burns, R. 1983. Extracellular enzyme-substrate interactions in soil. Pages 249–298 in: Microbes in their natural environment. J. H. Slater, R. Wittenbury, J. W. T. Wimpenny, editors. Cambridge University Press, London, UK.

Covington, W. W., and S. S. Sackett. 1984. The effect of a prescribed burn in southwestern ponderosa pine on organic matter and nutrients in woody debris and forest floor. Forest Science 30(1): 183-192.

De Cáceres, M. Legendre, P. Valencia, R. Cao, M. Chang, L. W. Chuyong, R. Condit, Z. Hao, C. Hsieh, S. Hubbell, D. Kenfack, k. ma, X. Mi, M. Noor, A. Kassim, H. Ren, S. Su, I. Sun, D. Thomas, W. Ye, and F. He. 2012. The variation of tree beta diversity across a global network of forest plots. Global Ecology and Biogeography 21(12):1191-1202.

Dennison, P. E., S. C. Brewer, J. D. Arnold, and M. A. Moritz. 2014. Large wildfire trends in the western United States, 1984–2011. Geophysical Research Letters 41(8): 2928-2933.

Fulé, P. Z., and W. W. Covington. 1998. Spatial patterns of Mexican pine-oak forests under different recent fire regimes. Plant Ecology 134(2): 197-209.

Gelfand, A. E., P. Diggle, P. Guttorp, and M. Fuentes. 2010. Handbook of spatial statistics. CRC press.

Harms, K. E., R. Condit, S. P. Hubbell, and R. B. Foster. 2001. Habitat associations of trees and shrubs in a 50-ha neotropical forest plot. Journal of Ecology 89(6):947-959.

Hubbell, S. P. 2001. The unified neutral theory of biodiversity and biogeography. Princeton University Press, Princton, New Jersey, USA.

Itoh, A., T. Yamakura, T. Ohkubo, M. Kanzaki, P. A. Palmiotto, J. V. LaFrankie, P. S. Ashton, and H. S. Lee. 2003. Importance of topography and soil texture in the

spatial distribution of two sympatric dipterocarp trees in a Bornean rainforest. Ecological Research 18(3): 307-320.

Jucker, T., B. Bongalov, D. F. Burslem, R. Nilus, M. Dalponte, S. L. Lewis, O. L. Phillips, L. Qie, and D. A. Coomes. 2018. Topography shapes the structure, composition and function of tropical forest landscapes. Ecology Letters 21(7): 989-1000.

Kanagaraj, R., T. Wiegand, L. S. Comita, and A. Huth. 2011. Tropical tree species assemblages in topographical habitats change in time and with life stage. Journal of Ecology 99(6): 1441-1452.

Leibold, M. A., and M. A. McPeek. 2006. Coexistence of the niche and neutral perspectives in community ecology. Ecology 87(6):1399-1410.

Long, W., R. Zang, Y. Ding, and Y. Huang. 2013. Effects of competition and facilitation on species assemblage in two types of tropical cloud forest. PLoS One 8(4): e60252.

Neary, D. G., K. C. Ryan, and L. F. DeBano. 2005. Wildland fire in ecosystems: effects of fire on soils and water. General Technical Report RMRS-GTR-42-vol. 4. Ogden, UT: US Department of Agriculture, Forest Service, Rocky Mountain Research Station.

Palmer, M. W., and P. M. Dixon. 1990. Small-scale environmental heterogeneity and the analysis of species distributions along gradients. Journal of Vegetation Science. 1(1): 57–65.

Pillay, T., and D. Ward. 2012. Spatial pattern analysis and competition between Acacia karroo trees in humid savannas. Plant Ecology 213(10): 1609-1619.

Potts, M. D., P. S. Ashton, L. S.Kaufman, and J. B. Plotkin. 2002. Habitat patterns in tropical rain forests: a comparison of 105 plots in northwest Borneo. Ecology 83(10): 2782-2797.

Punchi-Manage, R., T. Wiegand, K. Wiegand, S. Getzin, C. S. Gunatilleke, and I. N. Gunatilleke. 2014. Effect of spatial processes and topography on structuring species assemblages in a Sri Lankan dipterocarp forest. Ecology 95(2): 376-386.

Queenborough, S. A., D. F. Burslem, N. C. Garwood, and R. Valencia. 2007. Habitat niche partitioning by 16 species of Myristicaceae in Amazonian Ecuador. Plant Ecology 192(2): 193-207.

Rebertus, A., G. Williamson, and E. Moser. 1989. Fire-induced changes in Quercus laevis spatial pattern in Florida sandhills. The Journal of Ecology 638-650.

Sherene, T. 2017. Role of soil enzymes in nutrient transformation: A Review. Bio Bulletin 3(1): 109-131.

Siles, J. A., T. Cajthaml, S. Minerbi, and R. Margesin. 2016. Effect of altitude and season on microbial activity, abundance and community structure in Alpine forest soils. FEMS Microbiology Ecology 92(3).

Silvertown, J. 2004. Plant coexistence and the niche. Trends in Ecology & evolution 19(11): 605-611.

Sinsabaugh, R. L., R. K. Antibus, and A. E. Linkins. 1991. An enzymic approach to the analysis of microbial activity during plant litter decomposition. Agriculture, Ecosystems & Environment 34(1-4): 43-54.

Stein, A., K. Gerstner, and H. Kreft. 2014. Environmental heterogeneity as a universal driver of species richness across taxa, biomes and spatial scales. Ecology Letters 17(7): 866-880.

Tilman, D., and S. Pacala. 1993. The maintenance of species richness in plant communities. Pages 13-25 in R. E. Rick-lefs and D. Schluter, editors. Species diversity in ecological communities: historical and geographical perspectives. University of Chicago Press, Illinois.

Valencia, R., R. B. Foster, G. Villa, R. Condit, J. C. Svenning, C. Hernández, K. Romoleroux, E. Losos, E. Magård, and H. Balslev. 2004. Tree species distributions and local habitat variation in the Amazon: large forest plot in eastern Ecuador. Journal of Ecology 92(2): 214-229.

Westerling, A. L., H. G. Hidalgo, D. R. Cayan, and T. W. Swetnam. 2006. Warming and earlier spring increase western US forest wildfire activity. Science 313:940-943.

Whitfield, J. 2002. Neutrality versus the niche. Nature Publishing Group.

Zuleta, D., S. E. Russo, A. Barona, J. S. Barreto-Silva, D. Cardenas, N. Castaño, S. J. Davies, M. Detto, S. Sua, and B. L. Turner. 2020. Importance of topography for tree species habitat distributions in a terra firme forest in the Colombian Amazon. Plant and Soil 450(1): 133-149.

CHAPTER 2

SOIL ENZYME ACTIVITY AND SOIL NUTRIENTS JOINTLY INFLUENCE POST-FIRE HABITAT MODELS IN MIXED-CONIFER FORESTS OF YOSEMITE NATIONAL PARK, USA

Abstract

Disentangling the relative importance of habitat filtering and dispersal limitations at local scales (<1 km^2) in shaping species composition remains an important question in community ecology. Previous studies have examined the relative importance of these mechanisms using topography and selected soil properties. We examined both topography and edaphic properties from 160 locations in the recently burned 25.6 ha Yosemite Forest Dynamics Plot (YFDP) in Yosemite National Park, California, USA. In addition to eight soil chemical properties, we included phosphatases and urease enzymes in a definition of habitat niches, primarily because of their rapid changes with fire (compared to soil nutrients) and also their role in ecosystem function. We applied environmental variables to the distributions of 11 species. More species–habitat associations were defined by soil properties (54.5%) than topographically-defined habitat (45.4%). We also examined the relative importance of spatial and environmental factors in species assemblage. Proportions explained by spatial and environmental factors differed among species and demographic metrics (stem abundance, basal area increment, mortality, and recruitment). Spatial factors explained more variation than environmental factors in stem abundance, mortality, and recruitment. The contributions of urease and acid phosphatase to habitat definition were significant for species abundance and basal area increment. These results emphasize that a more complete

understanding of niche parameters is needed beyond simple topographic factors to explain species habitat preference. The stronger contribution of spatial factors suggests that dispersal limitation and unmeasured environmental variables have high explanatory power for species assemblage in this coniferous forest.

Introduction

Niche-based processes and neutral processes both shape species assemblages in ecological communities. Niche theory assumes that different species have their own niche and species adaptation to specific environmental heterogeneity and biotic interactions determine the species coexistence. In contrast, neutral theory emphasizes the role of stochastic events such as dispersal-assembly in shaping community structure. Neutral theory assumes that all individuals of all species are ecologically equivalent and the environmental variables play no role in community structure (Potts et al. 2004). Dispersal limitation controls the spread of individuals into various habitats while habitat filtering helps multi-species remained coexistence through interspecific competition for the same restricted resources (Keddy 1992).

Species demographic metrics including abundance (which defined by the species stems per 400 m^2), basal area increment (diameter growth at breast height), mortality (annually compounded of mortality), and recruitment (annually compounded ingrowth) play important roles in shaping species distributions under climate change. Understanding the relationships between species demographic metrics and habitats in forests is important not only in revealing community structure at different spatial scales, but also in providing valuable information regarding the environmental requirements of tree species in successful ecological restoration (Zhang et al. 2013). The effect of some

spatially structured habitat variables such as topographic and edaphic components could be reflected in species composition and distribution by habitat associations. However, topographic variables are commonly used as a proxy for habitat heterogeneity in governing community structure (Valencia et al. 2004, Kanagaraj et al. 2011) due to their impact on hydrological condition, flow patterns, and soil biogeochemical processes (Griffiths et al. 2009, Seibert et al. 2007), and topographic factors sometimes covary with the soil conditions and temperature (Aandahl 1949, Fu et al. 2004). In addition to topography, soil characteristics such as soil nutrients also restrict plant distribution.

Soil enzymes are produced by microorganisms, plants, and animals in the soil (Sherene 2017) and the enzymes originated by microorganism (bacteria and fungi) play key roles in mineralization of organic matter and nutrient cycling (Burns 1983, Sinsabaugh et al. 1991). Their activities depend on soil conditions (soil pH through its influence on the microorganisms, soil depth due to the plant roots concentrations on the soil surface, soil organic matter which is a source of substrate for the soil enzymes production) (Bielińska et al. 2013), climatic parameters (temperature through the effect on microbial biomass, precipitation by affecting water availability which influences on microbial activities, and geographic factors including elevation, longitude, and latitude by influence on soil organic matter affecting microbial abundance and activities) (Siles et al. 2016, Kumari and Rao 2017), and disturbance through effect on soil organic matter and microbial activities (Boerner et al. 2000). Fire changes soil enzyme activities through reduction of soil organic matter content, production of ash and char layers from soil organic matter, and change in soil temperature (Nannipieri et al. 1982). The degree to which these factors influence soil chemical properties and enzyme activity would be

expected to differ in burned areas and adjacent, small unburned patches (Lutz et al. 2017, Meddens et al. 2018).

In addition to the associations of species demographic metrics to habitats, recent studies have used theoretical explanations to dissociate the contribution of niche differentiation and dispersal limitation. The relative importance of environmental and spatial components can provide information with respect to habitat filtering and dispersal process dominance in shaping community assembly. The proportion explained by pure space is linked to dispersal processes and other unmeasured structured environmental factors. The fraction explained by environmental variables (pure environmental plus the spatially structured environmental factors) is related to species responses to measured environmental variables. If dispersal limitation is considered as the principal determinant of the variations in species composition, spatial variables will explain most of the variation. Otherwise, sites with the same species composition will be expected to have similar environmental conditions (Page and Shanker 2018). We examined the contribution of niche differentiation and dispersal limitation in explaining species demographic metrics. Species mortality depends on various factors including proximity to canopy gaps (Beckage and Clark 2003), climate variability (Neumann et al. 2017), and fire (Furniss et al. 2019, Furniss et al. 2020). The variation in species demographic metrics can be related to the effect of environmental conditions (Ferry et al. 2010, Herwitz and Young 1994), but understanding the relative importance of topography, soil, and spatial variables in controlling species demographic metrics at local would be a good approach to predict the potential response of species to the future climatic events.

In this study, we examined the habitat associations and determined the effects of edaphic (soil chemical and soil enzymes activities), topography, and space on species composition. Our objectives were to examine (1) species-environment associations in order to determine the total numbers of the species associated with habitats, (2) how much variation of species demographic metrics (stem abundance, basal area increment, mortality, and recruitment numbers) could be explained by spatial and environmental variables in order to determine the importance of dispersal limitation and niche differentiation on species assemblage, (3) the effect of fire on the levels of soil enzyme activities as explanatory variables in defining habitats, and (4) the importance of adding enzymatic activity to ascertain the effect of different environmental variables on improving habitat characterization.

Study area

Sited description

This study was conducted in the Yosemite Forest Dynamics Plot (YFDP) near Crane Flat in Yosemite National Park, central Sierra Nevada, California, USA (Fig. 2.1) (Lutz et al. 2012). The YFDP comprises 25.6 ha centered at 37.77°N, 119.82°W with dimensions of 800 m east to west and 320 m north to south. Elevation ranges between 1774.1 m to 1911.3 m.

Geology and soils

Soils of the plot derived from metamorphic parent material. The YFDP is situated on two soil polygons of the Clarks Lodge-Ultic Palexeralfs complex (fine sandy loam)

and the Typic Dystroxerepts-Humic Dystroxerepts complex (sandy loam) (Soil Survey Staff 2018).

Yosemite's climate is Mediterranean with hot, dry summers and cool, wet winters. Annual minimum and maximum temperatures are in January (-1.82 ºC to 10.01 ºC) and July (13.9 ºC to 27.14 ºC) (Lutz et al. 2010). The annual mean monthly minimum and maximum temperature were 6 ºC and 16 ºC respectively from 1981 to 2010; most of the precipitation falls from November through March, with an annual average of 1070 mm (Lutz et al. 2010, Larson et al. 2016). The YFDP is located in *Abies concolor-Pinus lambertiana* Forest (Keeler-Wolf et al. 2012).

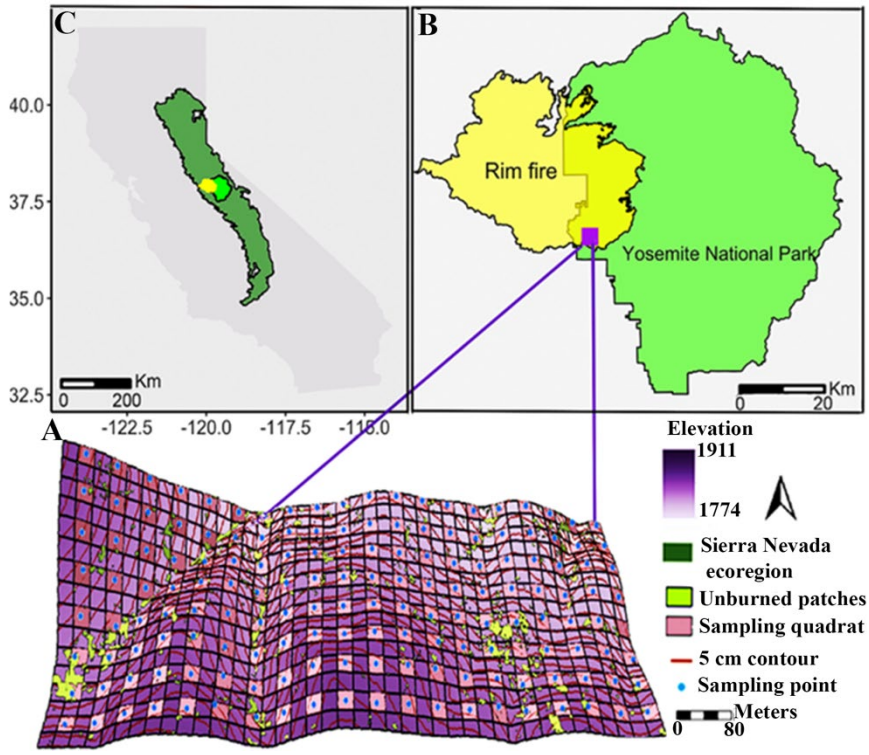

Fig. 2.1. Location of Yosemite Forest Dynamics Plot (YFDP, 25.6 ha; 320 m ×800 m) (A) in Yosemite National Park (B), California (C). The unburned patches ≥1 m^2 (following the Rim fire in 2013) include a total area 12,597 m^2 throughout the plot.

Climate

Thornthwaite-type water-balance models (Thornthwaite and Mather 1955, Lutz et al. 2010) display greatest level of annual water deficit in August (Deficit; 99 mm; Fig. 2.2 B), which have been increasing from 1981 to 2019 (Fig. 2.2 C).

Flora

The plot is located in *Abies concolor*-Mixed Conifer type (Keeler-Wolf et al. 2012). The five most abundant species includes *Abies concolor* (white fir), *Pinus lambertiana* (sugar pine), *Cornus nuttallii* (Pacific dogwood,) *Calocedrus decurrens* (incense-cedar), and *Quercus kelloggii* (California black oak) (Fig. 2.3; Fig. A.1). Shrub cover is dominated by California hazelnut (*Corylus cornuta* var. *californica*), Sierra Chinquapin (*Chrysolepis sempervirens*), and northern bilberry (*Vaccinium uliginosum*) (Lutz et al. 2012).

Fire history

Fire is an essential ecosystem process in Sierra Nevada forests (Stephens and Collins 2004). Sierra Nevada mixed-conifer forests were characterized by a frequent, low to moderate severity fire regime prior to European settlement (Weatherspoon et al. 1992), and the mean fire return interval in the YFDP was 29.5 years (Barth et al. 2015). Fire frequency declined in 1850 as a result of the Euro-American settlement and livestock grazing in the Yosemite national park (Scholl and Taylor 2010). The last widespread fire occurred in 1899 (Scholl and Taylor 2010) with fire having been excluded from 1900 to 2012. Since 1970 many of lighting- ignited fires have been allowed in the summer months if they met management plans (prescribed fire) (van Wagtendonk and Lutz 2007).

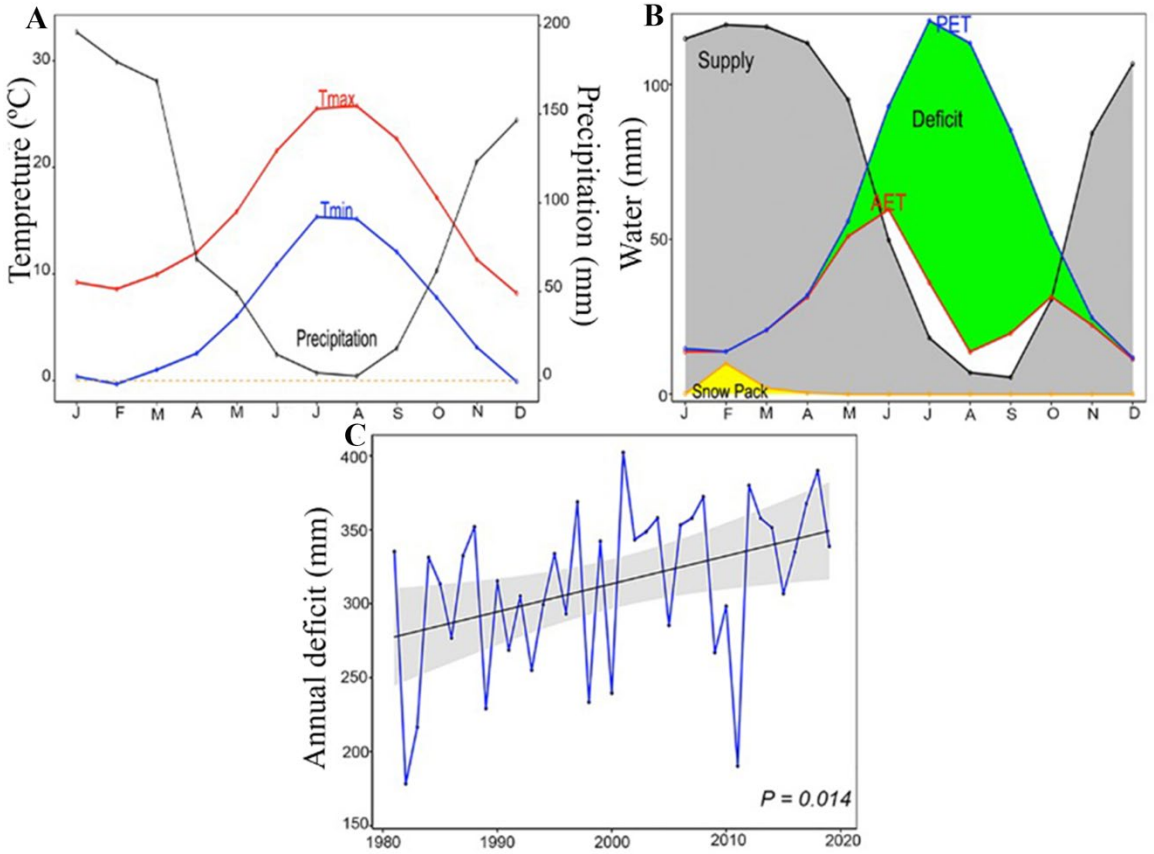

Fig. 2.2. Climate, water balance, and increasing climatic water deficit for the Yosemite Forest Dynamics Plot calculated using PRISM climate averages (1981 to 2019). The maximum and minimum temperature are mostly greater than freezing. The water supply (black closed circles) exceeds potential evapotranspiration (PET, blue closed circles) from November to May. Thornthwaite-type water balance models show that potential evapotranspiration exceeds actual evapotranspiration (AET) from mid-May through October, resulted in a drought summer months (B), which has been increasing between 1981 and 2019 (C).

In August 2013, the Rim Fire burned 104,131 ha, with approximately 31,263 ha within Yosemite National Park (Stavros et al. 2016).

The YFDP was burned on September first and second by a management-ignited (but subsequently unmanaged) backfire to slow the spread of the Rim fire (see Kane et al. 2015) for details regarding fire weather, (Blomdahl et al. 2019) for details regarding Landsat-derived fire severity and (Cansler et al. 2019) for details on surface fuel

consumption). The Rim Fire burned almost all litter and duff, leaving 3.22 Mg ha^{-1} and 13.1 Mg ha^{-1} respectively (Cansler et al. 2019. Larson et al. 2016). Within the YFDP, the overall effect of the Rim Fire was a burn severity, initial tree mortality, and surface fuel consumption similar to recent Yosemite fires (1984 and 2005) rather than the high severity present in parts of the Rim Fire footprint (Furniss et al. 2019, Van Wagtendonk and Lutz 2007, Kane et al. 2015, Lutz et al. 2018).

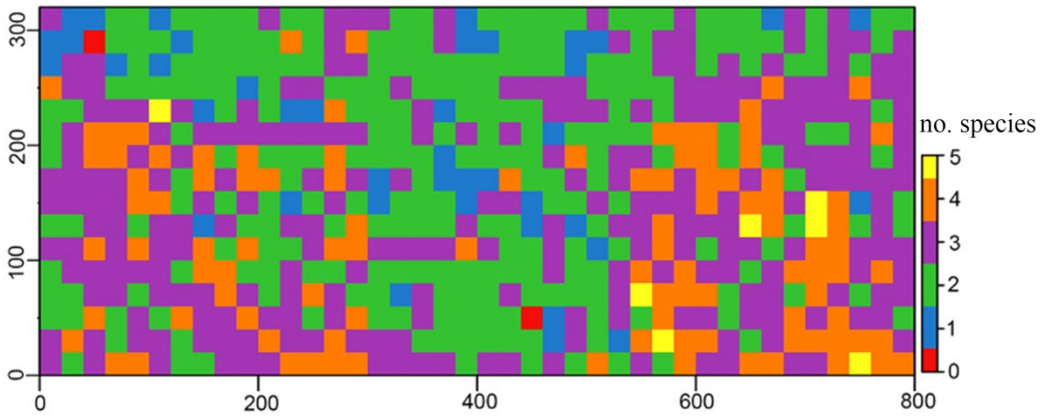

Fig. 2.3. Number of abundant species (out of five) including (*Abies concolor*, *Pinus lambertiana*, *Cornus nuttallii*, *Calocedrus decurrens*, and *Quercus kelloggii*) in all 20 m × 20 m quadrats in the Yosemite Forest Dynamics Plot.

Methods

Plot establishment

The YFDP is a rectangular plot totally 25.6 ha divided into 640 quadrats of 20 m × 20 m. A steel rod installed at the corner of each subplot and the steel tag of cell number wired to the rod.

Field sampling of trees

All trees ≥ 1 cm diameter at breast height (DBH) were identified, mapped, and tagged according to the Smithsonian ForestGEO protocols in 2009 and 2010 (Anderson-

Teixeira et al. 2015, Lutz 2015). Each tree was revisited annually between 2011 and 2019 and the status (live or dead) was checked each year, with tree diameters remeasured in 2014 and 2019. Unburned patches ≥1 m^2 (unburned litter and duff layer) were mapped at the beginning of the growing season immediately after fire (Blomdahl et al. 2019).

Soil sampling

Soil samples were collected at 160 points (98 samples from burned sites and 62 samples from unburned patches) within the YFDP in May 2017. Samples were air dried at temperature (22°C) and sieved to remove stones (with <2 mm sieve). The $BaCl_2$-method was used to determine the concentration of Ca (calcium), K (potassium), Mg (magnesium), and Mn (manganese). Phosphorus (P) was measured by Bray method (Bray and Kurtz 1945). Soil samples were extracted in 0.1 M $BaCl_2$ for two hours and the concentration of Ca, K, Mg, and Mn were determined by Inductivity Coupled Plasma Analyser (Jönsson et al. 2002). Cation exchange capacity (CEC) was calculated by summing the cations extracted (Ca^{2+}, Mg^{2+}, and K^{+}) and the soil's acidic cations. Total exchangeable bases (TEB) was obtained from summation of exchangeable K, Ca, Mg, and Na. Base saturation (BS) was calculated by dividing TEB by CEC value and multiplying by 100.

Soil enzyme measurement

Soil samples were collected at the same locations (160 quadrats; 98 burned patches and 62 unburned patches) for measuring the alkaline phosphatase, acid phosphatase, and urease activity in 2018. We collected three soil samples per quadrat and mixed them thoroughly. The mixed samples were considered as the representative of a

sample for each quadrat. Samples were sieved from quadrats and maintained at < 5℃ during transport to the lab. We allowed them to equilibrate at room temperature before starting enzymes measurements. Enzyme activity analysis was conducted using the methods developed by Dick (Dick 2020). Urease activity was assayed according to the method of Kandeler and Gerber (Kandeler and Gerber 1988). We used 2.5 milliliter (ml) of urea solution and 20 ml borate buffer containing disodium tetraborate for each 5 g soil sample and incubated them at 37 °C for two hours. A 30 ml potassium chloride (2 M)–hydrochloric acid (0.01 M) solution were added and the mixtures were shaken on a shaker for 30 minutes. Soil suspensions were filtered and filtrates analyzed for ammonium by colorimetric procedure. Phosphatases (acid and alkaline phosphatases) were measured by the method of Tabatabai and Bremner (1969) and Eivazi and Tabatabai (1977) which includes colorimetric estimation of p-nitrophenol release (acid solution of the p-nitrophenol is colorless and the alkaline solution has yellow color) when 1 g of soil is incubated with 0.2 ml toluene and 4 ml of buffered sodium p-nitrophenyl phosphate solution (pH for buffer were considered equal to 6.5 for acid phosphatase and 11 for alkaline phosphatase) at 37°C for 1 hour. After incubation, $CaCl_2$ –NaOH treatment was used to extract the p-nitrophenol released by phosphatase activity (see Appendix C for the detail).

Topographic variables and hydraulic conductivity measurements

Each tree was revisited annually between 2011 and 2019 and the status (live or dead) was checked each year, with tree diameters remeasured in 2014 and 2019. Unburned patches ≥1 m^2 (unburned litter and duff layer) were mapped at the beginning of

the growing season immediately after fire (Blomdahl et al. 2019). Topographic variables (elevation, aspect, and slope) of each 20 m × 20 m quadrat were calculated based on the surveyed position and elevation of the grid reference corners. Elevation was taken as the average of elevation of four corners of each quadrat and slope was measured as the mean angle of the four panels by connecting three corners of a quadrat. Aspects between 135° and 225° were considered south facing due to receive the most direct solar exposure (Furniss et al. 2017). Aspect >225° and <135° were considered as one group duo to the lower amount of sun radiation and temperature. As aspect is a land-surface variable, we used a cosine transformation to obtain a continuous gradient, describing the north-south gradient. Cumlative infiltration and hydraulic conductivity were calculated using mini disk infiltrometer in 56 burned and 39 unburned sites. The infiltrometer was placed on the soil surface and the water was pulled from the tube by soil suction. The volume of water was recorded at 30 second intervals and plotted (cumulative infiltration versus the square root of time) according to the methods of Zhang (1997):

$$\mathrm{K} = \frac{C_1}{A} \qquad \text{Eq. 1}$$

where C_1 is the slope for the cumulative infiltration vs. the square root of time, and A is a value that relates the van Genuchten parameters for a given soil texture class to both disk radius and the suction we selected. A is computed from below formula:

$$\mathrm{A} = \frac{11.65(\mathrm{n}^{0.1} - 1)\exp[2.92(\mathrm{n} - 1.9)\alpha\mathrm{h}]}{(\alpha \mathrm{r}_0)^{0.91}} \qquad (\mathrm{n} \geq 1.9) \qquad \text{Eq. 2}$$

$$\mathrm{A} = \frac{11.65(\mathrm{n}^{0.1} - 1)\exp[7.5(\mathrm{n} - 1.9)\alpha\mathrm{h}]}{(\alpha \mathrm{r}_0)^{0.91}} \qquad (\mathrm{n} < 1.9) \qquad \text{Eq. 3}$$

where r is the disk radius, h is the suction at the disk surface, n and α are the van Genuchten parameters for the soil. The van Genuchten parameters for the 12 texture classes were obtained from Carsel and Parrish (Carsel and Parrish 1988) (Table A.1.).

Analyses

Habitat definition

We identified two classes of habitat predictors (topographic and soil variables) to define habitat maps. Topographic variables were comprised of elevation, aspect, and slope. Soil variables were Ca, K, Mg, Mn, total exchangeable bases (TEB), base saturation (BS), P, pH, and soil enzymes, including acid and alkaline phosphatases and urease. We calculated topographic variables (elevation, aspect, and slope) at the 1 m × 1 m and 20 m × 20 m scales (Fig. A.2, Fig. 2.4). The optimal number of habitats was determined by elbow and gap statistic methods using the fviz_nbclust function from the factoextra package version 1.0.7 (Kassambara and Mundt 2017). In the elbow method, a K-means clustering algorithm was run on the data set and the total within-cluster sum of square (WSS) was calculated. By plotting the WSS curve and number of clusters, the point of inflection on the curve was chosen as the optimal number of clusters. We verified the appropriate number of clusters using complementary methods (gap statistic and NbClust function) (Fig. A.3). The hierarchical clustering was used to classify each quadrat into a habitat based on the environmental variables. Selective cuts across dendrogram were made to generate habitats based on the optimal number of habitats which were determined by previous step (Fig. A.4). All analyses were performed in R version 3.6.3 (R Core Team 2020).

We performed species-habitat association test on species with ≥25 stems (stem density ≥1 stem/ha) (eleven species) (Table 2.1; Fig. 2.5). This threshold for local abundance was applied to differentiate rare from abundant species (Furniss et al. 2017, Pitman et al. 1999). The associations of stem abundance in 2019, basal area increment from 2014 to 2019, mortality from 2014 to 2019, and recruitment from 2014 to 2019 in these eleven species were assessed within 160 quadrats (20 m × 20 m). The torus translation test was conducted by following the methods of Harms et al. (Harms et al. 2001). This test calculates the observed abundance of each species in each habitat type and compares these observed values with abundance values obtained from simulated habitat maps. Simulated maps were generated by shifting the actual habitat map in four directions by 20-m increments while the location of the stems did not change. A species was significantly positively (aggregated) or negatively (repelled) with a specific habitat type at ($\alpha = 0.05$) if observed abundance was higher (lower) than at least 97.5 % (or 2.5%) of the simulated abundance in simulated maps (Fig. A.5).

Principal coordinates of neighbor matrices

Principal coordinates of neighbor matrices (PCNM) proposed by Bocard and Legendre (2002) were used to model spatial variation. Generation of spatial variables was conducted using the pcnm function from the vegan package version 2.5-6 (Oksanen et al. 2013). The distance between spatial data was represented as a Euclidean distance matrix. This method creates a set of spatial explanatory variables and determines significant variables based on the statistically responding of response variable (Borcard et al. 2004). Data was normalized using the Hellinger transformation before PCNM analysis. PCNM function provides negative and positive eigenvalues as predictors but only positive

eigenvalues were selected as explanatory variables. The number of variables was reduced by selecting variables with a statistically significant contribution on variation of species abundance ($\alpha = 0.05$) using forward selection with the ordistep function (999 permutations) (Blanchet et al. 2008). The variation partitioning was conducted using the varpart function from the vegan package version 2.5-6 (Oksanen et al. 2013) to determine the explained proportion of variation in species composition by environmental, and spatial variables.

Results

Most soil properties were not significantly correlated with topography (Fig. A.6; Table A.2). Hydraulic conductivity was slightly greater in unburned sites but the difference between burned and unburned sites was not significant five years after fire occurrence (Fig. 2.6).

Differences in enzyme activity (urease, phosphatase, and alkaline phosphatase) and soil chemical properties between burned and unburned sites were significant for urease (p-value < 0.05) (Fig. 2.7), pH, Ca, and K (Table A.3, Fig. A.7) five years after fire. Additionally, correlation among enzyme activity (urease, phosphatase, and alkaline phosphatase) and soil chemical properties showed correlations were not significant (Table A.4). Hydraulic conductivity and alkaline phosphatase enzyme were added to the soil data as predictors which resulted in a lower explained proportion of edaphic component in species density (12% with three enzymes vs. 9% with three enzymes and hydraulic conductivity), basal area increment(15% with three enzymes vs. 18% with three enzymes), mortality (1% with three enzymes vs. 1% with three enzymes and hydraulic conductivity), and recruitment (2% with three enzymes vs. 1% with three

enzymes and hydraulic conductivity) compared to those with consideration of two enzymes (acid phosphatase and urease) (Figs. A.8 and A.9).

The number of habitats as identified by the combination of elbow method, gap statistic, and the diagnostics of the NbClust package, resulted in four habitats based on the topographic (slope, elevation, and aspect) and seven habitats based on soil variables.

Each 20 m × 20 m quadrat was assigned to a habitat (Fig. 2.8). All quadrats were allocated into four and seven habitats based on topographic (slope, elevation, and aspect) and soil variables respectively (Table A.5).

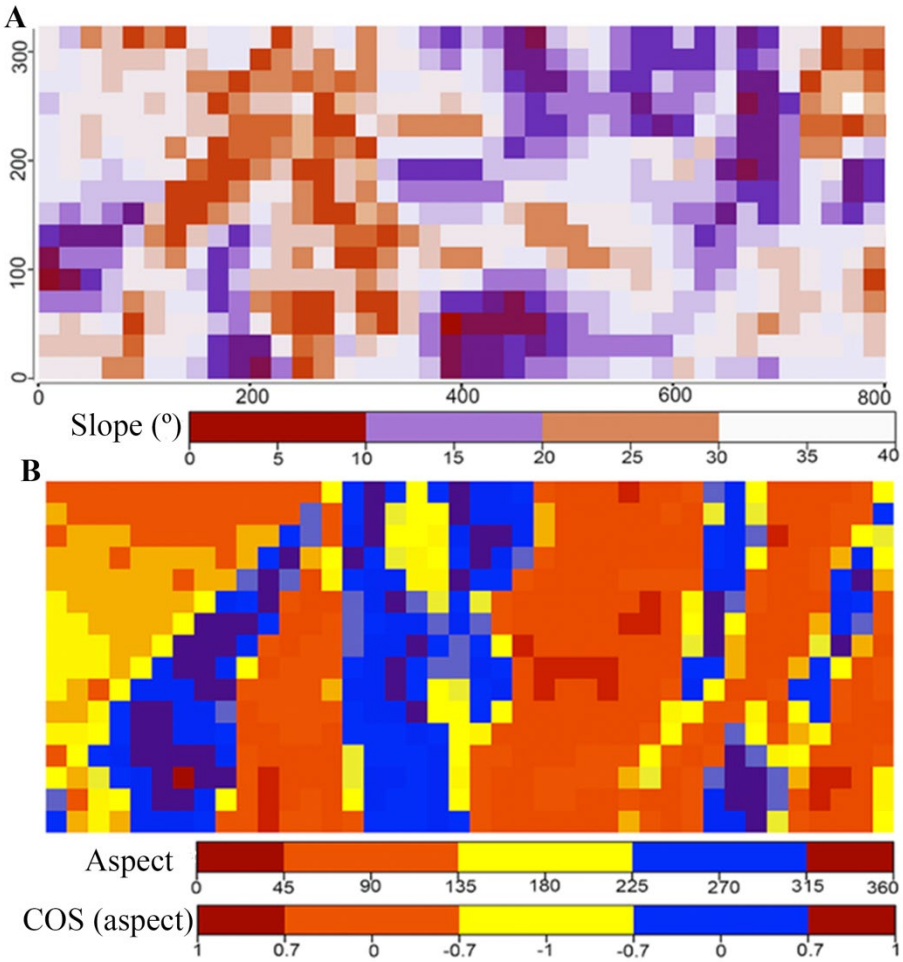

Fig. 2.4. Slope (A) and aspect (B) at the scale of 20 m × 20 m in the Yosemite Forest Dynamics Plot (25.6 ha), California, USA.

Table 2.1. Total number of live stems, basal area (BA, m^2 /ha), and basal area increment (BAI, m^2 /ha) of eleven species with 25 stems (dbh ≥ 1 cm) in the Yosemite Forest Dynamics Plot (25.6 ha) from 2014 to 2019. Number of stems and basal area increment (BAI) between 2014 and 2019 were calculated for those stems in 2014 that survived through 2019.

	2014				2019				2014 - 2019	
Species	**Stems ≥1 cm DBH**	**Stems ≥60 cm DBH**	**BA ≥1 cm DBH**	**BA ≥60 cm DBH**	**Stems ≥1 cm DBH**	**Stems ≥60 cm DBH**	**BA ≥1 cm DBH**	**BA ≥60 cm BDH**	**BAI ≥1 cm DBH**	**BAI ≥60 cm DBH**
Abies concolor	2815	403	15.25	8.56	2815	420	15.89	8.92	0.64	0.36
Pinus lambertiana	855	398	15.29	13.77	855	409	15.67	14.17	0.38	0.4
Cornus nuttallii	439		0.06		439		0.07		0.01	
Calocedrus decurrens	440	85	3.41	2.52	440	89	3.50	2.59	0.09	0.07
Quercus kelloggii	278	1	0.48	0.01	278	1	0.51	0.01	0.03	t
Arctostaphylos patula					82		t		t	
Cornus sericea	11		t		11		t		t	
Corylus cornuta var. californica					275		t		t	
Prunus virginiana	2		t		2		t		t	
Sambucus racemosa					35		t		t	
Chrysolepis sempervirens					36		t		t	

t - trace; less than 0.01 m^2 /ha.

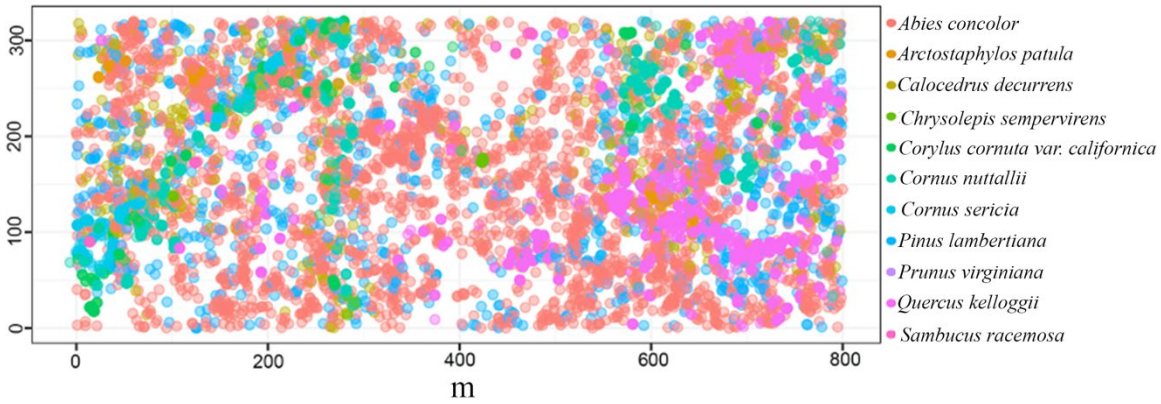

Fig. 2.5. Stem map of eleven species with ≥25 stems within the in the Yosemite Forest Dynamics Plot (25.6 ha), California, USA in 2019.

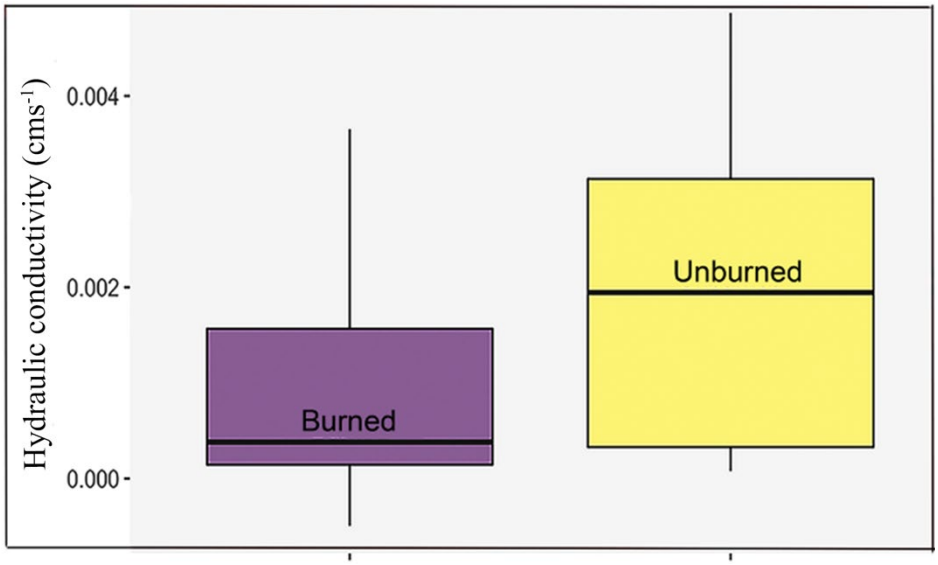

Fig. 2.6. Hydraulic conductivity between burned sites and unburned patches in the Yosemite Forest Dynamics Plot. Differences in hydraulic conductivity were non-significant (p-value > 0.05) between burned and unburned.

Table 2.2. Results of torus-translation test, the association of abundance in 2019 (per 400 m^2), basal area increment (per 400 $m^{2)}$ (BAI), mortality numbers (per 400 m^2), and recruitment numbers (per 400 m^2) of eleven species with greater than 25 stems with habitats, in the Yosemite Forest Dynamics Plot (25.6 ha), California. Ingrowth and mortality numbers show annually compounded numbers and increment of diameter growth at breast height was calculated between 2014 and 2019. Habitats defined by topographic variables (HSN: High Slope North facing, HSS: High Slope South facing, LSS: Low Slope South facing) and soil variables (h1: h7). The symbol "+" indicates positive association; "-" indicates negative association.

			Topography				Edaphic			
Species	**Density (stems ha^{-1})**	**Stems ≥ 1 cm dbh**	**Abundance**	**BAI**	**Mortality**	**Recruit.**	**Abundance**	**BAI**	**Mortality**	**Recruit.**
Abies concolor	111.8	2862	LSN+		LSN-		h3+			
Quercus kelloggii	50.1	1282					h3-	h7+/ h5-	h6+	
Pinus lambertiana	33.5	857	LSN+/LSS-				h3+/ h7-			
Cornus nuttallii	32	817	LSN-							
Calocedrus decurrens	17.6	450	LSN-				h7+/ h5-			
Corylus cornuta var. californica	10.7	275								h6+/ h2-
Cornus sericea	9.8	252				HSS-/HSN-				h1+
Arctostaphylos patula	34.5	82								
Chrysolepis sempervirens	1.4	36								
Sambucus racemosa	1.4	35								
Prunus virginiana	1	25								

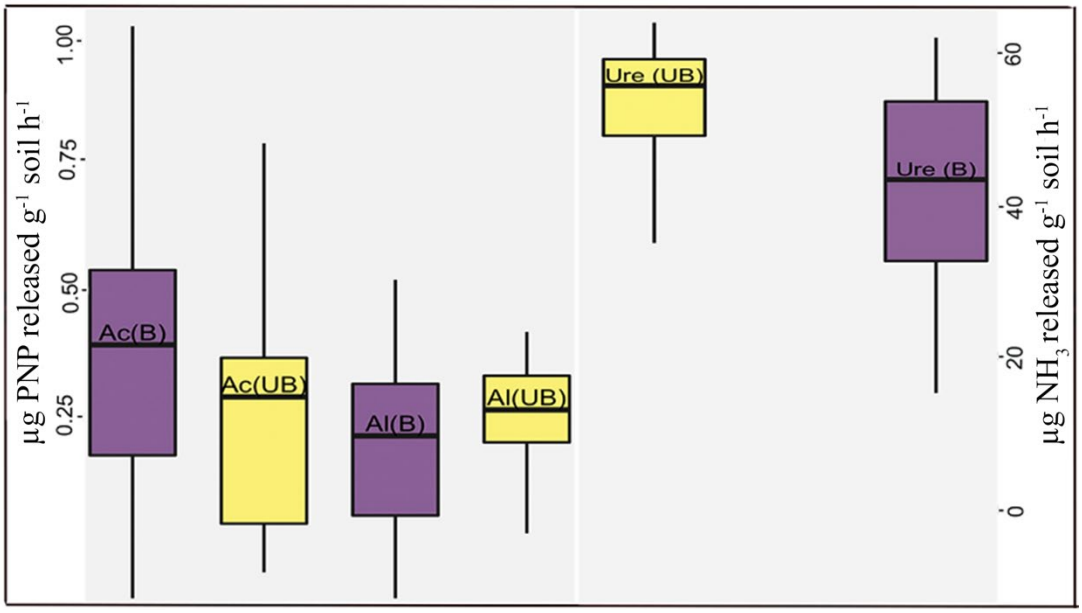

Fig. 2.7. Comparison of the soil enzymes of acid phosphatases (Ac), alkaline phosphatases (Al), and urease (Ure) activities between burned (B) and unburned (UB) sites. Differences was significant (p-value ≤ 0.05) only for urease. Box plots based on the first quartile, median (segment inside the box), and third quartile. Location of minimum and maximum data were shown in the first point below the box and last point above the box respectively. Units are µg p-nitrophenol and µg NH_3 released g^{-1} soil h^{-1}.

Among the eleven species, stem abundance of five species in 2019 (45.5% of stems) were negatively or positively associated with habitats (Table 2.2). The number of significantly associated species in habitats defined by soil variables, was slightly greater (6 versus 5) compared to total number of species associated with habitats defined based on topography. Total number of habitats associated species for basal area increment, mortality, and recruitment were lower than those of stem abundance (one (9.1%), two (18.2%), and two (18.2%) respectively).

Only 27 PCNMs were selected to predict the variation in community composition. The adjusted cumulative square for all 27 PCNMs was 27.9% (Table A.6). The proportion explained by spatial and environmental variables for stem abundance variation was 45% as opposed to 41%; for species basal area increase was 10% vs. 7%; for species

mortality numbers 53% vs. 52%; and for species recruitment, 52% vs. 51% with and without soil enzymes as a predictor respectively (Fig. 2.9).

The variation explained by spatial variables alone, was greater compared to other variables for the stem abundances, mortality and ingrowth numbers in the YFDP (Fig. 2.9). The contribution of only the topographic component in species abundance, basal area increment, and mortality number were decreased by removing soil enzymes data from edaphic predictors. Soil variables explained more variation than topographic variables in species abundance.

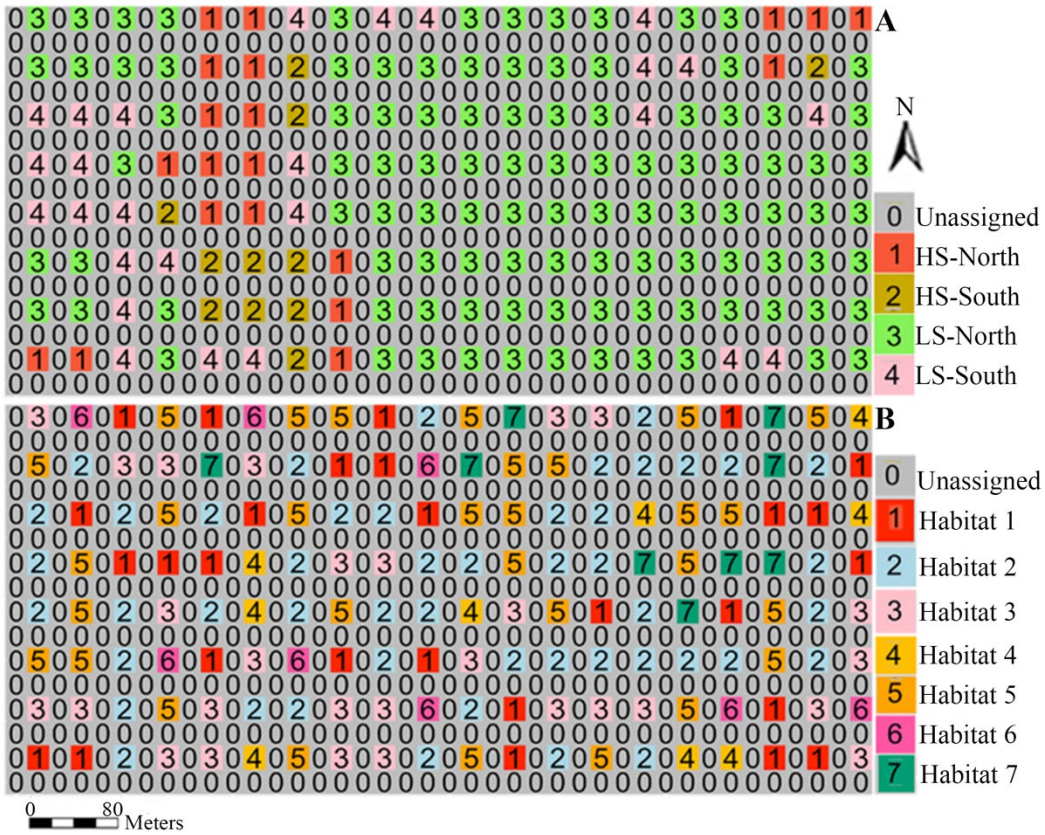

Fig. 2.8. Topographic habitat types (A) and habitat types derived from soil properties (B) at a scale of 20 m × 20 m in the Yosemite Forest Dynamics Plot. Every other quadrat was assigned to a specific habitat and the unassigned quadrats were removed from the analysis. "HS" and "LS" indicate high and low slope in habitats. "North" and "south" show north or south facing habitats.

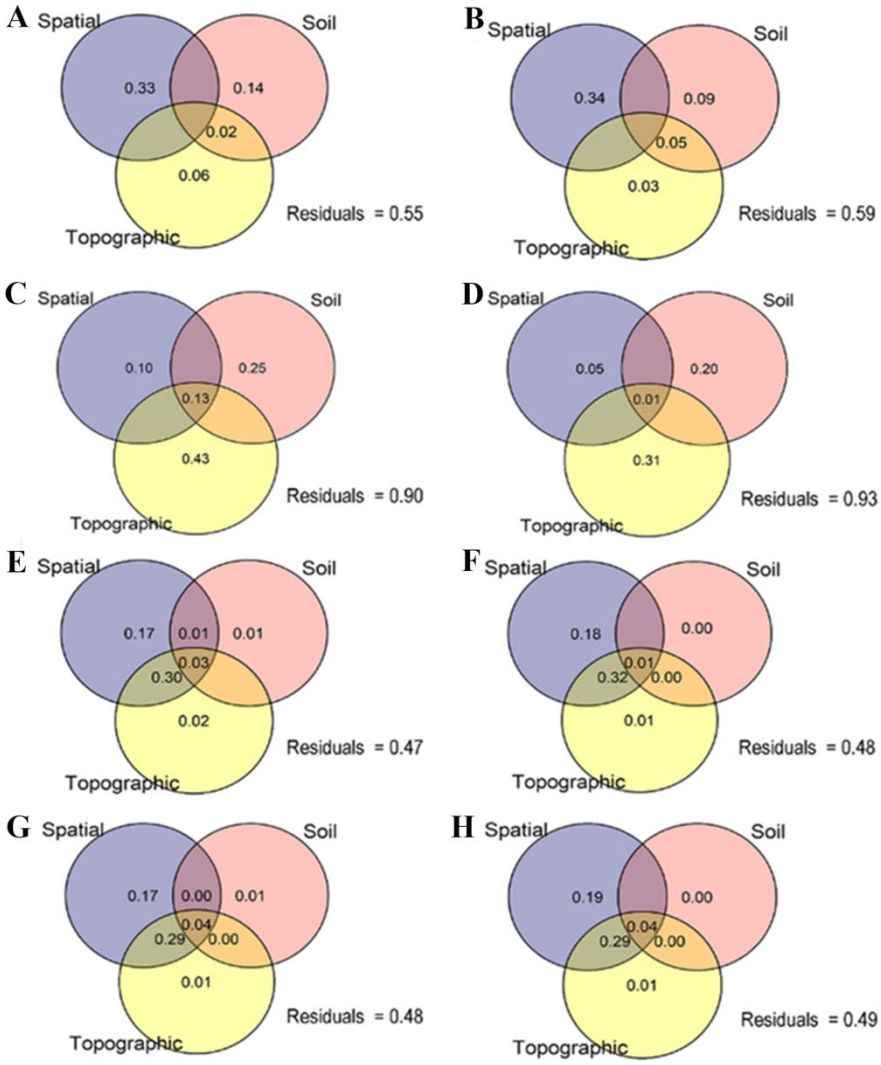

Fig. 2.9. Variation partitioning of 11 live species with ≥ 25 stems in the Yosemite Forest Dynamics Plot. The numbers correspond to the proportion of variations explained by spatial, edaphic (chemical properties with and without acid phosphatase and urease enzymes), and topographic variables in species abundance with (A) and without enzymes (B); basal area increment with (C) and without enzymes (D); mortality with (E) and without enzymes (F); and recruitment with (G) and without enzymes (H). Negative values of explained variation were not shown in the figures.

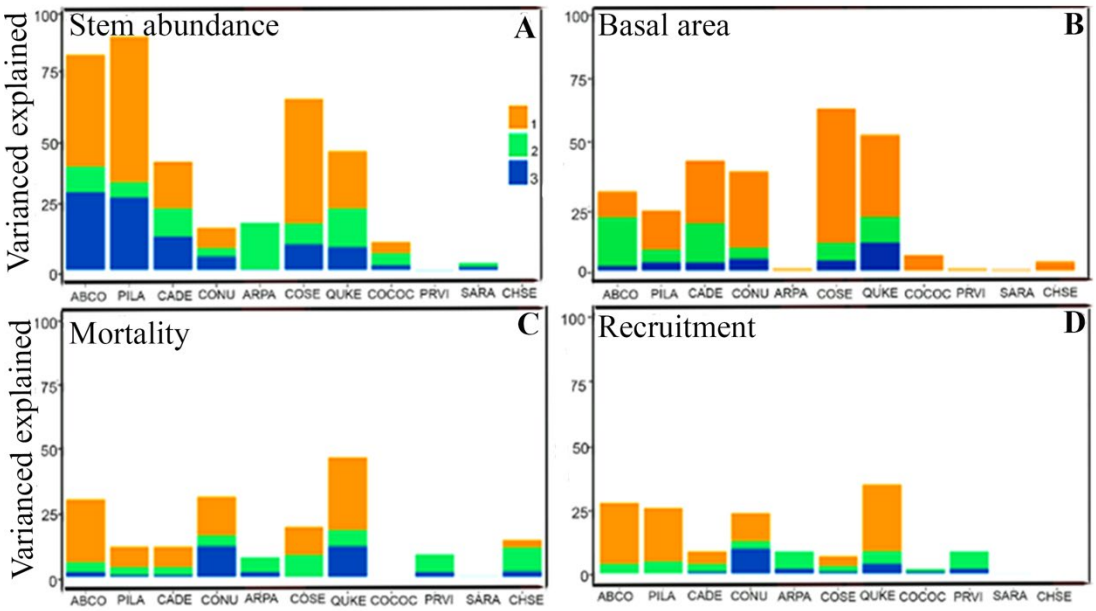

Fig. 2.10. Graphs show the contribution of spatial, soil and topographic variables with respect to each species stem abundance in 2019 (A), basal area increment in species (between 2014 to 2019) (B), mortality (between 2014 to 2019) (C), and recruitment (between 2014 to 2019) (D) in each quadrat (400 m^2) in the Yosemite Forest Dynamics Plot. 1= the pure spatial component; 2= the proportion explained by soil variables; 3= the proportion explained by topographic variables.

Table 2.3. Results of testing the significance of contribution for each component including spatial, topographic, and soil variables in species abundance (Abundance), basal area increment (BAI), morality, and recruitment. (1) refers to inclusion of two soil enzymes into edaphic factors and (2) refers to exclusion of enzymes from soil component

	Spatial		Topographic		Soil	
					(1)	(2)
	F	P	F	P	F	P
Abundance	9.1	0.001*	5.4	0.001*	2.1	0.002*
					1.5	0.012*
BAI	3.6	0.042*	3.1	0.008*	3.2	0.031*
					2.8	0.045*
Mortality	2.8	0.001*	19.0	0.001*	0.9	$0.581^{(ns)}$
					0.7	$0.794^{(ns)}$
Recruitment	3. 6	0.001*	2.8	0.001*	0.9	$0.479^{(ns)}$
					0.8	$0.706^{(ns)}$

* significant ($P \leq 0.05$), and ns, not significant ($P > 0.05$)

Spatial, topography, and soil resources (soil properties with and without enzymes) were all statistically significant in their contribution to species abundance and basal area increment (Table 2.3). Spatial and topographic variables were significant contributors to recruitment and mortality. The contributions of soil factors were not significant (soil properties with and without soil enzymes) explaining variations in recruitment and mortality (Table 2.3).

Discussion

Associations of different species with habitat types

About half of the species were positively (six species) or negatively (seven species) associated with specific habitats. Species which are positively associated with a specific habitat may be more competitive than the species which are negatively repelled or neutrally (no association with respect to habitat) associated with the same habitat (Zhang et al. 2012). Five species were associated with habitats defined by topographic variables. Slope is an important factor, likely due to its effect on water availability, especially during the dry seasons (Harms et al. 2001). Aspect often plays a role in species composition (Kutiel and Lavee 1999), by influencing on water potential, organic matter, irradiance availability at ground level, and the creation of different microclimates (Punchi-Manage et al. 2013). Generally, low slope north facing sites experienced cooler temperature, lower solar radiation and evapotranspiration rate due to the lower exposure of sunlight, higher runoff water accumulation due to the deep soil (Méndez-Toribio et al. 2017) and higher amount of organic matter. *Abies concolor* grows in the environment with the heterogenous soil conditions and shows the best growth on a moderate slopes

and level ground (Laacke 1990). The abundance in *Abies concolor* showed positive association with the low slope. Consistent with those results, mortality of *Abies concolor* was negatively associated with north-facing, low slopes (observed mortality number from habitat map was < 2.5% of the simulated mortality value from torus-translation). The importance of water availability as a restricting factor in *Abies concolor* development was also found by Laacke (Laacke 1990).

Recruitment of *Cornus sericea* was positively associated with habitat 1 (Table A.3). The levels of P concentration and K were high in these habitats. However, this positive association may be related to other factors including the high soil moisture in this habitat and the proximity to high abundances of parent plants at moist sites (considerable reproduction for this species is vegetative). *Quercus kelloggii* mortality was positively associated with habitat 6 where phosphorus, calcium, and urease enzyme levels were high. This association would be created as a result of higher competition in habitats with greater nutrient sources which would result in a greater number of observed mortalities. Basal area increment of *Quercus kelloggii* was positively associated with habitat 7, where phosphatase enzyme activity, Ca, K, and Mg were high. Additionally, *Quercus kelloggii* basal area increment was negatively associated with habitat 5 where Ca, Mg, and phosphatase levels were the lowest among all habitats and P concentration was not high. Zhang et al. (2010) determined the contribution of different soil chemical properties in explaining the variation in tree sizes in temperate forest and result showed that above 14% tree diameter variation could be explained by soil chemical variables. The effect of some soil nutrients on diameter growth in various system was confirmed in other studies. Neba et al. (2016) found that addition of Mg resulted in a better height and diameter

growth due to a better root growth and greater nutrient uptake from the soil. The important effect of P in dry matter production and basal area increment was also found by another study (Aydin and Uzun 2005). Increase in tree growth with the availability of Ca was presented by Baribault et al. (Baribault et al. 2012). In addition, a significant effect of Mg on stem diameter growth at breast height by increasing nutrient uptake confirmed by other studies (Gagnon 1965).

The habitat map created by edaphic variables produced a more heterogeneous pattern than a habitat map generated by topographic variables in this study (Fig. 2.8). The result was a greater number of species associated with edaphically-defined habitats in comparison with the number of species associated with topographically-defined habitats. The greater number of species associated with habitats in a more complex habitat map (heterogeneous pattern) due to the providing a wide range of niche which reduce species niche overlap and increase species diversity and abundance (Smith et al. 2014).

Niche vs. dispersal limitation drive variations in abundance and basal area increment

The role of niche and dispersal limitation in shaping forest communities was investigated by partitioning the variation in species demographic metrics into different portions determined by edaphic, topographic, and spatial variables. The variance explained by purely spatial variables was attributed to dispersal-assembly and responses of species to the unmeasured environmental variation (Baldeck et al. 2013). Although in general, variance partitioning analyses with observational data cannot distinguish unmeasured environmental variables and neutral processes (Legendre et al. 2009), this analysis included a more comprehensive environmental dataset than that used by

Legendre et al. (Legendre et al. 2009), which considered topography as the principal environmental factor. We thus decreased the effect of unmeasured environmental variables in the pure spatial fraction. However, other unmeasured environmental variables (such as light availability, soil temperature, soil moisture, and competition in the local tree neighborhood) undoubtedly contribute to the community structure. Dispersal limitation has a strong potential to structure communities at fine scales, especially in species with a lower dispersal ability which seeds are dispersed close to their parents (Gilbert and Lechowicz 2004, Girdler and Barrie 2008, Lin et al. 2013). Results showed more than 30% of total variation of species abundances was explained by spatial variables. The important effect of biotic processes such as dispersal limitation at finer scales confirmed by other study (Yuan et al. 2011). Stochasticity process such as demographic stochasticity as an important part of neutral theory, play important role at small scales (10 m to 20 m) and the importance of niche processes increase with scale (Shipley et al. 2012).

The incremental contribution of spatial and environmental factors varied among species (Table A.7; Table A.8). The variation in stem abundance explained by spatial variables was the highest for *Pinus lambertiana* which seeds are heavy with small wings that could result in a shorter dispersal distances (Kinloch and Scheuner 1990) (Fig. 2.10). *Abies concolor* grows on a variety of soil conditions and pH levels. In addition to fire history, their abundance mostly depends on water availability and temperature (Laacke 1990) supporting the high contribution of topographic variables in explaining variation in *Abies concolor* stem abundance (Fig. 2.10).

The contribution of environmental and spatial variables in forming mortality abundances across species

The higher contribution of the spatial variables in explaining the variation of species mortality may be related to strong neighborhood competition in species with limited dispersal ability due to a higher density of small individuals near the parent tree (Ma et al. 2016). As opposed to recruitment, mortality in old-growth forests is often due to insects, physical damage by wind, snow, other falling trees, disease, and intense neighborhood competition (Larson et al. 2015). Furniss et al. (2019) found that mortality following the fire was differentiated based on diameter class, and that large-diameter trees had higher survival rates than small-diameter trees. The changes in variation of species mortality explained by inclusion of soil enzymes into edaphic factors was nominal (1%). The negligible proportion of soil variables in explaining mortality indicates that soil variables are not differentiating factors for mortality in old-growth forests.

The variation in mortality explained by environmental and spatial components varied with species (Table A.9). This could be related to soil nutrient availability (Davies 2001, Bazzaz 1979). The contribution of topographic variables was the highest for Cornus nuttallii indicating the hydrological variations related to topography.

The contribution of environmental and spatial variables in forming ingrowth numbers across species

The fraction of spatial component in explaining variation of species recruitment was the highest among the other variables (Fig. 2.9). This showed the principal role of seed availability in recruitment at local scale (Eriksson 1995). The low contribution of environmental heterogeneity to recruitment may be related to the importance of other

factors, such as fecundity, germination rates, and initial growth rates of large-seeded species (Dalling and Hubbell 2002, Vera 1997). It is likely that other soil properties including temperature, especially during the January to March, affect the survival rate of seedlings due to the susceptibility of young seedlings to low temperature (Dzwonko and Gawroński 2002). In addition, other factors including litter layer depth which may prevent seedling emergences in small-seeded species (Dzwonko and Gawroński 2002).

The contribution of environmental and spatial components in explaining recruitment changed with species (Table A.10). The proportion of environmental variables was the lowest for *Chrysolepis sempervirens*, potentially due to the hypogeal (Baraloto and Forget 2007), clonal nature of this species and low sample size.

Edaphic effects

Compared to topography, we found the soil variables to explain a greater proportion of the variance in stem abundance (14% vs. 6%) (Fig. 2.9), although the total explained variance was low. Lin et al. (Lin et al. 2013) found that edaphic properties explained more variation in species distribution comparing to the topographic variables by having the direct effect on the plant growth at local scales which supported by other studies (Gleason et al. 2010, Zhao et al. 2015). Potassium, phosphorus, calcium (Naples and Fisk 2010), and micronutrients deficiency (Fay et al. 2015) can limit plant growth and function. We found that the distribution of 45.5% of species were associated with edaphic properties (Table 2.3), consistent with results showing that 40% of species distribution was associated with soil nutrients (John et al. 2007). The association of species to soil properties can be related to the direct effect of species characteristics on soil nutrients inputs and uptake which contribute to species-soil associations as a function

of species abundance (Gleason et al. 2010). We included soil enzymes in the list of soil variables due to their key role in the ecosystem dynamic and biochemical functioning through the decomposition of soil organic matter and release of nutrients such as nitrogen (urease enzyme), and phosphorus (phosphatase enzyme) (Sinsabaugh et al. 1991) into the soil. They catalyze many essential processes necessary for soil microorganisms life and affect the stabilization of soil structure. The relation of soil enzyme activities with several ecosystem processes (mineralization of nutrients such as N, P, and C), ease of measurement, and their rapid changes to soil disturbance made them an appropriate tool to evaluate the degree of soil health alteration following fire (Das and Varma 2010). The evaluation of soil health needs indicators of soil chemical and biological factors. Soil enzyme activity showed a significant difference in urease activity between burned and unburned patches four years after fire occurrence ($P = 0.01$). This decrease may be related to the reduced microbial activity and biomass in the soil after fire. The decrease may also reflect the decreased soil pH in the burned microsites compared to the unburned patches (5.56 versus 7.07; $P = 0.04$). The long-term changes in soil acidity may affect microbial activity in burned sites and resulted in a higher release of urease in the unburned patches (higher pH) compared to those in the burned sites. Additionally, the reduced urease activity, which is the first hydrolytic enzyme involved in the breakdown of urea, may be related to the increase in non-hydrolysable N forms after fire (Hernández et al. 1997, Xue et al. 2014).

We expected that the amount of inorganic N would have been higher (due to the activity of urease enzyme) in the unburned patches. However, there were no differences in $NH4^+$ ($P = 0.7$) between the burned and unburned sites. This result may be related to

the nutrient loss by leaching following the fire. Additionally, the availability of substrate (ammonium) to the nitrifying organisms may increase nitrification which in turn leads to a decrease in the level of ammonium in the soil. Furthermore, the inclusion of soil enzyme activity improved (albeit by 5%) the explanatory power of soil properties in explaining variation in species stem abundance and basal area increment (Fig. 2.9 A, B, C, D). Soil enzymes (acid phosphatase and urease) alone were significant (P= 0.01) in their contribution to species abundance and basal area increment even though the amounts of variation improvement explained by enzymes were small. The contribution of more explanatory variables (alkaline phosphatase and hydraulic conductivity shown in Fig. A.7) alone were not significant (P= 0.4) to species abundance and basal area increment.

Conclusion

The total number of species associated with habitats defined by soil properties was slightly greater than those associated with topographically-defined habitats. This finding suggests that niche partitioning caused by edaphic variables played a more important role compared to topographic variables in shaping species distributions. In addition, the contribution of spatial variables over topography and soil factors in explaining variation in species demographic metrics (stem abundance, mortality, and recruitment) indicates that community assembly was largely driven by spatially structured processes consistent with dispersal limitation and responses of species to the unmeasured environmental variables. Inclusion of two soil enzymes statistically improved predictions of species abundance and basal area increment suggesting that future studies of soil enzymes may improve habitat definitions in forests. Adding soil

enzymes to habitat definitions improved the explanatory power of edaphic variables to species abundance over the predictive ability of topography and soil nutrients alone. Species habitat associations and higher explanatory power of spatial factors compared to environmental variables suggest that both niche process and dispersal limitations affect species distributions, but dispersal processes and unmeasured environmental variables were more important. The implication of a stronger contribution of neutral processes could reduce some concerns about the effects of increasing disturbance, decreasing habitat heterogeneity, and climate change on local species extinction in the future.

Literature Cited

Aandahl, A. R. 1949. The Characterization of slope positions and their influence on the total nitrogen content of a few virgin soils of western Iowa 1. Soil Science Society of America Journal 13(c):449-454.

Anderson-Teixeira, K. J., S. J. Davies, A. C. Bennett, E. B. Gonzalez-Akre, H. C. Muller-Landau, S. J. Wright, K. Abu Salim, J. L. Baltzer, Y. Bassett, N. A. Bourg, E. N. Broadbent, W. Y. Brockelman, S. Bunyavejchewin, D. F. R. P. Burslem, N. Butt, M. Cao, D. Cardenas, K. Clay, R. S. Condit, M. Detto, X. Du, A. Duque, D. L. Erikson, C. E.N. Ewango, C. D. Fletcher, G. S. Gilbert, N. Gunatilleke, S. Gunatilleke, Z. Hao, W. H. Hargrove, T. B. Hart, B. Hao, F. He, F. M. Hoffman, R. Howe, S. P. Hubbell, P. A. Jansen, M. Jiang, M. Kanzaki, D. Kenfack, M. F. Kinnaird, J. Kumar, A. J. Larson, Y. Li, X. Li, S. Liu, S. K.Y. Lum, J. A. Lutz, K. Ma, D. Maddalena, J. R. Makana, Y. Malhi, T. Marthews, S. McMahon, W. J. McShea, H. Memiaghe, X. Mi, T. Mizuno, J. A. Myers, V. Novotny, A. A. de Oliveira, D. Orwig, R. Ostertag, J. den Ouden, G. Parker, R.

Phillips, A. Rahman, K. Sri-ngernyuang, R. Sukumar, I. F. Sun, W. Sungpalee, S. Tan, S. C. Thomas, D. Thomas, J. Thompson, B. L. Turner, M. Uriarte, R. Valencia, M. I. Vallejo, A. Vicentini, T. Vrška, X. Wang, G. Weiblen, A. Wolf, H. Xu, W. Xugao, S. Yap, and J. Zimmerman. 2015. CTFS-ForestGEO: A worldwide network monitoring forests in an era of global change. Global Change Biology 21(2): 528-549. http://dx.doi.org/10.1111/gcb.12712.

Aydin, I., and F. Uzun. 2005. Nitrogen and phosphorus fertilization of rangelands affects yield, forage quality and the botanical composition. European Journal of Agronomy 23(1): 8-14.

Baldeck, C. A., K. E. Harms, J. B. Yavitt, R. John, B. L. Turner, R. Valencia, H. Navarrete, S. J. Davies, G. B. Chuyong, and D. Kenfack. 2013. Soil resources and topography shape local tree community structure in tropical forests. Proceedings of the Royal Society B: Biological Sciences 280(1753): 20122532.

Baraloto, C., and P. M. Forget. 2007. Seed size, seedling morphology, and response to deep shade and damage in neotropical rain forest trees. American Journal of Botany 94(6): 901-911.

Baribault, T. W., R. K. Kobe, and A. O. Finley. 2012. Tropical tree growth is correlated with soil phosphorus, potassium, and calcium, though not for legumes. Ecological Monographs 82(2): 189-203.

Barth, M. A., A. J. Larson, and J. A. Lutz. 2015. A forest reconstruction model to assess changes to Sierra Nevada mixed-conifer forest during the fire suppression era. Forest Ecology and Management 354: 104-118. https://doi.org/10.1016/j.foreco.2015.06.030.

Bazzaz, F. 1979. The physiological ecology of plant succession. Annual review of Ecology and Systematics 10(1): 351-371.

Beckage, B., and J. S. Clark. 2003. Seedling survival and growth of three forest tree species: the role of spatial heterogeneity. Ecology 84(7) :1849-1861.

Bielińska, E. J., B. Kołodziej, and D. Sugier. 2013. Relationship between organic carbon content and the activity of selected enzymes in urban soils under different anthropogenic influence. Journal of Geochemical Exploration 129:52-56.

Blanchet, F. G., P. Legendre, and D. Borcard. 2008. Forward selection of explanatory variables. Ecology 89(9): 2623-2632.

Blomdahl, E. M., C. A. Kolden, A. J. Meddens, and J. A. Lutz. 2019. The importance of small fire refugia in the central Sierra Nevada, California, USA. Forest Ecology and Management 432: 1041-1052. https://doi.org/10.1016/j.foreco.2018.10.038.

Boerner, R. E., K. L. Decker, and E. K. Sutherland. 2000. Prescribed burning effects on soil enzyme activity in a southern Ohio hardwood forest: a landscape-scale analysis. Soil Biology and Biochemistry 32(7): 899-908.

Borcard, D., and P. Legendre. 2002. All-scale spatial analysis of ecological data by means of principal coordinates of neighbour matrices. Ecological Modelling 153(1-2): 51-68.

Borcard, D., P. Legendre, C. Avois-Jacquet, and H. Tuomisto. 2004. Dissecting the spatial structure of ecological data at multiple scales. Ecology 85: 1826-1832.

Bray, R. H., and L. T. Kurtz. 1945. Determination of total, organic, and available forms of phosphorus in soils. Soil Science 59(1): 39-46.

Burns, R. 1983. Extracellular enzyme-substrate interactions in soil. Pages 249–298 in J. H. Slater, R. Wittenbury, and J. W. T. Wimpenny, editors. Microbes in their natural environment. Cambridge University Press, London, UK.

Cansler, C. A., M. E. Swanson, T. J. Furniss, A. J. Larson, and J. A. Lutz. 2019. Fuel dynamics after reintroduced fire in an old-growth Sierra Nevada mixed-conifer forest. Fire Ecology 15(1): 16. https://doi.org/10.1186/s42408-019-0035-y.

Carsel, R. F., and R. S. Parrish. 1988. Developing joint probability distributions of soil water retention characteristics. Water Resources Research 24(5): 755-769.

Dalling, J. W., and S. P. Hubbell. 2002. Seed size, growth rate and gap microsite conditions as determinants of recruitment success for pioneer species. Journal of Ecology 90: 557-568.

Das, S. K., and A. Varma. 2010. Role of enzymes in maintaining soil health. Pages 25-42 in Soil Enzymology. Springer, Berlin, Heidelberg.

Davies, S. J. 2001. Tree mortality and growth in 11 sympatric Macaranga species in Borneo. Ecology 82(4): 920-932.

Dick, R. P. 2020. Methods of soil enzymology. Pages 154–196. Soil Science Society of America, Madison, WI, USA.

Dzwonko, Z., and S. Gawroński. 2002. Influence of litter and weather on seedling recruitment in a mixed oak–pine woodland. Annals of Botany 90(2): 245-251.

Eivazi, F., and M. Tabatabai. 1977. Phosphatases in soils. Soil Biology and Biochemistry 9(3): 167-172.

Eriksson, O. 1995. Seedling recruitment in deciduous forest herbs: the effects of litter, soil chemistry and seed bank. Flora 190(1): 65-70.

Fay, P.A.; S. M. Prober., W.S. Harpole, J. M. Knops, J. D. Bakker, E. T. Borer, E. M. Lind, A. S. MacDougall, E.W. Seabloom, and P.D. Wragg. 2015. Grassland productivity limited by multiple nutrients. Nature Plants 1(7): 1-5.

Ferry, B., F. Morneau, J. D. Bontemps, L. Blanc, and V. Freycon. 2010. Higher treefall rates on slopes and waterlogged soils result in lower stand biomass and productivity in a tropical rain forest. Journal of Ecology 98(1): 106-116.

Fu, B., S. Liu, K. Ma, and Y. Zhu. 2004. Relationships between soil characteristics, topography and plant diversity in a heterogeneous deciduous broad-leaved forest near Beijing, China. Plant and soil 261(1-2): 47-54.

Furniss, T. J., V. R. Kane, A. J. Larson, and J. A. Lutz. 2020. Detecting tree mortality with Landsat-derived spectral indices: Improving ecological accuracy by examining uncertainty. Remote Sensing of Environment 237: 111497. https://doi.org/10.1016/j.rse.2019.111497.

Furniss, T. J., A. J. Larson, V. R. Kane, and J. A. Lutz. 2019. Multi-scale assessment of post-fire tree mortality models. International Journal of Wildland Fire 28(1): 46-61. https://doi.org/10.1071/WF18031

Furniss, T. J., A. J. Larson, and J. A. Lutz. 2017. Reconciling niches and neutrality in a subalpine temperate forest. Ecosphere 8(6): e01847. https://doi.org/10.1002/ecs2.1847.

Gagnon, J. 1965. Effect of magnesium and potassium fertilization on a 20-year-old red pine plantation. The Forestry Chronicle 41(3): 290-294.

Gilbert, B., and M. J. Lechowicz. 2004. Neutrality, niches, and dispersal in a temperate forest understory. Proceedings of the National Academy of Sciences 101(20): 7651-7656.

Girdler, E. B., and B. T. C. Barrie. 2008. The scale-dependent importance of habitat factors and dispersal limitation in structuring Great Lakes shoreline plant communities. Plant Ecology 198(2): 211-223.

Gleason, S.M., J. Read, A. Ares, and D. J. Metcalfe. 2010. Species–soil associations, disturbance, and nutrient cycling in an Australian tropical rainforest. Oecologia, 162(4): 1047-1058.

Griffiths, R. P., M. D. Madritch, and A. K. Swanson. 2009. The effects of topography on forest soil characteristics in the Oregon Cascade Mountains (USA): Implications for the effects of climate change on soil properties. Forest Ecology and Management 257(1): 1-7.

Harms, K. E., R. Condit, S. P. Hubbell, and R. B. Foster. 2001. Habitat associations of trees and shrubs in a 50-ha neotropical forest plot. Journal of Ecology 89(6): 947-959.

Hernández, T.; C. Garcia, I. Reinhardt. 1997. Short-term effect of wildfire on the chemical, biochemical and microbiological properties of Mediterranean pine forest soils. Biology and Fertility of Soils 25(2): 109-116.

Herwitz, S. R., and S. S. Young. 1994. Mortality, recruitment, and growth rates of montane tropical rain forest canopy trees on Mount Bellenden-Ker, Northeast Queensland, Australia. Biotropica 350-361.

John, R., J.W. Dalling, K.E. Harms, J. B. Yavitt, R.F. Stallard, M. Mirabello, S. P. Hubbell, R. Valencia, H. Navarrete, and M.Vallejo. 2007. Soil nutrients influence spatial distributions of tropical tree species. Proceedings of the National Academy of Sciences. 104(3): 864-869.

Jönsson, U., U. Rosengren, B. Nihlgård, and G Thelin. 2002. A comparative study of two methods for determination of pH, exchangeable base cations, and aluminum. Communications in Soil Science and Plant Analysis 33(19-20): 3809-3824.

Kanagaraj, R., T. Wiegand, L. S. Comita, and A. Huth. 2011. Tropical tree species assemblages in topographical habitats change in time and with life stage. Journal of Ecology 99(6): 1441-1452.

Kandeler, E., and H. Gerber. 1988. Short-term assay of soil urease activity using colorimetric determination of ammonium. Biology and Fertility of Soils 6(1): 68-72.

Kane, V. R., C. A. Cansler, N. A. Povak, J. T. Kane, R. J. McGaughey, J. A. Lutz, D. J. Churchill, and M. P. North. 2015. Mixed severity fire effects within the Rim fire: relative importance of local climate, fire weather, topography, and forest structure. Forest Ecology and Management 358: 62-79. https://doi.org/10.1016/j.foreco.2015.09.001.

Kassambara, A., and F. Mundt. 2017. Factoextra: Extract and visualize the results of multivariate data analyses package. Version 1.0.7. https://cran.r-project.org/web/packages/factoextra/index.html.

Keddy, P. A. 1992. Assembly and response rules: two goals for predictive community ecology. Journal of Vegetation Science 3(2):157-164.

Keeler-Wolf, T., P. Moore, E. Reyes, J. Menke, D. Johnson, and D. Karavidas. 2012. Yosemite National Park vegetation classification and mapping project report. Natural Resource Report NPS/YOSE/NRTR—2012/598. National Park Service, Fort Collins, Colorado.

Kinloch, B. B., and W. H. Scheuner. 1990. Pinus lambertiana Dougl. Pages 370-379 in R. Burns, and B. Honkala, editors. Silvics of North America. U.S. Dept. of Agriculture, Forest Service, Washington, USA.

Kumari, J. A., and P. C. Rao. 2017. Effect of Temperature on Soil Enzyme Urease Activity-productivity. International Journal of Humanities, Arts, Medicine and Science 5: 65-72.

Kutiel, P., and H. Lavee. 1999. Effect of slope aspect on soil and vegetation properties along an aridity transect. Israel Journal of Plant Sciences 47(3):169-178.

Laacke, R. 1990. Abies concolor (Gord. & Glend.) Lindl. ex Hildebr. White Fir. Pages 36-46 in R. Burns, and B. Honkala, editors. Silvics of North America. U.S. Dept. of Agriculture, Forest Service, Washington, USA.

Larson, A. J., C. A. Cansler, S. G. Cowdery, S. Hiebert, T. J. Furniss, M. E. Swanson, and J. A. Lutz. 2016. Post-fire morel (Morchella) mushroom abundance, spatial structure, and harvest sustainability. Forest Ecology and Management 377: 16-25. https://doi.org/10.1016/j.foreco.2016.06.038

Larson, A. J., J. A. Lutz, D. C. Donato, J. A. Freund, M. E. Swanson, J. HilleRisLambers, D. G. Sprugel, and J. F. Franklin. 2015. Spatial aspects of tree mortality strongly differ between young and old-growth forests. Ecology 96(11): 2855-2861. https://doi.org/10.1890/15-0628.1

Legendre, P., X. Mi, H. Ren, K. Ma, M. Yu, I. F. Sun, and F. He. 2009. Partitioning beta diversity in a subtropical broad-leaved forest of China. Ecology 90(3): 663-674.

Lin, G., D. Stralberg, G. Gong, Z. Huang, W. Ye, and L. Wu. 2013. Separating the effects of environment and space on tree species distribution: from population to community. PLoS One 8(2): e56171.

Lutz, J. A. 2015. The evolution of long-term data for forestry: large temperate research plots in an era of global change. Northwest Science 89(3): 255-269. https://doi.org/10.3955/046.089.0306.

Lutz, J. A., A. J. Larson, and M. E. Swanson. 2018. Advancing fire science with large forest plots and a long-term multidisciplinary approach. Fire 1(1): 5. https://doi.org/10.3390/fire1010005

Lutz, J. A., A. J. Larson, M. E. Swanson, and J. A. Freund. 2012. Ecological importance of large-diameter trees in a temperate mixed-conifer forest. PLoS One 7(5): e36131. https://doi.org/10.1371/journal.pone.0036131.

Lutz, J. A., J. R. Matchett, L. W. Tarnay, D. F. Smith, K. M. Becker, T. J. Furniss, and M. L. Brooks. 2017. Fire and the distribution and uncertainty of carbon sequestered as aboveground tree biomass in Yosemite and Sequoia & Kings Canyon National Parks. Land 6(1): 10. https://doi.org/10.3390/land6010010.

Lutz, J. A., J. W. Van Wagtendonk, and J. F. Franklin. 2010. Climatic water deficit, tree species ranges, and climate change in Yosemite National Park. Journal of Biogeography 37(5): 936-950. https://doi.org/10.1111/j.1365-2699.2009.02268.x.

Ma, L., J. Lian, G. Lin, H. Cao, Z. Huang, and D. Guan. 2016. Forest dynamics and its driving forces of sub-tropical forest in South China. Scientific reports 6: 22561.

Meddens, A. J., C. A. Kolden, J. A. Lutz, A. M. Smith, C. A. Cansler, J. T. Abatzoglou, G. W. Meigs, W. M. Downing, and M. A. Krawchuk. 2018. Fire refugia: What are they, and why do they matter for global change? BioScience 68(12): 944-954.

Méndez-Toribio, M., G. Ibarra-Manríquez, A. Navarrete-Segueda, and H. Paz. 2017. Topographic position, but not slope aspect, drives the dominance of functional strategies of tropical dry forest trees. Environmental Research Letters 12(8): 085002.

Nannipieri, P., B. Ceccanti, C. Conti, and D. Bianchi. 1982. Hydrolases extracted from soil: their properties and activities. Soil Biology and Biochemistry 14(3): 257-263.

Naples, B.K., and M.C. Fisk. 2010. Belowground insights into nutrient limitation in northern hardwood forests. Biogeochemistry 97(2-3): 109-121.

Neba, G. A., D. M. Newbery, and G. B. Chuyong. 2016. Limitation of seedling growth by potassium and magnesium supply for two ectomycorrhizal tree species of a Central African rain forest and its implication for their recruitment. Ecology and evolution 6(1): 125-142.

Neumann, M., V. Mues, A. Moreno, H. Hasenauer, and R. Seidl. 2017. Climate variability drives recent tree mortality in Europe. Global change biology 23(11): 4788-4797.

Oksanen, J., F. G. Blanchet, R. Kindt, P. Legendre, P. R. Minchin, R. O'hara, G. L. Simpson, P. Solymos, M. H. H. Stevens, and H. Wagner. 2013. Vegan: Community ecology package. Version 2.5-6. https://cran.r-project.org/web/packages/vegan/index.html.

Page, N. V., and K. Shanker. 2018. Environment and dispersal influence changes in species composition at different scales in woody plants of the Western Ghats, India. Journal of Vegetation Science 29(1): 74-83.

Pitman, N. C., J. Terborgh, M. R. Silman, and P. Nuñez V. 1999. Tree species distributions in an upper Amazonian forest. Ecology 80(8): 2651-2661.

Potts, M. D., S. J. Davies, W. H. Bossert, S. Tan, and M. N. Supardi. 2004. Habitat heterogeneity and niche structure of trees in two tropical rain forests. Oecologia 139(3): 446-453.

Prism Climate Group. 2019. Climatological normals, 1981-2019. The PRISM Group, Oregon State University, Oregon, USA. http://prism.oregonstate.edu

Punchi-Manage, R., S. Getzin, T. Wiegand, R. Kanagaraj, C. Savitri Gunatilleke, I. Nimal Gunatilleke, K. Wiegand, and A. Huth. 2013. Effects of topography on structuring local species assemblages in a Sri Lankan mixed dipterocarp forest. Journal of Ecology 101(1): 149-160.

R Core Team. 2020. R: A Language and Environment for Statistical Computing. Version 3.6.3. R Core Team, R Foundation for Statistical Computing, Vienna, Austria.

Scholl, A. E., and A. H. Taylor. 2010. Fire regimes, forest change, and self-organization in an old-growth mixed-conifer forest, Yosemite National Park, USA. Ecological Applications 20(2): 362-380.

Seibert, J., J. Stendahl, and R. Sørensen. 2007. Topographical influences on soil properties in boreal forests. Geoderma 141(1-2): 139-148.

Sherene, T. 2017. Role of soil enzymes in nutrient transformation: A Review. Bio Bulletin 3(1): 109-131.

Shipley, B., C. T. Paine, and C. Baraloto. 2012. Quantifying the importance of local niche-based and stochastic processes to tropical tree community assembly. Ecology 93(4): 760-769.

Siles, J. A., T. Cajthaml, S. Minerbi, and R. Margesin. 2016. Effect of altitude and season on microbial activity, abundance and community structure in Alpine forest soils. FEMS microbiology ecology 92.

Sinsabaugh, R. L., R. K. Antibus, and A. E. Linkins. 1991. An enzymic approach to the analysis of microbial activity during plant litter decomposition. Agriculture, Ecosystems & Environment 34(1-4): 43-54.

Smith, R. S., E. L. Johnston, and G. F. Clark. 2014. The role of habitat complexity in community development is mediated by resource availability. PloS One 9(7): e102920.

Soil Survey Staff, 2018. Natural Resources Conservation Service, United States Department of Agriculture. Web Soil Survey. Available online at the following link: http://websoilsurvey.sc.egov.usda.gov/. Accessed (8 May. 2018).

Stavros, E. N., Z. Tane, V. R. Kane, S. Veraverbeke, R. J. McGaughey, J. A. Lutz, C. Ramirez, and D. Schimel. 2016. Unprecedented remote sensing data over King and Rim megafires in the Sierra Nevada Mountains of California. Ecology 97(11): 3244-3244.

Stephens, S. L., and B. M. Collins. 2004. Fire regimes of mixed conifer forests in the north-central Sierra Nevada at multiple spatial scales. Northwest Science 78(1): 12-23.

Tabatabai, M., and J. Bremner. 1969. Use of p-nitrophenyl phosphate for assay of soil phosphatase activity. Soil Biology and Biochemistry 1: 301-307.

Thornthwaite, C., and J. Mather. 1955. The Water Balance, Publications in Climatology 8 (1): 1–104.

Valencia, R., R. B. Foster, G. Villa, R. Condit, J. C. Svenning, C. Hernández, K. Romoleroux, E. Losos, E. Magård, and H. Balslev. 2004. Tree species distributions and local habitat variation in the Amazon: large forest plot in eastern Ecuador. Journal of Ecology 92(2): 214-229.

Van Wagtendonk, J. W., and J. A. Lutz. 2007. Fire regime attributes of wildland fires in Yosemite National Park, USA. Fire Ecology 3(2): 34-52.

Vera, M. 1997. Effects of altitude and seed size on germination and seedling survival of heathland plants in north Spain. Plant Ecology 133(1): 101-106.

Weatherspoon, C. P., S. J. Husari, and J. W. Van Wagtendonk. 1992. Fire and fuels management in relation to owl habitat in forests of the Sierra Nevada and southern California. Pages 247-260 in: J. Verner, K. S. McKelvey, B. R. Noon, R. J. Gutierrez, G. I. Gould, T. W. Beck. General Technical Report. PSW-GTR-133. Albany, CA: Pacific Southwest Research Station, Forest Service, US Department of Agriculture.

Xue, L., Q. Li, and H. Chen. 2014. Effects of a wildfire on selected physical, chemical and biochemical soil properties in a Pinus massoniana forest in South China. Forests 5(12): 2947-2966.

Yuan, Z., A. Gazol, X. Wang, F. Lin, J. Ye, X. Bai, B. Li, and Z. Hao. 2011. Scale specific determinants of tree diversity in an old growth temperate forest in China. Basic and Applied Ecology 12(6): 488-495.

Zhang, C., X. Zhao, X. Zhao, and K. Gadow. 2010. Partitioning temperate plant community structure at different scales. Acta Oecol 36: 306–313.

Zhang, C., Y. Zhao, X. Zhao, and K. Gadow. 2012. Species-habitat associations in a northern temperate forest in China. Silva Fenn 46(4): 501-519.

Zhang, R. 1997. Determination of soil sorptivity and hydraulic conductivity from the disk infiltrometer. Soil Science Society of America Journal 61(4): 1024-1030.

Zhang, Z.-h., G. Hu, and J. Ni. 2013. Effects of topographical and edaphic factors on the distribution of plant communities in two subtropical karst forests, southwestern China. Journal of Mountain Science 10(1): 95-104.

Zhao, L., W. Xiang, W. Li, P. Lei, X. Deng, X. Fang, and C. Peng. 2015. Effects of topographic and soil factors on woody species assembly in a Chinese subtropical evergreen broadleaved forest. Forests 6(3): 650-669.

CHAPTER 3

THE POST-FIRE ASSEMBLY PROCESSES OF TREES SPECIES BASED ON SPATIAL ANALYSIS OF A SIERRA NEVADA MIXED-CONIFER FOREST

Abstract

Understanding the mechanisms underlying tree spatial arrangements may provide significant insights onto the processes in the maintenance species coexistence. We examined the potential role of habitat heterogeneity, dispersal limitation, fire history, unilateral intraspecific and interspecific interactions of adults on juveniles, and negative density dependence in shaping the spatial patterns of four dominant tree species (*Abies concolor, Pinus lambertiana*, *Calocedrus decurrens*, and *Quercus kelloggii*) after fire in the Yosemite Forest Dynamics Plot, California, USA. We used the univariate pair correlation function and implemented three point pattern processes (homogeneous Poisson process, inhomogeneous Poisson process, and homogeneous Thomas process) to evaluate the potential contribution of habitat filtering and dispersal limitation, bivariate null model to evaluate unilateral intra/interspecific interactions of adults on juveniles. We also used the pairwise correlation function to investigate the spatial patterns of density dependence. To understand the effect of fire, we used the univariate pair correlation function to investigate pattern changes during the six years following reintroduced fire. We compared spatial pattern changes in both sprouting species (*Quercus kelloggii*) and seeding species (*Abies concolor*), and also examined the changes in patterns of large-diameter individuals of *Abies concolor*, *Pinus lambertiana*, and *Calocedrus decurrens* in 2013 (pre-fire), 2016 (two years post-fire), and 2019. The homogeneous Thomas process was the better model at finer scales (0 m to 5 m) and the inhomogeneous Poisson

processes was the fit model at coarser scales (5 m to 60 m) which suggests that the joint effects of dispersal limitation and habitat heterogeneity contribute to the spatial patterns of these three dominant tree species. Furthermore, the results showed that the young individuals of *Abies concolor* and *Pinus lambertiana* were more commonly found around the conspecific adults. Juvenile regeneration to the 1 cm diameter threshold was highly aggregated following the fire. Large-diameter trees of *Abies concolor*, *Pinus lambertiana*, and *Calocedrus decurrens* generally did not exhibit patterns different from complete spatial randomness (*Calocedrus decurrens*), or displayed only slight aggregation (*Abies concolor* and *Pinus lambertiana*). In addition, *Abies concolor* showed positive conspecific density dependence in the immediate post-fire period.

Introduction

Studying processes underlying tree species spatial distribution provide insights into mechanisms that maintain species coexistence. Niche-based processes theory assumes that each species has their own niche and is restricted by various ecological factors (Whitfield 2002). Adaptation of species along with environmental heterogeneity and biotic interactions determine the species coexistence. In contrast, neutral processes emphasize the role of stochastic ecological processes such as dispersal limitation in species assembly (Hubbell 2001, Zhou and Zhang 2008). Species can be distributed in clumped (aggregated), uniform (dispersed), and random patterns. Considering forest trees, aggregated spatial patterns are more common than random distributions (Condit et al. 2000, Zhang et al. 2013, Engone Obiang et al. 2019).

Species spatial patterns can reflect various ecological processes including abiotic microhabitat heterogeneity (Harms et al. 2001, Queenborough et al. 2007), seed dispersal

limitations (Valencia et al. 2004), local disturbance events (Briggs and Gibson 1992), interspecific and intraspecific interactions, competition between neighboring trees (Pillay and Ward 2012), and negative density dependence (Wang et al. 2018). According to niche theory, different species adapt along particular environmental gradients and show habitat preference (or avoidance). Species are often relatively more abundant in their preferred habitats. Therefore, habitat heterogeneity may potentially affect species distributions and lead to increases in species spatial aggregations. Dispersal limitation (based on neutral process) predicts species spatial aggregation due to the localized dispersal events and regardless of underlying habitat heterogeneity (Dalling et al. 2002, Hubble 2001, Plotkin et al. 2002).

Species spatial patterns can also reflect disturbance history (i.e., fire). Fire has been one of the dominant disturbances in the most forests of western North America and it was historically frequent in the forests of the Sierra Nevada. Fire generally causes higher mortality among small diameter classes, but leaves the large-diameter cohort relatively unaffected (Furniss et al. 2019). However, fire combined with other mortality agents (bark beetles, fungi and drought) can introduce considerable uncertainty into post-fire patterns of trees (Furniss et al. 2020a, Furniss et al. 2020b). Large-diameter trees in particular play important ecological roles in sequestering biomass and reproductive output (Lutz et al. 2018b), but despite their multifaceted importance to forest ecosystem structure (e.g., Lutz et al. 2012, 2013, 2020), there is still lack of information about the factors regulating their spatial distribution. We might expect that heterogeneous fire severity leads to patchy mortality of large-diameter trees that might result in aggregated patterns following the fire.

Mixed fire severity results in mortality of overstory trees in some areas which are appropriate regions for tree regeneration. Fire influences microhabitat by unequal consumption of organic matter (Neary et al. 2005, Blomdahl et al. 2019), increasing light availability, decreasing nitrogen from the forest floor (Murphy et al. 2006), and decreasing forest floor interception (Covington and Sackett 1984). Additionally, the effect of fire on regeneration depends on the species physiology. *Quercus* species vigorously resprout after fire, taking advantage of the deep root system from mature top killed trees, which increases their access to deeper water sources and carbohydrate mobilization, causing their growth rates to be high (Zhu et al. 2012) especially compared to seeder species (i.e., *Abies concolor*).

Species interactions affect the species assembly and can structure the spatial pattern through altering growth (Saha et al. 2014), mortality pattern (Liao et al. 2015), and biomass accumulation (Yang et al. 2019), with the strength of the interaction often depending on whether close neighbors are conspecific or heterospecific. Adult trees would have unfavorable and favorable effects on survivorship and spatial pattern of juveniles within the neighboring area through competition, light availability and organic matter depth (Pardos et al. 2007), ameliorating the effects of wind, predators, and parasites existence (Janzen 1971).

In addition, conspecific density can contribute to species spatial arrangement through negative density dependence (CNDD) or positive density dependence (PNDD, facilitation). CNDD occurred when conspecific densities are high and host-specific natural enemies (predators, herbivores, and pathogens) reduce offspring survival (Janzen 1970). CNDD can be considered as a mechanism which would lead to regular pattern by

decreasing conspecific aggregation through the negative correlation between the seedling survival and conspecific adults (Inman-Narahari et al. 2016).

The study aimed to examine: (1) the potential contributions of dispersal limitation and habitat filtering in three dominant tree species spatial patterns at different scales, (2) the possible intraspecific and interspecific interactions between the adults and juveniles in four most abundant species, (3) the changes in regeneration spatial pattern in seeder and sprouter species through the years followed by the fire, (4) the possible effect of fire on the large-diameter trees spatial patterns, and (5) the influence of density-dependent processes in forming dominant tree species spatial arrangements in the Yosemite Forest Dynamics Plot.

Methods

Study area

The study was carried out in the Yosemite Forest Dynamics Plot (YFDP), a 25.6 ha (320 m × 800 m) plot established according to the Smithsonian ForestGEO protocols near Crane Flat in Yosemite National Park, central Sierra Nevada, California, USA (Fig 3.1) (Anderson-Teixeira et al. 2015, Lutz 2015). The YFDP is further divided into 640 quadrats of 20 m × 20 m. The climate is Mediterranean, with hot, dry summers and cool, wet winters. Annual minimum and maximum temperatures are in January (-1.82 ºC to 10.01 ºC) and July (13.9 ºC to 27.14 ºC) (Lutz et al. 2010). Mean annual precipitation is 1070 mm, with most precipitation occurring between November and March (Lutz et al. 2010). Elevation ranges from 1774.1 m to 1911.3 m. The principal tree species are *Abies concolor* (white fir), *Pinus lambertiana* (sugar pine), *Cornus nuttallii* (Pacific dogwood,)

Calocedrus decurrens (incense-cedar), and *Quercus kelloggii* (California black oak) (Lutz et al. 2012), with distribution and abundance of these species jointly controlled by climate and fire (van Wagtendonk et al. 2020). The YFDP was burned in August 2013 by a management-ignited backfire to prevent the spread of the Rim fire (details about fire behavior and fire effects: Stavros et al. 2016, Lutz et al. 2017, Blomdahl et al. 2019, and Cansler et al. 2019).

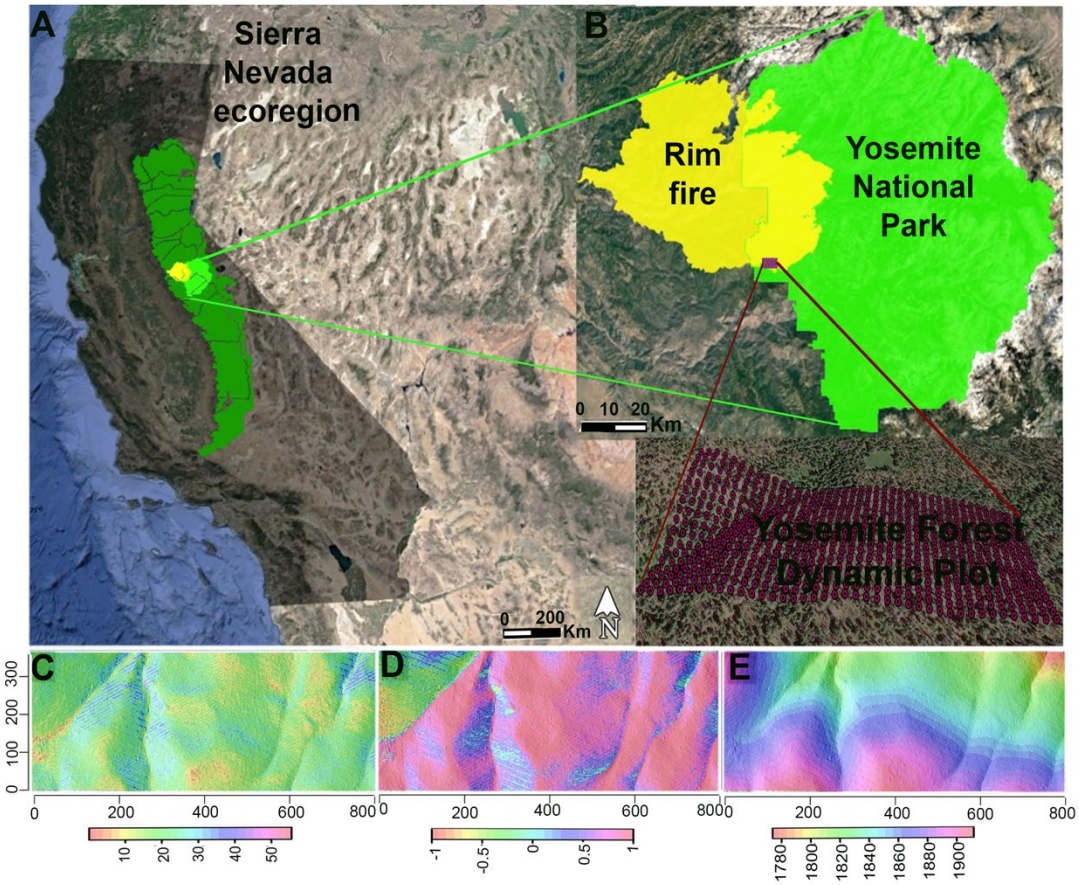

Fig. 3.1. Locations of Yosemite National Park and Yosemite Forest Dynamics Plot in California (A, B). Topographic maps of the 25.6 ha plot including slope (C), aspect (D), and elevation (E). Imagery from google earth 2020 (Google Earth Pro 2020).

Field methods

Within the YFDP, each tree was revisited annually between 2011 and 2019 and the status (live or dead) was checked each year, with tree diameters remeasured in 2014 and 2019. We analyzed the four most abundant tree species; *Abies concolor*, *Pinus lambertiana*, *Calocedrus decurrens*, and *Quercus kelloggii* (2862, 857, 450, and 1282 live stems, respectively, in 2019). To evaluate the potential influence of topographic variables on species spatial patterns, elevation, aspect, and slope were calculated in each 20 × 20 m using the surveyed elevations of the quadrat corners. Each quadrat was divided into four triangular planes (each triangle is formed by connecting three corners of the quadrat) and the slope was calculated by taking the mean angular deviation of these panels. Elevation was calculated by averaging the elevations of four corners of the quadrat (Harms et al. 2001).

Data analysis

Null models and spatial point process models

We used the pair correlation function to analyze the spatial pattern of individuals ≥1 cm diameter at breast height (Stoyan and Stoyan 1994, Illian et al. 2008). The Ripley's k-function is the expected number of individuals in a circle with radius r centered at optional individual divided by the intensity of the pattern (Ripley 1976). The univariate pair correlation function, g(r), which the circle in Ripley's k-function is replaced by ring was used to analyze the spatial arrangement of tree distributions (Stoyan and Stoyan 1994). The g(r) is the expected density of points falling within a circular ring of radius (r) around a focal tree divided by the intensity of the pattern (Stoyan and Stoyan 1994). If

g(r) ~1, then the inter-tree distances are consistent with complete spatial randomness. If g(r) values are larger than one, indicate that trees are more aggregated (clustered) than expected at radius r. Values of g(r) less than one indicate that trees are more dispersed than expected at distance r. Point process models use one of several random distributions of points as a null model (Harvey et al. 1983). We used three null models – complete spatial randomness, inhomogeneous Poison processes, and homogeneous Thomas processes.

Complete spatial randomness (CSR)

The simplest and perhaps most common null model for univariate point patterns is complete spatial randomness (CSR), which indicates that the spatial distributions of trees is not influenced by any underlying biological mechanisms at any distance (Wiegand and A. Moloney 2004). For CSR patterns, each point has the same probability of occurring at any place in the study area. Gradients due to first order environmental differences are not considered.

Inhomogeneous Poisson process (IPP)

The inhomogeneous Poisson process (IPP) considers first order gradients in the dataset. In this null model, the distribution of points is assumed based on an intensity function (λ) that depends on the interaction between environmental covariates and tree species density (Wiegand et al. 2007). In this study, three topographic variables including aspect, slope and elevation selected as environmental variables. We used the heterogeneous Poisson process to estimate the effect of topographic heterogeneity on the local tree species density.

Homogeneous Thomas process (HTP)

This point process is a Poisson cluster process which can model the impact of dispersal limitation (independent of the habitat heterogeneity) with the aggregation of the offspring around the parent trees. This process is modeled by two steps (Illian et al. 2008). First the locations of parent trees are generated from a homogeneous Poisson point process with $\lambda > 0$ on simulation window. Second a number of offspring with mean $\mu > 0$ are independently generated around each parent. These offspring form the clusters and displaced from the parent by independent Gaussian dispersal kernel with standard deviation σ. For all analyses, 999 Monte Carlo simulations were used to evaluate departures of g(r) from the null models. The 95% confidence envelopes were estimated from the twenty fifth lowest and twenty fifth highest values obtained from 999 simulations using the “spatstat” package (version 1.64-1; Baddeley 2020) in R version 3.6.3 (R Core Team 2020). The distance associated to the Thomas process is the distance which g(r) =1 (Mitchell et al. 2019).

Best spatial model at different scales

The goodness-of-fit of the homogeneous Poisson process, inhomogeneous Poisson process, and homogeneous Thomas process were calculated by Akaike's information criterion (AIC). AIC were calculated using the "nmle" package (version 3.1-149; Pinheiro et al. 2020). To evaluate the best model at different spatial distances, distances were divided into the six categories: 0-2 m, 2-5 m, 5-10 m, 10-20 m, 20-40 m, and 40-60 m and the AIC were calculated over each scale range.

Antecedent conditions null model

Point pattern analysis can be employed to analyze spatial distribution and unilateral interactions of juveniles with mature individuals (Batllori et al. 2010). This bivariate null model keeps the locations of antecedent (mature trees) pattern constant and randomizes the juvenile patterns (Wiegand and Moloney 2004). We used 999 Monte-Carlo simulations and used the 25 largest and 25 smallest to define a 95% confidence interval. When the observed pattern falls above the 97.5% confidence interval, there is positive spatial correlation between juveniles and adult or clustered distribution. When the observed pattern falls below the 2.5% confidence interval adult trees negatively affect juvenile density and yield an overdispersed spatial distribution. Juveniles were considered to be those trees with 1 cm ≤ dbh < 5 cm and adults were considered to be those trees with dbh ≥ 20 cm in 2019 (diameter cutoffs as selected by Furniss et al. 2017). Stems ≥ 5 and < 20 cm were not included in the analysis because of the uncertainty in their reproductive status based on diameter threshold alone (Furniss et al. 2017). The sensitivity analysis on ±50% range of diameter threshold values was implemented on diameter threshold values (2.5 cm to 7.5 cm < threshold values dbh for juveniles and threshold values ≥ 10 cm to 30 cm dbh for adults) (Figs. B2, B3).

Assessing spatial pattern

The spatial pattern was assessed using the univariate pair correlation function g(r). Changes in spatial pattern following the fire were examined for large-diameter trees and juvenile regeneration in 2013, 2016, and 2019 (different post-fire years). Large-diameter trees were considered to be those with dbh ≥ 60 cm. We limited our analysis to tree species with more than 70 stems since we needed sufficient number of individuals to

detect patterns in point pattern statistics (Wiegand et al. 2007); those species were *Abies concolor*, *Pinus lambertiana*, and *Calocedrus decurrens*. The changes in juveniles spatial pattern were investigated in a sprouting species (*Quercus kelloggii*) and a non-sprouting species (*Abies concolor*). We applied a 9-meter radius as the local neighborhood (Lutz et al. 2012). We used the goodness-of-fit test proposed by Loosmore and Ford (Loosmore and Ford 2006) and "ecespa" package (de la Cruz Rot 2008) was used to examine the spatial pattern against the CSR. We set $\alpha = 0.05$ and applied a Bonferroni correction for multiple tests (n=23), resulting in a threshold p-value of 0.002.

Conspecific negative density dependence

Conspecific density dependent dependence (CNDD) was calculated with $g_{d,\,d+l}(r) - g_{l,\,d+l}(r)$, which compares the conspecific neighborhood of trees that died and survived (subscripts show tree status: dead (d), live (l)). Dead trees were individuals that survived from fire but died in 2015-2019 and live trees indicate the trees that survived through the time period (2015-2019). Positive and negative values indicate that the neighborhood of trees that died were more (less) crowded than the neighborhood of trees that survived. Random labeling null model was implemented to generate 999 simulation. The goodness-of-fit test, proposed by Loosmore and Ford (Loosmore and Ford 2006) was used to calculate P-value at inter-tree distances up to 4 m for inference.

Results

The observed (g) functions from CSR showed that species fell above the simulation envelopes which suggested no regular patterns under the CSR null model (Fig. 3.2 A; Fig. B.4 A; Fig. B.5 A).

Topographic effect

Abies concolor, *Pinus lambertiana*, and *Calocedrus decurrens* were aggregated at the scales ≤ 15 m scale (Fig. 3.2 B; Fig. B.4 B; Fig. B.5 B). The percentage of aggregated species decreased with the increased in the spatial distance. Also, the species densities were predicted based on the covariates data (topographic) (Fig. 3.3).

Dispersal limitation effect

Abies concolor, *Pinus lambertiana*, and *Calocedrus decurrens* showed aggregated patterns at scales lower than 5 meters, as with the inference of topographic effect (Fig. 3.2 C; Fig B.4 C; Fig. B.5 C).

Best spatial model

The homogeneous Thomas process was generally a better model in explaining species spatial pattern at finer scales (Table B.3). The inhomogeneous Poisson process performed better at coarser scales and the relative importance of homogeneous Thomas process decreased with distance. The result of the goodness-of-fit obtained from Monte Carlo simulation were relatively consistent with the results from AIC.

Spatial patterns of juvenile and adult trees

Juveniles of *Abies concolor*, *Pinus lambertiana*, and *Quercus kelloggii* were clustered around conspecific adults at 0-2 m, 0-6.5 m, and 0-6.5 m scales, respectively (Fig. 3.4 A, C, E, G; see species totals in Table B.1 and species spatial distribution in Fig. B.6 A, C, E, G). Only juveniles of *Quercus kelloggii* exhibited a significant attraction with adults of other species at 0-2.5 m scales (Fig. 3.4 B, D, F, H; see species spatial distribution in Fig. S.6 B, D, F, H).

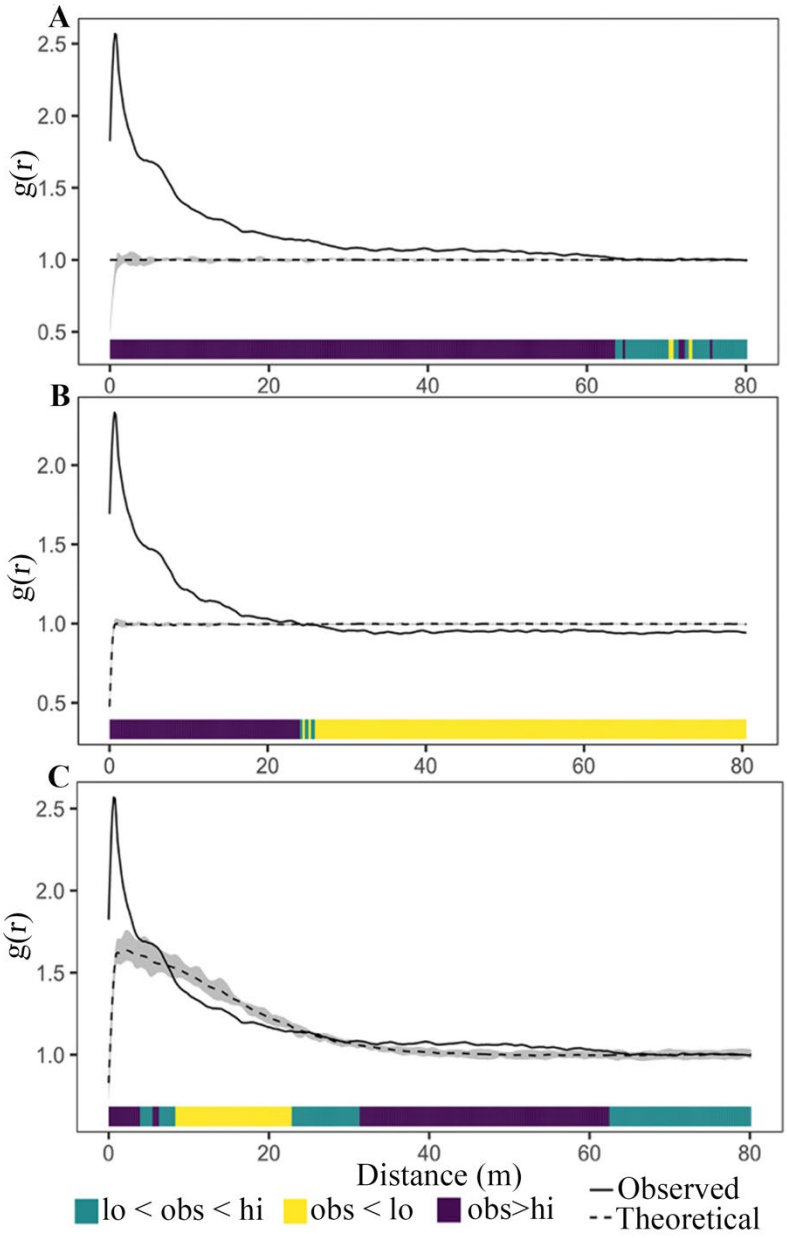

Fig. 3.2. Panels display the results of different point process models of *Abies concolor* in 2019 in the Yosemite Forest Dynamics Plot. The gray regions indicate the boundaries of the 999 Monte Carlo simulation under the homogeneous Poisson process (A), heterogeneous Poisson process (B), and homogeneous Thomas process (C). The bold black lines show the calculated g function from observed data and the black dashed lines indicate the mean of simulated values. Green, yellow, and violet colors show randomness, segregation, and clustering respectively.

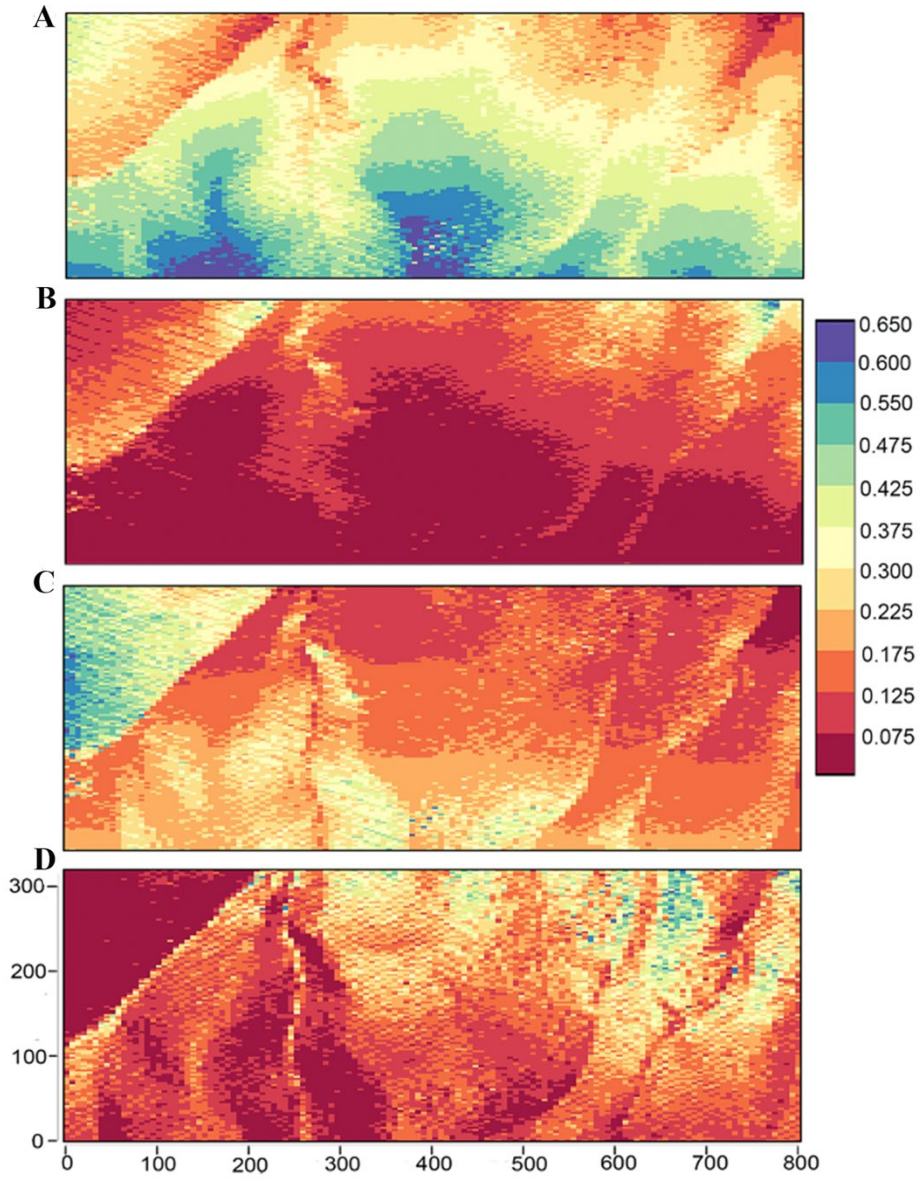

Fig. 3.3. Intensity estimation (stem/ha-1) for *Abies concolor* (A), *Calocedrus decurrens* (B), *Pinus lambertiana* (C), *Quercus kelloggii* (D) based on the slope, elevation, and aspect in 2019 in the Yosemite Forest Dynamics Plot.

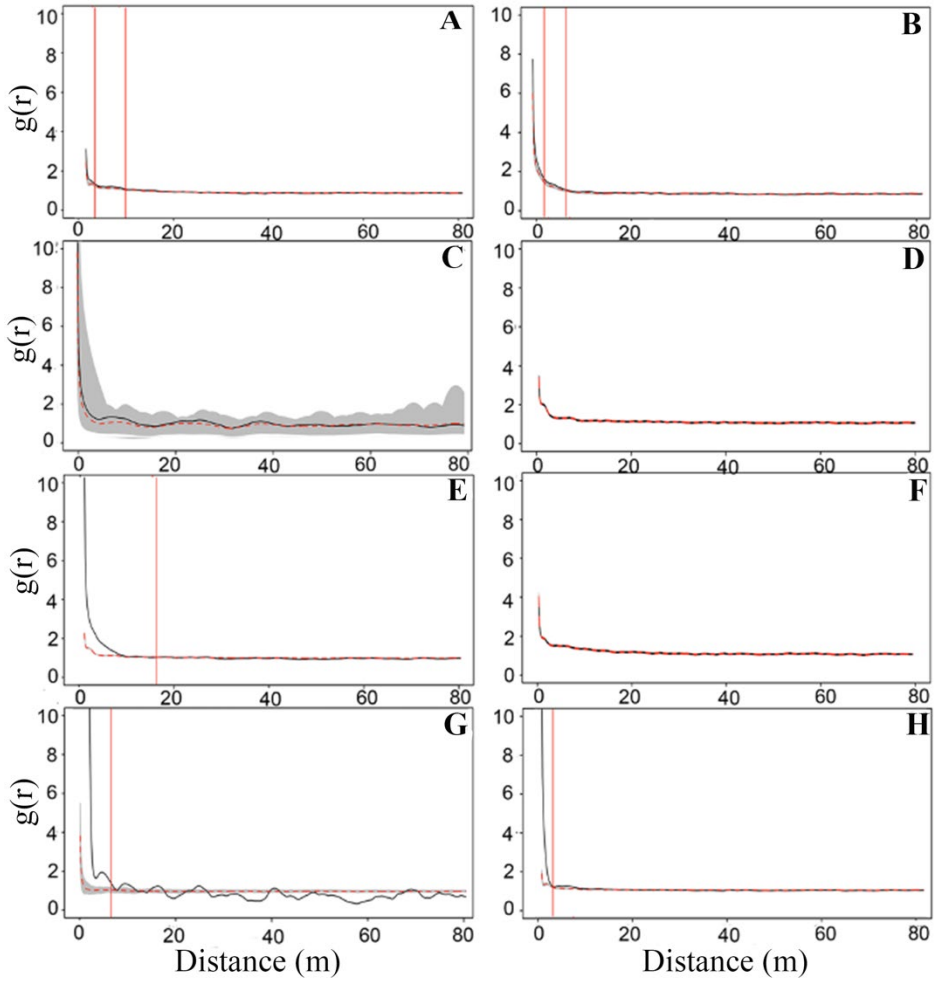

Fig. 3.4. Left panels show the bivariate spatial pattern analysis to assess the interaction between juvenile (1 cm ≤ stems dbh < 5 cm dbh) around conspecific adults (individuals ≥ 20 cm dbh) in *Abies concolor* (A), *Calocedrus decurrens* (C), *Pinus lambertiana* (E), *Quercus kelloggii* (G) in 2019 in the Yosemite Forest Dynamics Plot. The right panels display the bivariate spatial pattern analysis to estimate the distribution of juvenile (1 cm ≤ stems dbh < 5 cm) of *Abies concolor* (B), *Calocedrus decurrens* (D), *Pinus lambertiana* (F), *Quercus kelloggii* (H) around other species adult trees (individuals ≥ 20 cm dbh) in 2019. The gray areas represent the 999 Monte Carlo simulation envelopes under the antecedent condition null model and the black lines indicate the calculated g function from observed data. The red dashed lines indicate the significant aggregation pattern.

Overall changes in tree spatial patterns

The changes in spatial pattern of regeneration (1 cm ≤ dbh < 5 cm) were investigated for *A. concolor* and *Q. kelloggii* in 2013 (pre-fire), 2016 (little post-fire), and 2019 (Fig. 3.5; Table B.2; Fig. B.7). Most of the post-fire recruitments (2014-2015) of these species are from small seedlings that survived the fire. The regeneration in *A. concolor* displayed significant aggregation pattern at the 0-9 m scale in 2013, 2016, and 2019 (Monte Carlo goodness-of-fit test; 2013, 2016, and 2019, all P = 0.001). The significant aggregation from complete spatial randomness was observed for *Q. kelloggii* in 2016 and 2019 (Monte Carlo goodness-of-fit test; 2016 and 2019: P = 0.001). The g(r) value for *A. concolor* in 2016 rose significantly at small scale, reached to the aggregation peak at about 8 m and decreased gradually at coarse scale. The *A. concolor* spatial pattern in 2019 was approximately same as 2016, but with a greater magnitude. The spatial arrangement was different from complete spatial randomness from 0-9 m for *Q. kelloggii* in 2016 (Monte Carlo goodness-of-fit test; 2016: P = 0.001). The g(r) value decreased from 22-42 m and showed spatial inhibition at around 42 m.

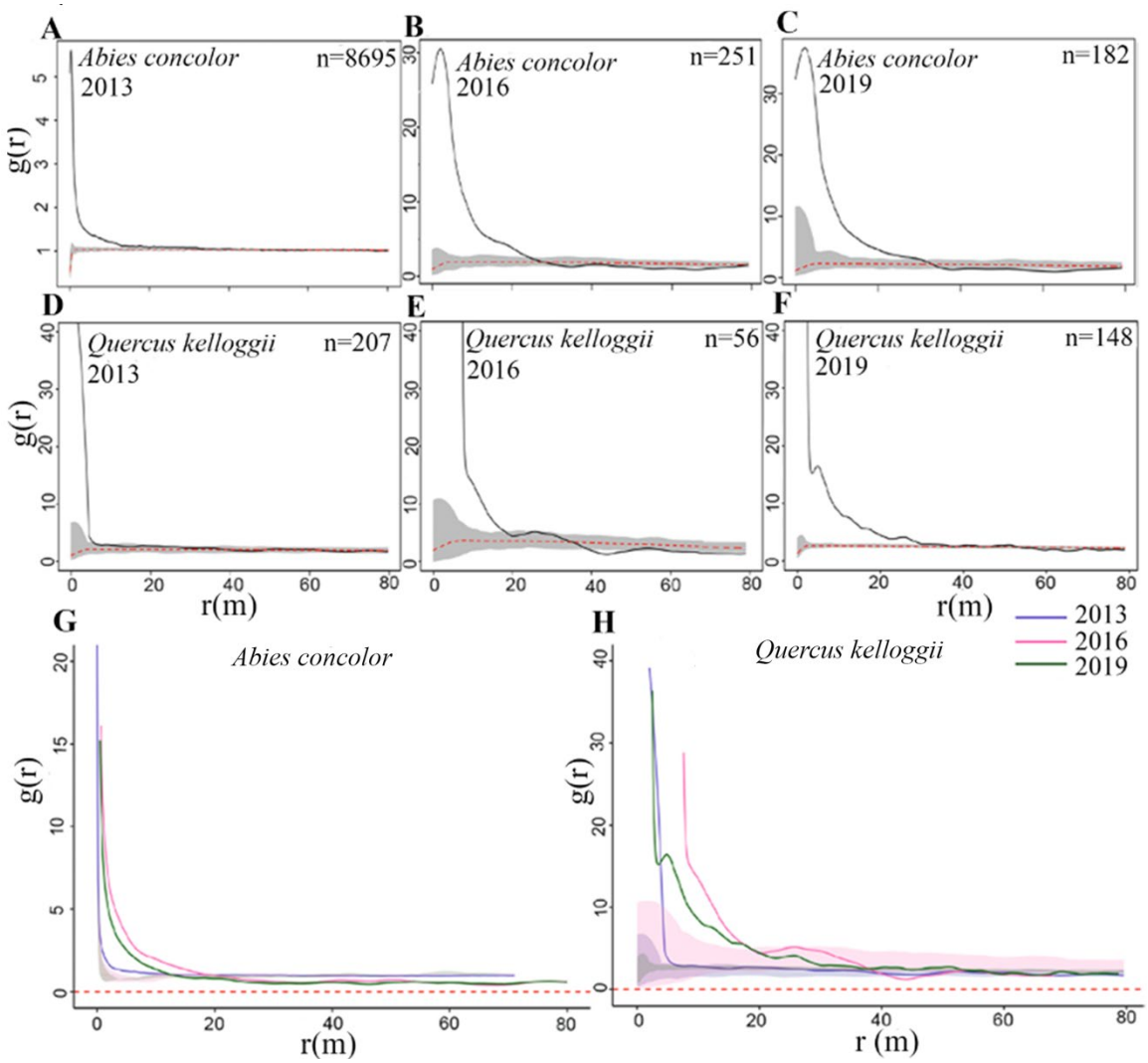

Fig. 3.5. Univariate live juvenile regeneration (1 cm ≤ dbh < 5 cm) spatial pattern in 2013, 2016, and 2019 in the Yosemite Forest Dynamics Plot. The panels (G and H) show the overall change in spatial pattern of three species in 2013, 2016, and 2019. Black lines display the observed g(r), values above (below) simulation envelope indicate aggregated (dispersed) pattern. The gray areas were obtained from the 25th highest and 25th lowest values from 999 Monte Carlo simulations.

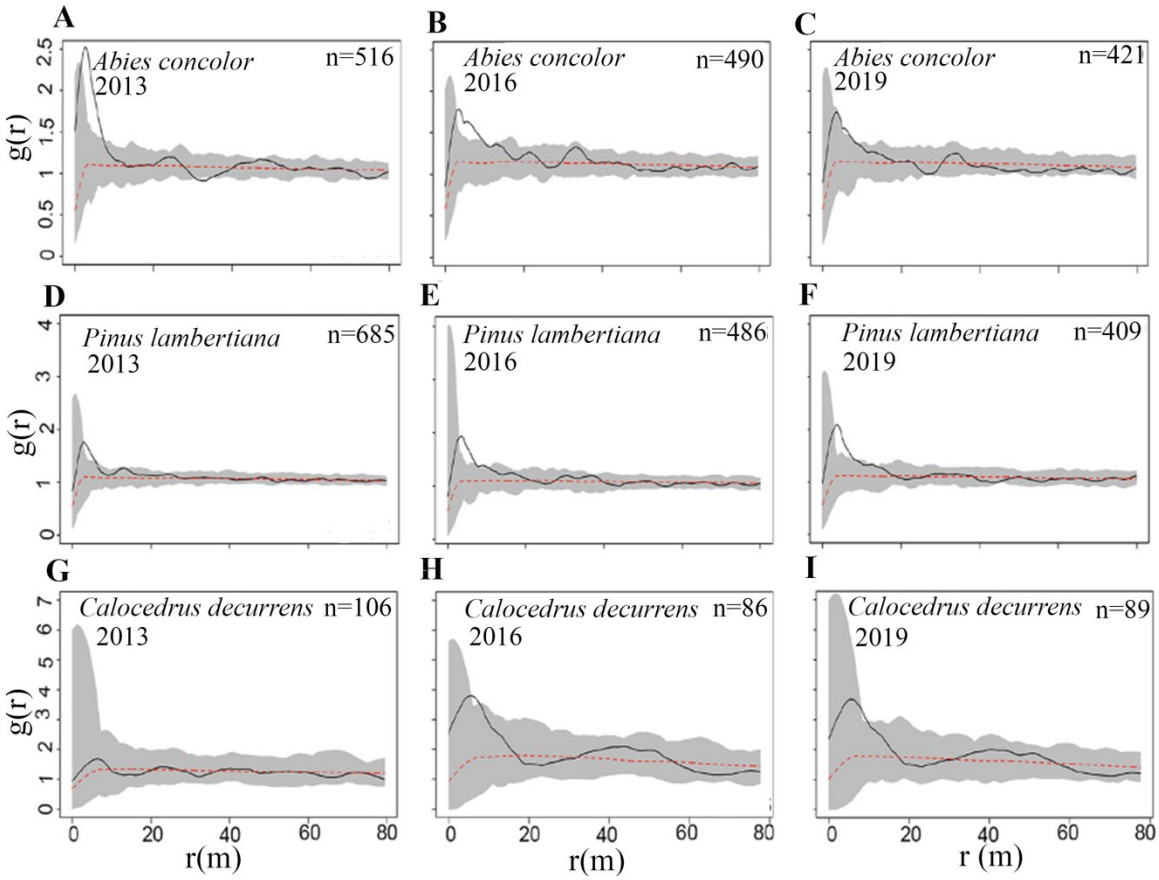

Fig. 3.6. Univariate live large tree (dbh ≥ 60 cm) spatial pattern in 2013, 2016, and 2019 in the Yosemite Forest Dynamics Plot. Black lines display the observed g(r), values above (below) simulation envelope indicate aggregated (dispersed) pattern. The gray areas were obtained from the 25th highest and 25th lowest values from 999 Monte Carlo simulations.

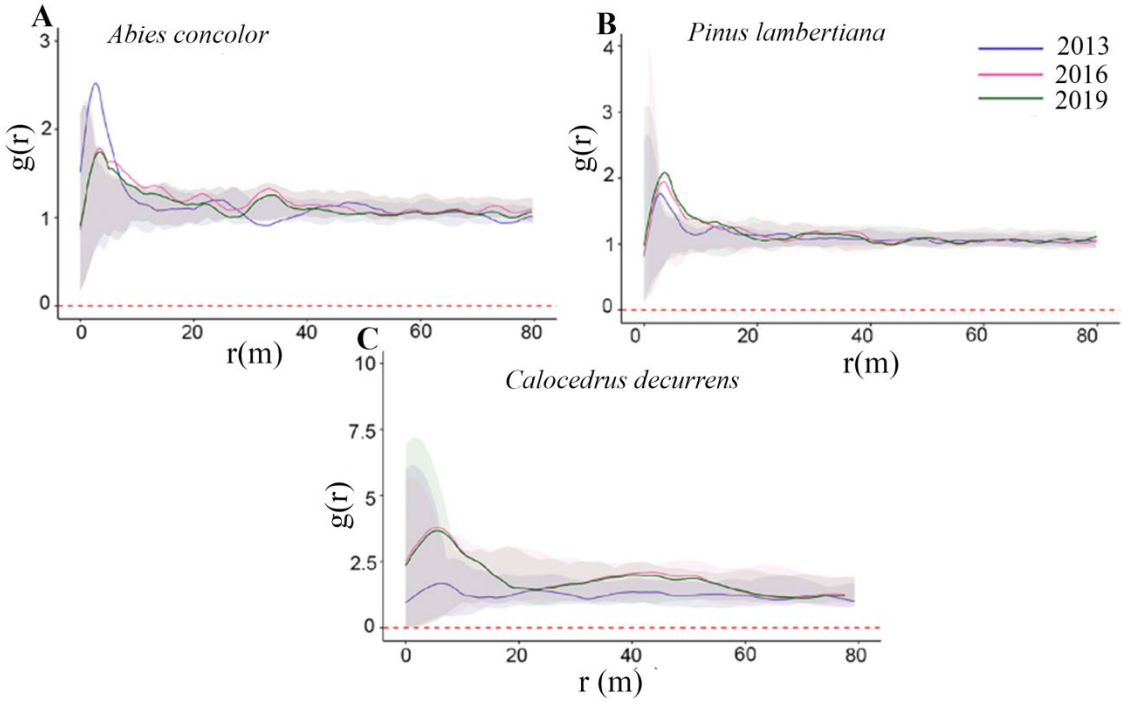

Fig. 3.7. The panels (A, B, C) show the overall change in spatial pattern of three species in 2013, 2016, and 2019. The colorful areas were obtained from the 25th highest and 25th lowest values from 999 Monte Carlo simulations in each year.

The spatial pattern of large-diameter *A. concolor* was different from complete randomness from 0-9 m (Monte Carlo goodness-of-fit test; 2013 and 2016: P = 0.001; Fig. 3.6 and Fig. 3.7). The g(r) values indicate spatial randomness from 0-9 in 2019 (Monte Carlo goodness-of-fit test; 2019: P = 0.003). The spatial pattern of *P. lambertiana* in 2013, 2016, 2019 were different from complete randomness (exhibited the significant clustering) from 0-9 m (Monte Carlo goodness-of-fit test; 2013, 2016, and 2019: P = 0.001). The spatial arrangement at all scales did not change from 2016 to 2019 in P. lambertiana. The spatial pattern of large-diameter *C. decurrens* was not different from complete randomness from 0-9 m (Monte Carlo goodness-of-fit test; 2013, 2016, 2019: P = 0.001, 0.002, 0.001).

Conspecific negative density dependence

The diameter distributions (Fig. B.10) showed that the plot characterized by abundant trees in the smaller diameter classes in 2019. The number of living *Quercus kelloggii* was relatively greater than those of dead *Quercus kelloggii*. Also, the dead stems were in the smaller diameter classes (Fig. B.9). The results (Fig. 3.8) showed that live *A. concolor* have more conspecific neighbors (living and dead) at 1-4 meters than do dead *A. concolor* which indicate the conspecific positive density dependent.

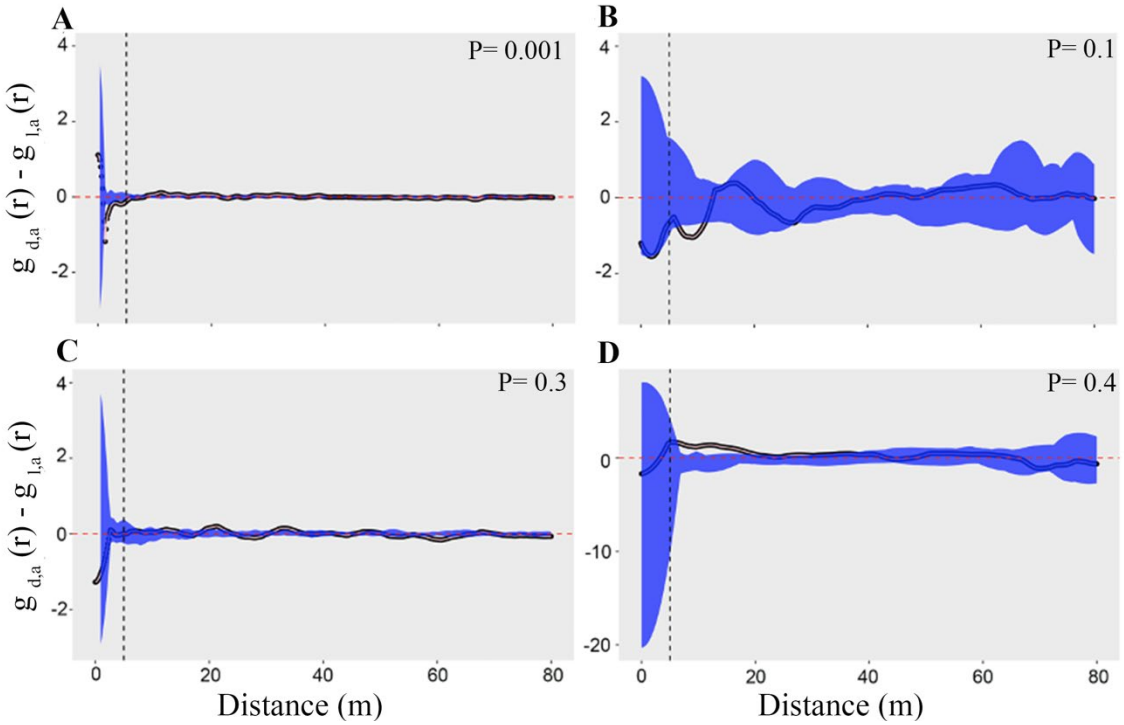

Fig. 3.8. Density dependence mortality in *Abies concolor* (A), *Calocedrus decurrens* (B), *Pinus lambertiana* (C), and *Quercus kelloggii* (D) in 2019 in the Yosemite Forest Dynamics Plot. The g(r) function indicates the pair correlation function, r is distance, and subscripts l, d, and a indicate live, dead, and all trees. Only values above (or below) the simulation envelope display that the dead trees had more (or less) crowded initial conspecific neighborhoods than survivors. P-values are based on goodness-of-fit test implemented at distance at distances of 0-4 m (shown by the vertical black dotted lines in the panels). The blue areas represent the simulation envelopes under the random labelling null model.

Discussion

Effect of random process, habitat heterogeneity, and dispersal limitation on the formation of the spatial patterns of abundant species

The homogeneous Thomas process was the better model in describing the spatial pattern of three species comparing to inhomogeneous Poisson process at finer scales, consistent with a greater contribution of neutral processes and unmeasured environmental variables compare to the habitat heterogeneity at these scales. Dispersal limitation introduced a mechanism in which a parent defines the location of an individual. Poor seed dispersal is related to a greater clumping pattern (Hubbell 1979). In species with animal dispersal mode, it is expected to have a higher dispersal ability and less aggregated pattern comparing to species with wind or gravity dispersal mode. Seeds in *P. lambertiana* are not often dispersed great distance by wind, because they are large and heavy (Habeck 1992). Furthermore, secondary mechanisms of dispersal (food-storing rodents and birds) contribute substantially in *P. lambertiana* seed dispersion by dispersing seeds away from parent trees (Vander Wall 2003). In addition, seeds of *A. concolor* disperse shorter distances due to their short and broad wing relative to its weight (Zouhar 2001). The better contribution of dispersal limitation in comparison with the environmental heterogeneity in shaping species spatial aggregation relative to environmental heterogeneity was consistent with several studies (Hardy and Sonké 2004, Seidler and Plotkin 2006, Wang et al. 2010).

However, the results displayed the contribution of habitat heterogeneity in forming tree species spatial patterns at coarser scales (>5 m), indicating the joint effects of the dispersal limitation and habitat heterogeneity in forming the species spatial pattern

(Tamjidi and Lutz 2020). Dispersal limitation apparently first generates the template for tree distribution (seed aggregation close to the parent trees), but species habitat requirements may result in uneven seedlings survival (if species survival depends on the habitat characteristics) and modify the sapling and adult distribution. Thus, the spatial pattern of seedling and young trees may display the combination of both habitat heterogeneity and dispersal limitation. Therefore, it is better to evaluate the potential contribution of two processes simultaneously while examining spatial distribution.

Biotic interactions of the four abundant species

The analysis of juveniles around adults can be considered as an approach to examine the facilitation or microhabitat selection. According to this analysis, in three out of four species including *A. concolor*, *P. lambertiana*, *Q. kelloggii*, we found juveniles aggregated around conspecific adults. This also can be related to dispersal limitation in these species as the regeneration occurred near seed source. The microhabitat close to the parent trees may facilitate seedling establishment resulting in juveniles tendency to aggregate around the adults. Additionally, positive interactions with mycorrhizal fungi may facilitate the establishment of conspecifics. The vast majority of tree species are colonized by either arbuscular (AM) or ectomycorrhizal (ECM) fungi in most temperate forest. AM trees do not have fungal external structures that protect root cells from entering pathogens. In contrast, ECM trees have fungal structure that prevent pathogens entry. *A. concolor* and *P. lambertiana* juveniles were clustered around the conspecific adults at <2 m and <6.5 m scales respectively. These aggregated patterns can be related to mycorrhizal association (both are ECM trees and have ectomycorrhizal fungi), which caused positive interactions among their juveniles with conspecific trees (Molina et al.

1993, Johnson et al. 2018). Furthermore, the aggregation of *A. concolor* juveniles around the conspecific adults at fine scales may have arisen from a lower mortality risk with proximity to conspecific neighbors in old-growth conifer forests (Das et al. 2008). The juveniles of *Q. kelloggii* exhibited attractions with conspecific and other species adults at the short distances due to the quick regeneration by sprouting in a response to fire. (Martínez et al. 2010), (Teste et al. 2009). This result displayed that tree species affected by facilitation were around 50% (50% with conspecific mature trees). The results of antecedent condition null model would be better if we applied it to specific pairs of species, but due to the lack of enough sample size in particular species, we conducted it in all species.

Effect of disturbance on the spatial pattern of juveniles regeneration and large-diameter trees

Fire can alter plant community composition by generating post-fire conditions which favor of the establishment of some species and changing the species composition in remaining forest (van Wagtendonk et al. 2020). The fire severity was classified as low-and-moderate severity fire regime with small unburned and high severity patches (Lutz et al. 2018a, Blomdahl et al. 2019). Fires with low and moderate severity regimes in areas of topographic variability create a mosaic with patches including open patches, patches with spaced single trees, and patches with aggregated trees in the forest (Kane et al. 2015, Jeronimo et al. 2019, Ng et al. 2020). Open patches of mineral soil are favorable sites for seedling establishment and increased soil moisture and reduced competition in these patches (Zald et al. 2008) may promote seedling and saplings survival. Furthermore, burned patches may show a moderate rise in the availability of resources including soil

nutrients, light, and water increasing the chances of establishment and survival (Tamjidi and Lutz 2020). The decreased attraction between juveniles and adults at greater distance indicates that light was not dominant drivers of regeneration success (unsurprising in this post-fire forest).

Oak's traits and growth strategies, allows it to take advantage of post-fire conditions. The better adaptation of oak can be traced to the ability to make root reserves by allocating carbohydrates to root growth (Johnson et al. 2019), producing deep post-fire root systems from top killed trees (Green et al. 2010). These characteristics allow oak to have a post-fire competitive advantage over seeders due to their shorter time to contribute to measured recruitment, i.e., 1 cm DBH (Van Wilgen et al. 2012). The abundance of sprouter and survived seeder species seedlings from fire event may affect post-fire forest composition. In our study, most of the regeneration (three and six years following the fire) in *A. concolor* was from small seedlings that survived the fire because of their location in small fire refugia or completely unburned patches. All of the recruitment for *Q. kelloggii* was from sprouting and resulted in strongly aggregated post-fire pattern of at scale about 1 m. Our results suggest that post-fire regeneration had a tendency to aggregate at distances up to 20 m, consistent with Fulé and Covington (1998).

The degree of disturbance affects the spatial pattern of large- diameter trees in different ways (Armesto et al. 1986, Le et al. 2016). Although low-to-moderate intensity fire often do not have direct effect on large-diameter tree mortality, it can result in injuries which would impact on large-diameter trees physiological functionality (Bär et al. 2019). Small patches of high-severity fire can kill most or all large-diameter trees, but lower severity patches leave even medium-sized trees alive (Becker and Lutz 2016). Spatial patterns of

A. concolor were clumped at scales of 0-9 m in 2013 and 2016. The survival of the large-diameter of *A. concolor* in refugia (Fulé and Covington 1998, Condit et al. 2000) would result in a clustering pattern following the fire. Random spatial distributions of large-diameter trees were observed in most scales following the fire. The spatial pattern of large-diameter *P. lambertiana* did not change a lot from 2013 to 2019, most likely due to its fire resistance. Clustering patterns at 0-9 m scales was observed in the *P. lambertiana* and *A. concolor* following the fire occurrence. This can be related to the survived stems in scattered fire refugia (Davis et al. 2005, Lutz et al. 2012). The post-fire spatial pattern in *C. decurrens* did not different from CSR which can be related to the fire-resistant characteristic in large-trees (fire-intolerant when they are small).

Effect of Conspecific negative density dependence in regulating dominant tree species spatial pattern

The conspecific negative density dependent (CNDD) was examined to assess the possible effect of density-dependent mortality on spices spatial patterns. We did not detect significant CNDD regulation at scales < 4 m in four abundant tree species. The observed intraspecific association (from antecedent condition null model) can confirm the results which displayed the attraction between conspecific adults and juveniles in *A. concolor* and *P. lambertiana*. Additionally, the positive density dependence in *A. concolor* at < 4 m scales was observed which is possibly related to the fungal structure in the roots of some species. It caused saplings clustered around conspecific trees due to their protection against pathogens and affecting saplings survival (Johnson et al. 2018).

Conclusion

Understanding processes underlying spatial arrangement reveals important clues for mechanisms of species coexistence. Investigating the effect of environmental heterogeneity, dispersal limitation, biotic interactions, and disturbance in spatial patterns development would help us to predict plant community responses to environmental changes as a result of global change. This study displayed that the both seed dispersal limitation and habitat heterogeneity shape the spatial distribution of abundant species. We found that fire can play a key role in forest composition by creating opportunities for tree species to be reorganized following the fire, although a longer time period is needed to study the regeneration spatial pattern as the most of recruits analyzed here are from small seedlings survived during the fire. Additionally, a more comprehensive study of the effect of fire on tree mortality spatial pattern is needed to examine the fire influence in species spatial pattern. The results of conspecific negative density dependence indicate the slight role of CNND in shaping abundant spatial distribution. Explaining the coexistence of species remains a challenge and future work could investigate the contribution of other ecological factors including bark beetles, pathogens, climate and drought, post-fire mortality pattern, physical mortality agent including (wind and crushing), and other environmental heterogeneity (including light, soil moisture, temperature) in species spatial pattern.

Literature Cited

Anderson-Teixeira, K. J., S. J. Davies, A. C. Bennett, E. B. Gonzalez-Akre, H. C. Muller-Landau, S. J. Wright, K. Abu Salim, J. L. Baltzer, Y. Bassett, N. A. Bourg, E. N. Broadbent, W. Y. Brockelman, S. Bunyavejchewin, D. F. R. P. Burslem, N. Butt,

M. Cao, D. Cardenas, K. Clay, R. S. Condit, M. Detto, X. Du, A. Duque, D. L. Erikson, C. E.N. Ewango, C. D. Fletcher, G. S. Gilbert, N. Gunatilleke, S. Gunatilleke, Z. Hao, W. H. Hargrove, T. B. Hart, B. Hao, F. He, F. M. Hoffman, R. Howe, S. P. Hubbell, P. A. Jansen, M. Jiang, M. Kanzaki, D. Kenfack, M. F. Kinnaird, J. Kumar, A. J. Larson, Y. Li, X. Li, S. Liu, S. K.Y. Lum, J. A. Lutz, K. Ma, D. Maddalena, J. R. Makana, Y. Malhi, T. Marthews, S. McMahon, W. J. McShea, H. Memiaghe, X. Mi, T. Mizuno, J. A. Myers, V. Novotny, A. A. de Oliveira, D. Orwig, R. Ostertag, J. den Ouden, G. Parker, R. Phillips, A. Rahman, K. Sri-ngernyuang, R. Sukumar, I. F. Sun, W. Sungpalee, S. Tan, S. C. Thomas, D. Thomas, J. Thompson, B. L. Turner, M. Uriarte, R. Valencia, M. I. Vallejo, A. Vicentini, T. Vrška, X. Wang, G. Weiblen, A. Wolf, H. Xu, W. Xugao, S. Yap, and J. Zimmerman. 2015. CTFS-ForestGEO: A worldwide network monitoring forests in an era of global change. Global Change Biology 21(2): 528-549. http://dx.doi.org/10.1111/gcb.12712.

Armesto, J., J. Mitchell, and C. Villagran. 1986. A comparison of spatial patterns of trees in some tropical and temperate forests. Biotropica 1-11.

Baddeley, A. 2020. Spatstat: Spatial point pattern analysis, model-fitting, simulation, tests. R package version 3.6.3.

Bär, A., S. T. Michaletz, and S. Mayr. 2019. Fire effects on tree physiology. New Phytologist 223(4): 1728-1741.

Batllori, E., J. J. Camarero, and E. Gutiérrez. 2010. Current regeneration patterns at the tree line in the Pyrenees indicate similar recruitment processes irrespective of the past disturbance regime. Journal of Biogeography 37(10): 1938-1950.

Becker, K. M. L., and J. A. Lutz. 2016. Can low-severity fire reverse overstory compositional change in montane forests of the Sierra Nevada, USA? Ecosphere 7(12): e01484. doi: http://dx.doi.org/10.1002/ecs2.1484.

Blomdahl, E. M., C. A. Kolden, A. J. Meddens, and J. A. Lutz. 2019. The importance of small fire refugia in the central Sierra Nevada, California, USA. Forest Ecology and Management 432:1041-1052. https://doi.org/10.1016/j.foreco.2018.10.038.

Briggs, J. M., and D. J. Gibson. 1992. Effect of fire on tree spatial patterns in a tallgrass prairie landscape. Bulletin of the Torrey Botanical Club:300-307.

Brown, C., J. B. Illian, and D. F. Burslem. 2016. Success of spatial statistics in determining underlying process in simulated plant communities. Journal of Ecology 104(1): 160-172.

Cansler, C. A., M. E. Swanson, T. J. Furniss, A. J. Larson, and J. A. Lutz. 2019. Fuel dynamics after reintroduced fire in an old-growth Sierra Nevada mixed-conifer forest. Fire Ecology 15(1): 16. https://doi.org/10.1186/s42408-019-0035-y.

Condit, R., P. S. Ashton, P. Baker, S. Bunyavejchewin, S. Gunatilleke, N. Gunatilleke, S. P. Hubbell, R. B. Foster, A. Itoh, and J. V. LaFrankie. 2000. Spatial patterns in the distribution of tropical tree species. Science 288(5470): 1414-1418.

Covington, W. W., and S. S. Sackett. 1984. The effect of a prescribed burn in southwestern ponderosa pine on organic matter and nutrients in woody debris and forest floor. Forest Science 30(1): 183-192.

Dalling, J. W., H. C. Muller-Landau, S. J. Wright, and S. P. Hubbell. 2002. Role of dispersal in the recruitment limitation of neotropical pioneer species. Journal of Ecology 90(4): 714-727.

Das, A., J. Battles, P. J. van Mantgem, and N. L. Stephenson. 2008. Spatial elements of mortality risk in old-growth forests. Ecology 89(6): 1744-1756.

Davis, M. A., C. Curran, A. Tietmeyer, and A. Miller. 2005. Dynamic tree aggregation patterns in a species-poor temperate woodland disturbed by fire. Journal of Vegetation Science 16(2): 167-174.

De la Cruz Rot, M., and M. M. De la Cruz Rot. 2020. ecespa: Functions for Spatial Point Pattern Analysis. R package version 1.1-11. https://cran.r-project.org/web/packages/ecespa/index.html. Downloaded 27 March 2020.

Engone Obiang, N. L., D. Kenfack, N. Picard, J. A. Lutz, P. Bissiengou, H. R. Memiaghe, and A. Alonso. 2019. Determinants of spatial patterns of canopy tree species in a tropical evergreen forest in Gabon. Journal of Vegetation Science 30(5): 929-939.

Fulé, P. Z., and W. W. Covington. 1998. Spatial patterns of Mexican pine-oak forests under different recent fire regimes. Plant Ecology 134:197-209.

Furniss, T. J., A. J. Larson, V. R. Kane, and J. A. Lutz. 2020a. Wildfire and drought moderate the spatial elements of tree mortality. Ecosphere, 11(8): e03214. https://doi.org/10.1002/ecs2.3214.

Furniss, T. J., V. R. Kane, A. J. Larson, and J. A. Lutz. 2020b. Detecting tree mortality with Landsat-derived spectral indices: Improving ecological accuracy by examining uncertainty. Remote Sensing of Environment 237: 111497. https://doi.org/10.1016/j.rse.2019.111497.

Furniss, T. J., A. J. Larson, V. R. Kane, and J. A. Lutz. 2019. Multi-scale assessment of post-fire tree mortality models. International Journal of Wildland Fire 28(1):46-61. https://doi.org/10.1071/WF18031.

Furniss, T. J., A. J. Larson, and J. A. Lutz. 2017. Reconciling niches and neutrality in a subalpine temperate forest. Ecosphere 8(6): e01847. https://doi.org/10.1002/ecs2.1847.

Gelfand, A. E., P. Diggle, P. Guttorp, and M. Fuentes. 2010. Handbook of spatial statistics. CRC press.

Green, S. R., M. A. Arthur., and B. A. Blankenshi. 2010. Oak and red maple seedling survival and growth following periodic prescribed fire on xeric ridgetops on the Cumberland Plateau. Forest Ecology and Management, 259(12): 2256-2266.

Google Earth Pro. (August 11, 2017). Yosemite Forest Dynamics Plot, ON USA. 37.77° N and 119.92° W. http://www.google.com/earth/index.html. (Accessed April 1, 2013).

Hardy, O. J., and B. Sonké. 2004. Spatial pattern analysis of tree species distribution in a tropical rain forest of Cameroon: assessing the role of limited dispersal and niche differentiation. Forest Ecology and Management 197(1-3): 191-202.

Harms, K. E., R. Condit, S. P. Hubbell, and R. B. Foster. 2001. Habitat associations of trees and shrubs in a 50-ha neotropical forest plot. Journal of Ecology 89(6): 947-959. https://doi.org/10.1111/j.1365-2745.2001.00615.x

Harvey, P. H., R. K. Colwell, J. W. Silvertown, and R. M. May. 1983. Null models in ecology. Annual review of Ecology and Systematics 14: 189-211.

Habeck, R. J. 1992. *Pinus lambertiana*. Fire Effects Information System. US Department of Agriculture, Forest Service, Rocky Mountain Research Station, Fire Sciences Laboratory.

Hubbell, S. P. 1979. Tree dispersion, abundance, and diversity in a tropical dry forest. Science 203: 1299-1309.

Hubbell, S. P. 2001. The unified neutral theory of biodiversity and biogeography (MPB-32). Princeton University Press.

Illian, J., A. Penttinen, H. Stoyan, and D. Stoyan. 2008. Statistical analysis and modelling of spatial point patterns. John Wiley & Sons.

Inman-Narahari, F., R. Ostertag, S. P. Hubbell, C. P. Giardina, S. Cordell, and L. Sack. 2016. Density-dependent seedling mortality varies with light availability and species abundance in wet and dry Hawaiian forests. Journal of Ecology 104(3): 773-780.

Janzen, D. H. 1970. Herbivores and the number of tree species in tropical forests. The American Naturalist 104(942): 501-528.

Janzen, D. H. 1971. Escape of juvenile *Dioclea megacarpa* (Leguminosae) vines from predators in a deciduous tropical forest. The American Naturalist 105: 97-112.

Jeronimo, S. M. A., V. R. Kane, D. J. Churchill, J. A. Lutz, M. P. North, G. P. Asner, and J. F. Franklin. 2019. Forest structure and pattern vary by climate and landform across active-fire landscapes in the montane Sierra Nevada. Forest Ecology and Management 437: 70-86. https://doi.org/10.1016/j.foreco.2019.01.033.

Johnson, D. J., K. Clay, and R. P. Phillips. 2018. Mycorrhizal associations and the spatial structure of an old-growth forest community. Oecologia 186: 195-204.

Johnson, P. S., S. R. Shifley, R. Rogers, D. C. Dey, and J. M. Kabrick. 2019. The ecology and silviculture of oaks. Cabi.

Kane, V. R., C. A. Cansler, N. A. Povak, J. T. Kane, R. J. McGaughey, J. A. Lutz, D. J. Churchill, and M. P. North. 2015. Mixed severity fire effects within the Rim fire: Relative importance of local climate, fire weather, topography, and forest structure. Forest Ecology and Management 358: 62-79. http://dx.doi.org/10.1016/j.foreco.2015.09.001.

Le, N., D. Thi, N. Van Thinh, and R. Mitlöhner. 2016. Effect of disturbance regimes on spatial patterns of tree species in three sites in a tropical evergreen forest in Vietnam. International Journal of Forestry Research 3:1-16.

Liao, J., J. Bogaert, and I. Nijs. 2015. Species interactions determine the spatial mortality patterns emerging in plant communities after extreme events. Scientific Reports 5:11229.

Loosmore, N. B., and E. D. Ford. 2006. Statistical inference using the G or K point pattern spatial statistics. Ecology 87(8): 1925-1931.

Lutz, J. A. 2015. The evolution of long-term data for forestry: large temperate research plots in an era of global change. Northwest Science, 89(3): 255-269. https://doi.org/10.3955/046.089.0306

Lutz, J., A. Larson, and M. Swanson. 2018a. Advancing fire science with large forest plots and a long-term multidisciplinary approach. Fire 1(1):5. https://doi.org/10.3390/fire1010005.

Lutz, J. A., T. J. Furniss, D. J. Johnson, S. J. Davies, D. Allen, A. Alonso, K. J. Anderson-Teixeira, A. Andrade, J. Baltzer, and K. M. Becker. 2018b. Global

importance of large-diameter trees. Global Ecology and Biogeography 27(7): 849-864. https://doi.org/10.1111/geb.12747.

Lutz, J. A., A. J. Larson, M. E. Swanson, and J. A. Freund. 2012. Ecological importance of large-diameter trees in a temperate mixed-conifer forest. PLoS One 7(5): e36131. doi: https://doi.org/10.1371/journal.pone.0036131.

Lutz, J. A., Larson, A. J., Freund, J. A., Swanson, M. E., & Bible, K. J. 2013. The importance of large-diameter trees to forest structural heterogeneity. PLoS One 8(12): e82784. https://doi.org/10.1371/journal.pone.0082784.

Lutz, J. A., J. R. Matchett, L. W. Tarnay, D. F. Smith, K. M. Becker, T. J. Furniss, and M. L. Brooks. 2017. Fire and the distribution and uncertainty of carbon sequestered as aboveground tree biomass in Yosemite and Sequoia & Kings Canyon National Parks. Land 6(1):10. https://doi.org/10.3390/land6010010.

Lutz, J. A, S. Struckman, T. J. Furniss, C. A. Cansler, S. J. Germain, L. L. Yocom, D. J. McAvoy, C. A. Kolden, A. M. S. Smith, M. E. Swanson, and A. J. Larson. 2020. Large-diameter trees dominate snag and surface biomass following reintroduced fire. Ecological Processes 9:41. https://doi.org/10.1186/s13717-020-00243-8.

Lutz, J. A., J. W. Van Wagtendonk, and J. F. Franklin. 2010. Climatic water deficit, tree species ranges, and climate change in Yosemite National Park. Journal of Biogeography 37(5): 936-950. https://doi.org/10.1111/j.1365-2699.2009.02268.x.

Martínez, I., T. Wiegand, F. González-Taboada, and J. R. Obeso. 2010. Spatial associations among tree species in a temperate forest community in North-western Spain. Forest Ecology and Management 260(4): 456-465.

Mitchell, E. G., S. Harris, C. G. Kenchington, P. Vixseboxse, L. Roberts, C. Clark, A. Dennis, A. G. Liu, and P. R. Wilby. 2019. The importance of neutral over niche processes in structuring Ediacaran early animal communities. Ecology Letters 22(12): 2028-2038.

Molina, R. 1993. Biology, ecology, and social aspects of wild edible mushrooms in the forests of the Pacific Northwest: a preface to managing commercial harvest. US Department of Agriculture, Forest Service, Pacific Northwest Research Station..

Murphy, J., D. Johnson, W. W. Miller, R. F. Walker, and R. R. Blank. 2006. Prescribed fire effects on forest floor and soil nutrients in a Sierra Nevada forest. Soil Science 171(3): 181-199.

Neary, D. G., K. C. Ryan, and L. F. DeBano. 2005. Wildland fire in ecosystems: effects of fire on soils and water. General Technical Report RMRS-GTR-42-vol. 4. US Department of Agriculture, Forest Service, Rocky Mountain Research Station, Ogden, UT.

Ng, J., M. P. North, A. J. Arditti, M. R. Cooper, and J. A. Lutz. 2020. Topographic variation in tree group and gap structure in Sierra Nevada mixed-conifer forests with active fire regimes. Forest Ecology and Management 472: 118220. https://doi.org/10.1016/j.foreco.2020.118220.

Pardos, M., F. Montes, I. Aranda, and I. Cañellas. 2007. Influence of environmental conditions on germinant survival and diversity of Scots pine (*Pinus sylvestris* L.) in central Spain. European Journal of Forest Research 126 (1): 37-47.

Pillay, T., and D. Ward. 2012. Spatial pattern analysis and competition between *Acacia karroo* trees in humid savannas. Plant Ecology 213: 1609-1619.

Pinheiro, J., D. Bates, S. DebRoy, and D. Sarkar. 2020. R Core Team. nlme: Linear and Nonlinear Mixed Effects Models. R package version 3.1-149.

Plotkin, J. B., J. Chave, and P. S. Ashton. 2002. Cluster analysis of spatial patterns in Malaysian tree species. The American Naturalist 160(5): 629-644.

Queenborough, S. A., D. F. Burslem, N. C. Garwood, and R. Valencia. 2007. Habitat niche partitioning by 16 species of Myristicaceae in Amazonian Ecuador. Plant Ecology 192: 193-207.

R Core Team. 2020. R: A Language and Environment for Statistical Computing. Version 3.6.3. R Core Team, R Foundation for Statistical Computing, Vienna, Austria.

Ripley, B. D. 1976. The second-order analysis of stationary point processes. Journal of Applied Probability, 13(2): 255-266.

Saha, S., C. Kuehne, and J. Bauhus. 2014. Intra-and interspecific competition differently influence growth and stem quality of young oaks (*Quercus robur* L. and *Quercus petraea* (Mattuschka) Liebl.). Annals of Forest Science 71(3): 381-393.

Seidler, T. G., and J. B. Plotkin. 2006. Seed dispersal and spatial pattern in tropical trees. PLoS Biology 4(11) :e344.

Stavros, E. N., Z. Tane, V. R. Kane, S. Veraverbeke, R. J. McGaughey, J. A. Lutz, C. Ramirez, and D. Schimel. 2016. Unprecedented remote sensing data over the King and Rim megafires in the Sierra Nevada Mountains of California. Ecology 97(11): 3244. http://dx.doi.org/10.1002/ecy.1577

Stoyan, D., and H. Stoyan. 1994. Fractals, random shapes, and point fields: methods of geometrical statistics. John Wiley & Sons Inc.

Tamjidi, J., and J. A. Lutz. 2020. Soil enzyme activity and soil nutrients jointly influence post-fire habitat models in mixed-conifer forests of Yosemite National Park, California, USA. Fire 3(4): 54. https://doi.org/10.3390/fire3040054.

Teste, F. P., S. W. Simard, and D. M. Durall. 2009. Role of mycorrhizal networks and tree proximity in ectomycorrhizal colonization of planted seedlings. Fungal Ecology 2(1): 21-30.

Valencia, R., R. B. Foster, G. Villa, R. Condit, J. C. Svenning, C. Hernández, K. Romoleroux, E. Losos, E. Magård, and H. Balslev. 2004. Tree species distributions and local habitat variation in the Amazon: large forest plot in eastern Ecuador. Journal of Ecology 92(2): 214-229.

Vander Wall, S. B. 2003. Effects of seed size of wind-dispersed pines (Pinus) on secondary seed dispersal and the caching behavior of rodents. Oikos 100(1): 25-34.

Van Wagtendonk, J. W., P. E. Moore, J. L. Yee, and J. A. Lutz. 2020. The distribution of woody species in relation to climate and fire in Yosemite National Park, California, USA. Fire Ecology 16: 22. https://doi.org/10.1186/s42408-020-00079-9.

Van Wilgen, B. W., D. M. Richardson, F. J. Kruger, and H. J. van Hensbergen. 2012. Fire in South African mountain fynbos: ecosystem, community and species response at Swartboskloof. Springer Science & Business Media.

Wang, H., H. Peng, G. Hui, Y. Hu, and Z. Zhao. 2018. Large trees are surrounded by more heterospecific neighboring trees in Korean pine broad-leaved natural forests. Scientific Reports 8: 1-11.

Wang, X., J. Ye, B. Li, J. Zhang, F. Lin, and Z. Hao. 2010. Spatial distributions of species in an old-growth temperate forest, northeastern China. Canadian Journal of Forest Research 40: 1011-1019.

Whitfield J. 2002. Ecology: neutrality versus the niche. Nature 417(6888): 480–1.

Wiegand, T., and K. A Moloney. 2014. Handbook of spatial point-pattern analysis in ecology. Chapman and Hall. CRC Press.

Wiegand, T., and K. A. Moloney. 2004. Rings, circles, and null-models for point pattern analysis in ecology. Oikos 104: 209-229.

Wiegand, T., C. S. Gunatilleke, I. N. Gunatilleke, and A. Huth. 2007. How individual species structure diversity in tropical forests. Proceedings of the National Academy of Sciences 104: 19029-19033.

Yang, X.-z., W.-h. Zhang, and Q.-y. He. 2019. Effects of intraspecific competition on growth, architecture and biomass allocation of Quercus Liaotungensis. Journal of Plant Interactions 14: 284-294.

Zald, H. S., A. N. Gray, M. North, and R. A. Kern. 2008. Initial tree regeneration responses to fire and thinning treatments in a Sierra Nevada mixed-conifer forest, USA. Forest Ecology and Management 256(1-2): 168-179.

Zhang, Z.-h., G. Hu, and J. Ni. 2013. Effects of topographical and edaphic factors on the distribution of plant communities in two subtropical karst forests, southwestern China. Journal of Mountain Science 10: 95-104.

Zhu, W.-Z., J.-S. Xiang, S.-G. Wang, and M.-H. Li. 2012. Resprouting ability and mobile carbohydrate reserves in an oak shrubland decline with increasing elevation on

the eastern edge of the Qinghai–Tibet Plateau. Forest Ecology and Management 278: 118-126.

Zhou, S., and D. Zhang. 2008. Neutral theory in community ecology. Frontiers of Biology in China 3(1): 1-8.

Zouhar, K. 2001. *Abies concolor*. Fire Effects Information System. U.S. Department of Agriculture, Forest Service, Rocky Mountain Research Station, Fire Sciences Laboratory.

CHAPTER 4

CONCLUSION

Understanding the mechanisms that shape species distribution and govern species demographic metrics are fundamental goals in ecology. Some of the most important factors shaping species distribution in a forest are the species responses to the environmental heterogeneity, dispersal limitation of propagules (Hubbell 2001), biotic interaction (Wisz et al. 2013), stand development processes (Connell and Slatyer 1977), and disturbance events (Briggs and Gibson 1992). Fire has been one of the dominant disturbances in the most of the forests in western North America and is an essential ecosystem process in Sierra Nevada forests (Stephens and Collins 2004). Among the various hypotheses regarding the mechanism, niche theory and neutral theory have been considered as primary processes of species distributions (Leibold and McPeek 2006, Smith and Lundholm 2010). According to the niche theory, various species have their own niche and different species coexist by occupying different resources. Species adaptation to the specific conditions determines the distribution of various species along the environmental gradients. Therefore, in a community dominated by niche theory, different species display preference for the specific habitats and show habitat associations (Itoh et al. 2003). On the other hand, neutral theory is associated with spatial dynamics such as dispersal limitation and assumes that environmental variables play no role in community structure (Potts et al. 2004)

My second chapter examined the association of species with habitats defined by topographic and soil variables. Soil enzymes were added to the soil chemical properties due to their role in ecosystem function. Additionally, the relative importance of spatial

and environmental variables was examined in order to determine the importance of dispersal limitation and niche differentiation on species demographic metrics and assemblage. I found that more species associated with habitats were defined by soil properties rather than topographically-defined habitats. Adding soil enzymes to habitat definitions improved the explanatory power of edaphic variables to species abundance over the predictive ability of topography and soil nutrients alone. These results emphasize that a more complete understanding of niche parameters is needed in explaining species habitat preference. Spatial factors explained more variation than environmental factors in stem abundance, mortality, and recruitment which suggest that dispersal limitation and unmeasured environmental variables have high explanatory power for species assemblage in this forest. These finding could reduce some concerns about the effects of increasing disturbance, decreasing habitat heterogeneity, and climate change on local species extinction in the future.

The findings in my third chapter examined the potential role of habitat heterogeneity, dispersal limitation, fire history, unilateral intraspecific and interspecific interactions of adults on juveniles, and negative density dependence in determining the spatial pattern of four dominant tree species. I found that both seed dispersal limitation and habitat heterogeneity shape the spatial distribution of abundant species at different scales. Although, we found that fire can play a key role in forest composition by creating opportunities for tree species to be reorganized following the fire, a longer time period and a more comprehensive study of the effect of fire on tree mortality spatial pattern are needed to study the effect of fire on species spatial pattern. Furthermore, conspecific negative density dependence played slight role in shaping abundant spatial distribution.

Considering these results provide that explaining the coexistence of species remains a challenge and future work could investigate the contribution of other ecological factors in species spatial pattern.

Literature Cited

Briggs, J. M., and D. J. Gibson. 1992. Effect of fire on tree spatial patterns in a tallgrass prairie landscape. Bulletin of the Torrey Botanical Club 300-307.

Connell, J. H., and R. O. Slatyer. 1977. Mechanisms of succession in natural communities and their role in community stability and organization. The American Naturalist 111(982): 1119-1144.

Hubbell, S. P. 2001. The unified neutral theory of biodiversity and biogeography. Princeton University Press, Princton, New Jersey, USA.

Itoh, A., T. Yamakura, T. Ohkubo, M. Kanzaki, P. A. Palmiotto, J. V. LaFrankie, P. S. Ashton, and H. S. Lee. 2003. Importance of topography and soil texture in the spatial distribution of two sympatric dipterocarp trees in a Bornean rainforest. Ecological Research 18(3): 307-320.

Leibold, M. A., and M. A. McPeek. 2006. Coexistence of the niche and neutral perspectives in community ecology. Ecology 87(6):1399-1410.

Potts, M. D., S. J. Davies, W. H. Bossert, S. Tan, and M. N. Supardi. 2004. Habitat heterogeneity and niche structure of trees in two tropical rain forests. Oecologia 139(3): 446-453.

Smith, T. W., and J. T. Lundholm. 2010. Variation partitioning as a tool to distinguish between niche and neutral processes. Ecography 33(4): 648-655.

Stephens, S. L., and B. M. Collins. 2004. Fire regimes of mixed conifer forests in the north-central Sierra Nevada at multiple spatial scales. Northwest Science 78(1): 12-23.

Wisz, M. S., J. Pottier, W. D. Kissling, L. Pellissier, J. Lenoir, C. F. Damgaard, and R. K. Heikkinen. 2013. The role of biotic interactions in shaping distributions and realised assemblages of species: implications for species distribution modelling. Biological reviews 88(1): 15-30.

APPENDICES

APPENDIX A: Chapter 2 Supplemental Tables and Figures

Table A.1. Van Genuchten parameters for 12 soil texture classes and A values for a disk with a 2.25 cm radius and suction values between 0.5 cm to 6 cm.

			h_0						
			-0.5	-1	-2	-3	-4	-5	-6
Soil Texture			A						
Sand	0.145	2.68	2.84	2.40	1.73	1.24	0.89	0.64	0.46
Loamy Sand	0.124	2.28	2.99	2.79	2.43	2.12	1.84	1.61	1.40
Sandy Loam	0.075	1.89	3.88	3.88	3.89	3.91	3.93	3.98	4.00
Loam	0.036	1.56	5.46	5.72	6.27	6.87	7.53	8.25	9.05
Silt	0.016	1.37	7.92	8.18	8.71	9.29	9.90	10.55	11.24
Silt Loam	0.020	1.41	7.10	7.37	7.93	8.53	9.19	9.98	10.64
Sandy Clay Loam	0.059	1.48	3.21	3.52	4.24	5.11	6.15	7.41	8.92
Clay Loam	0.019	1.31	5.86	6.11	6.64	7.23	7.86	8.55	9.30
Silty Clay Loam	0.010	1.23	7.89	8.09	8.51	8.95	9.41	9.90	10.41
Sandy Clay	0.027	1.23	3.34	3.57	4.09	4.68	5.36	6.14	7.04
Silty Clay	0.005	1.09	6.08	6.17	6.36	6.56	6.76	6.97	7.18
Clay	0.008	1.09	4.00	4.10	4.30	4.51	4.74	4.98	5.22

Table A.2. Correlation between environmental variables at 20 m ×20 m scale in the Yosemite Forest Dynamics Plot. Elev, P, Ca, Mn, Mg, EN-P, EN-U, EN-A, BS, and TEB represent elevation, phosphorus, calcium, manganese, magnesium, phosphatase enzyme, urease enzyme, alkaline phosphatase enzyme, base saturation, and total exchangeable bases respectively.

	Elev	Slope	Aspect	EN-P	EN-U	EN-A	pH	P	Ca	Mg	BS	K	TEB	Mn
Elev	-													
Slope	-0.18	-												
Aspect	-0.05	0.20	-											
EN-P	-0.11	0.07	-0.01	-										
EN-U	-0.24	-0.08	-0.11	0.02	-									
EN-A	-0.14	0.06	-0.03	0.96	0.06	-								
pH	-0.22	-0.05	-0.05	0.04	0.27	0.24	-							
P	-0.07	0.00	-0.05	-0.09	-0.03	-0.10	-0.08	-						
Ca	-0.22	0.05	0.07	0.03	0.09	0.15	0.64	0.13	-					
Mg	-0.25	0.04	-0.12	0.03	-0.02	0.1	0.30	0.28	0.73	-				
BS	-0.13	-0.15	-0.04	0.14	0.24	0.23	0.54	0.01	0.39	0.15	-			
K	-0.18	-0.11	-0.10	0.13	0.04	0.20	0.42	0.05	0.46	0.60	0.29	-		
TEB	-0.23	0.05	0.06	0.03	0.08	0.16	0.63	0.14	1.00	0.75	0.39	0.49	-	
Mn	0.26	0.01	0.03	-0.11	-0.21	-0.20	-0.52	0.41	-0.05	0.13	-0.33	-0.11	-0.05	-

Table A.3. Soil chemical properties (mean ± sd) in burned and unburned patches in the Yosemite Forest Dynamics Plot. P, Ca, Bs, K, Mg, TEB, Mn, NH_4^+, and NO_3^- indicate phosphorus, calcium, base saturation, potassium, magnesium, total exchangeable bases, manganese, ammonium, and nitrate respectively.

Soil properties	Variables	Burned	Unburned	Sig
Chemical properties	pH	5.56±0.74	7.07±0.33	0.04*
	P (mg kg^{-1})	23.66±21.71	19.09±17.33	0.26
	Ca (mg kg^{-1})	3570.65±3534.83	2304.66±1610.84	0.04*
	Bs (%)	95.87±5.01	94.27±4.25	0.35
	K (mg kg^{-1})	161.60±50.61	133.80±44.60	t*
	Mg (mg kg^{-1})	110.58±73.61	95.70±56.10	0.28
	TEB (cmol kg^{-1})	19.17±18.24	12.44±8.43	0.15
	Mn (mg kg^{-1})	41.01±36.25	47.3±38.90	0.40
	NH_4^+ (mg kg^{-1})	1.24±1.27	1.59±1.44	0.70
	NO_3^- (mg kg^{-1})	1.27±1.96	1.24±1.69	0.76

t - trace; less than 0.01.

Table A.4. Correlation among soil enzymes including URE (urease), ACP (acid phosphatase), and ALP (alkaline phosphatase) and soil chemical properties.

Soil properties	URE	ACP	ALP
pH	0.102	-0.146	0.028
P	0.090	0.090	-0.072
Ca	0.039	-0.145	-0.012
Bs	0.057	-0.086	-0.068
K	0.029	-0.006	0.029
Mg	-0.015	-0.073	-0.012
TEB	0.048	-0.143	-0.035
Mn	-0.093	-0.065	-0.002
NH_4^+	0.037	-0.131	0.067

Table A.5. Average properties (mean ± sd) for four and seven habitats at 20 m × 20 m scale in the Yosemite Forest Dynamics Plot.

Habitat	Mean Elevation	Slope	Aspect	pH	P	Ca	Bs	K
High Slope-North	1858 ± 28.3	24 ± 4	0.67 ± 0.33	6.04 ± 0.66	27.61 ± 21.52	2926.79 ± 2225.72	94.62 ± 7.61	146.14 ± 58.72
High Slope-South	1856 ± 28	15 ± 4	0.69 ± 0.31	6.14 ± 0.71	27.42 ± 24.75	2667.99 ± 1518.53	95.87 ± 5.40	175.92 ± 77.94
Low Slope-North	1846 ± 20.6	13 ± 1	0.71 ± 0.29	6.06 ± 0.37	33.34 ± 36.37	2938.10 ± 2093.01	97.22 ± 1.07	165.60 ± 36.97
Low Slope-South	1860 ± 5.1	10 ± 9	0.79 ± 0.21	6.50 ± 0.00	24.70 ± 4.38	2682.05 ± 359.28	98.55 ± 0.49	226.60 ± 52.60
Habitat 1	1856 ± 22.9	15.4 ± 4	0.53 ± 0.47	6.14 ± 0.60	27.42 ± 24.04	2667.99 ± 2162.47	95.8 ± 27.28	175.92 ± 0.17
Habitat 2	1864 ± 9.0	19 ± 0	0.54 ± 046	5.80 ± 0.40	12.22 ± 7.52	2003.16 ± 601.02	95.80 ± 2.96	179.02 ± 22.13
Habitat 3	1859 ± 25.7	23 ± 2	0.61 ± 0.39	6.11 ± 0.68	28.71 ± 23.36	3024.34 ± 2280.23	96.24 ± 3.87	151.29 ± 60.33
Habitat 4	1857 ± 28.3	14 ± 3	0.71 ± 0.29	6.16 ± 0.74	28.97 ± 24.91	2790.60 ± 1631.51	95.77 ± 5.80	173.58 ± 83.02
Habitat 5	1879 ± 17.2	20 ± 8	0.63 ± 0.37	5.76 ± 0.57	20.10 ± 7.61	1652.46 ± 986.70	88.86 ± 12.94	163.51 ± 61.42
Habitat 6	1824 ± 35.6	26 ± 7	0.71 ± 0.29	6.10 ± 0.32	37.64 ± 16.27	3098.37 ± 1148.49	92.00 ± 15.84	140.28 ± 42.04
Habitat 7	1827 ± 15.3	18 ± 6	0.71 ± 0.29	6.40 ± 0.55	23.50 ± 13.74	4862.91 ± 2396.60	98.61 ± 61.67	202.15 ± 61.67

Table A.5 (continued). Average properties (mean ± sd) for four and seven habitats at 20 m × 20 m scale in the Yosemite Forest Dynamics Plot.

Habitat	K	Mg	TEB	Mn	Acid Phosphatase	Alkaline Phosphatase	Urease
High Slope-North	146.14 ± 58.72	92.88 ± 53.99	15.7 ± 11.56	48.09 ± 35.74	0.41 ± 0.20	0.36 ± 0.16	46.80 ± 11.05
High Slope-South	175.92 ± 77.94	94.09 ± 48.74	14.54 ± 7.93	38.99 ± 37.54	0.46 ± 0.20	0.37 ± 0.14	47.01 ± 15.36
Low Slope-North	165.60 ± 36.97	93.52 ± 38.88	15.8 ± 10.74	44.12 ± 14.05	0.36 ± 0.20	0.39 ± 0.16	47.80 ± 11.32
Low Slope-South	226.60 ± 52.60	76.60 ± 20.50	14.60 ± 1.69	29.35 ± 8.41	0.44 ± 0.01	0.41 ± 0.17	49.75 ± 1.06
Habitat 1	175.92 ± 0.17	94.09 ± 240.25	14.5 ± 11.16	38.99 ± 25.68	0.37 ± 0.10	0.35 ± 0.19	45.18 ± 12.15
Habitat 2	179.02 ± 22.13	86.92 ± 24.21	11.18 ± 3.14	56.00 ± 44.56	0.38 ± 0.15	0.37 ± 0.14	50.25 ± 10.46
Habitat 3	151.29 ± 60.33	91.27 ± 50.54	16.2 ± 11.81	42.93 ± 33.10	0.43 ± 0.20	0.33 ± 0.13	49.22 ± 9.90
Habitat 4	173.58 ± 83.02	97.28 ± 51.67	15.18 ± 8.53	40.45 ± 40.59	0.43 ± 0.20	0.43 ± 0.17	50.23 ± 10.10
Habitat 5	163.51 ± 61.42	58.16 ± 24.96	9.15 ± 5.23	73.75 ± 37.35	0.37 ± 0.10	0.43 ± 0.17	41.83 ± 13.73
Habitat 6	140.28 ± 42.04	115.38 ± 80.50	16.78 ± 6.22	35.95 ± 9.72	0.30 ± 0.10	0.32 ± 0.10	56.70 ± 1.69
Habitat 7	202.15 ± 61.67	162.45 ± 17.80	26.1 ± 11.90	35.25 ± 11.90	0.42 ± 0.21	0.40 ± 0.11	52.15 ± 7.69

Table A.6. Significant spatial variables selected by forward selection ($P < 0.05$) showing adjusted cumulative square of sum of all variables, F-test (F), and p-value (P = significant variable) show in the table.

	Variable	Cumulative Adjusted R^2	F	P
	PCNM 4	0.01	3.87	0.004
	PCNM 79	0.03	3.80	0.003
	PCNM 28	0.04	3.24	0.002
	PCNM 88	0.06	3.28	0.005
	PCNM 25	0.07	3.32	0.006
	PCNM 70	0.08	3.14	0.007
	PCNM 1	0.10	3.12	0.007
	PCNM 3	0.11	3.05	0.011
	PCNM 6	0.12	2.85	0.008
	PCNM 12	0.13	2.79	0.008
	PCNM 44	0.14	2.75	0.015
	PCNM104	0.15	2.71	0.021
	PCNM 71	0.16	2.74	0.019
Space	PCNM 35	0.17	2.70	0.012
	PCNM 75	0.18	2.74	0.015
	PCNM 13	0.19	2.76	0.014
	PCNM 64	0.20	2.62	0.017
	PCNM 67	0.21	2.62	0.021
	PCNM 5	0.22	2.63	0.019
	PCNM 78	0.22	2.41	0.016
	PCNM 72	0.23	2.25	0.024
	PCNM 48	0.24	2.21	0.036
	PCNM 85	0.24	2.17	0.038
	PCNM 49	0.25	2.18	0.039
	PCNM 32	0.26	2.17	0.040
	PCNM 2	0.26	2.17	0.034
	PCNM 22	0.27	2.16	0.049

Table A.7. The contribution of spatial, soil and topographic variables for each species within the Yosemite Forest Dynamics Plot with respect to stem density in each quadrat (400 m^2) in 2019. 1 = the pure spatial component; 2 = the spatially structured environmental component; 3 = the pure Environmental component; 4 = the proportion explained by soil variables; 5 = the proportion explained by topographic variables; 6 = the topographically structured edaphic component.

Species	1	2	3	4	5	6
Abies concolor	0.430	0.300	0.040	0.130	0.300	0.120
Pinus lambertiana	0.560	0.280	0.000	0.060	0.280	0.040
Calocedrus decurrens	0.180	0.060	0.070	0.110	0.130	0.040
Cornus nuttallii	0.070	0.060	0.030	0.036	0.054	0.030
Arctostaphylos patula	0.000	0.080	0.040	0.180	0.004	0.020
Cornus sericea	0.480	0.040	0.060	0.080	0.100	0.060
Quercus kelloggii	0.220	0.000	0.270	0.100	0.200	0.030
Corylus cornuta var. californica	0.044	0.020	0.030	0.046	0.020	0.020
Prunus virginiana	0.000	0.001	0.004	0.001	0.004	0.002
Sambucus racemosa	0.000	0.012	0.010	0.016	0.014	0.000
Chrysolepis sempervirens	0.000	0.001	0.004	0.200	0.000	0.053

Table A.8. The contribution of spatial, soil and topographic variables for each species within the Yosemite Forest Dynamics Plot with respect to basal area increment in each quadrat (400 m^2) from 2009 to 2014. Numbers 1 = the pure spatial component; 2 = the spatially structured environmental component; 3 = the pure Environmental component; 4 = the proportion explained by soil variables; 5 = the proportion explained by topographic variables; 6 = the topographically structured edaphic component.

Species	1	2	3	4	5	6
Abies concolor	0.100	0.207	0.080	0.190	0.019	0.080
Pinus lambertiana	0.152	0.059	0.039	0.050	0.033	0.015
Calocedrus decurrens	0.244	0.094	0.243	0.153	0.032	0.062
Cornus nuttallii	0.295	0.087	0.030	0.046	0.046	0.221
Arctostaphylos patula	0.008	0.000	0.000	0.000	0.000	0.000
Cornus sericea	0.520	0.050	0.070	0.070	0.040	0.019
Quercus kelloggii	0.319	0.072	0.031	0.100	0.110	0.072
Corylus cornuta var. californica	0.062	0.060	0.000	0.000	0.000	0.060
Prunus virginiana	0.080	0.000	0.000	0.000	0.000	0.000
Sambucus racemosa	0.070	0.000	0.000	0.000	0.000	0.000
Chrysolepis sempervirens	0.038	0.010	0.000	0.000	0.000	0.010

Table A.9. The contribution of spatial, soil and topographic variables for each species within the Yosemite Forest Dynamics Plot with respect to mortality in each quadrat (400 m^2) from 2014 to 2019. Numbers 1 = the pure spatial component; 2 = the spatially structured environmental component; 3 = the pure Environmental component; 4 = the proportion explained by soil variables; 5 = the proportion explained by topographic variables; 6 = the topographically structured edaphic component.

Species	1	2	3	4	5	6
Abies concolor	0.340	0.223	0.060	0.040	0.030	0.040
Pinus lambertiana	0.080	0.010	0.030	0.030	0.010	0.020
Calocedrus decurrens	0.080	0.010	0.030	0.030	0.010	0.020
Cornus nuttallii	0.150	0.040	0.120	0.040	0.120	0.010
Arctostaphylos patula	0.000	0.000	0.090	0.060	0.020	0.000
Cornus sericea	0.109	0.083	0.000	0.084	0.020	0.020
Quercus kelloggii	0.280	0.011	0.070	0.060	0.120	0.000
Corylus cornuta var. californica	0.000	0.000	0.000	0.002	0.001	0.000
Prunus virginiana	0.000	0.000	0.090	0.070	0.020	0.000
Sambucus racemosa	0.000	0.000	0.000	0.004	0.002	0.000
Chrysolepis sempervirens	0.029	0.015	0.048	0.090	0.025	0.002

Table A.10. The contribution of spatial, soil and topographic variables for each species within the Yosemite Forest Dynamics Plot with respect to recruitment in each quadrat (400 m^2) from 2014 to 2019. Numbers 1 = the pure spatial component; 2 = the spatially structured environmental component; 3 = the pure Environmental component; 4 = the proportion explained by soil variables; 5 = the proportion explained by topographic variables; 6 = the topographically structured edaphic component.

Species	1	2	3	4	5	6
Abies concolor	0.240	0.040	0.000	0.040	0.000	0.040
Pinus lambertiana	0.210	0.050	0.000	0.050	0.000	0.000
Calocedrus decurrens	0.050	0.000	0.040	0.030	0.010	0.010
Cornus nuttallii	0.110	0.030	0.100	0.030	0.100	0.010
Arctostaphylos patula	0.000	0.000	0.090	0.070	0.020	0.000
Cornus sericea	0.040	0.020	0.031	0.022	0.010	0.020
Quercus kelloggii	0.260	0.070	0.060	0.050	0.040	0.000
Corylus cornuta var. californica	0.000	0.037	0.042	0.011	0.001	0.000
Prunus virginiana	0.000	0.000	0.090	0.070	0.020	0.000
Sambucus racemosa	0.000	0.001	0.000	0.002	0.002	0.002
Chrysolepis sempervirens	0.000	0.001	0.000	0.002	0.000	0.001

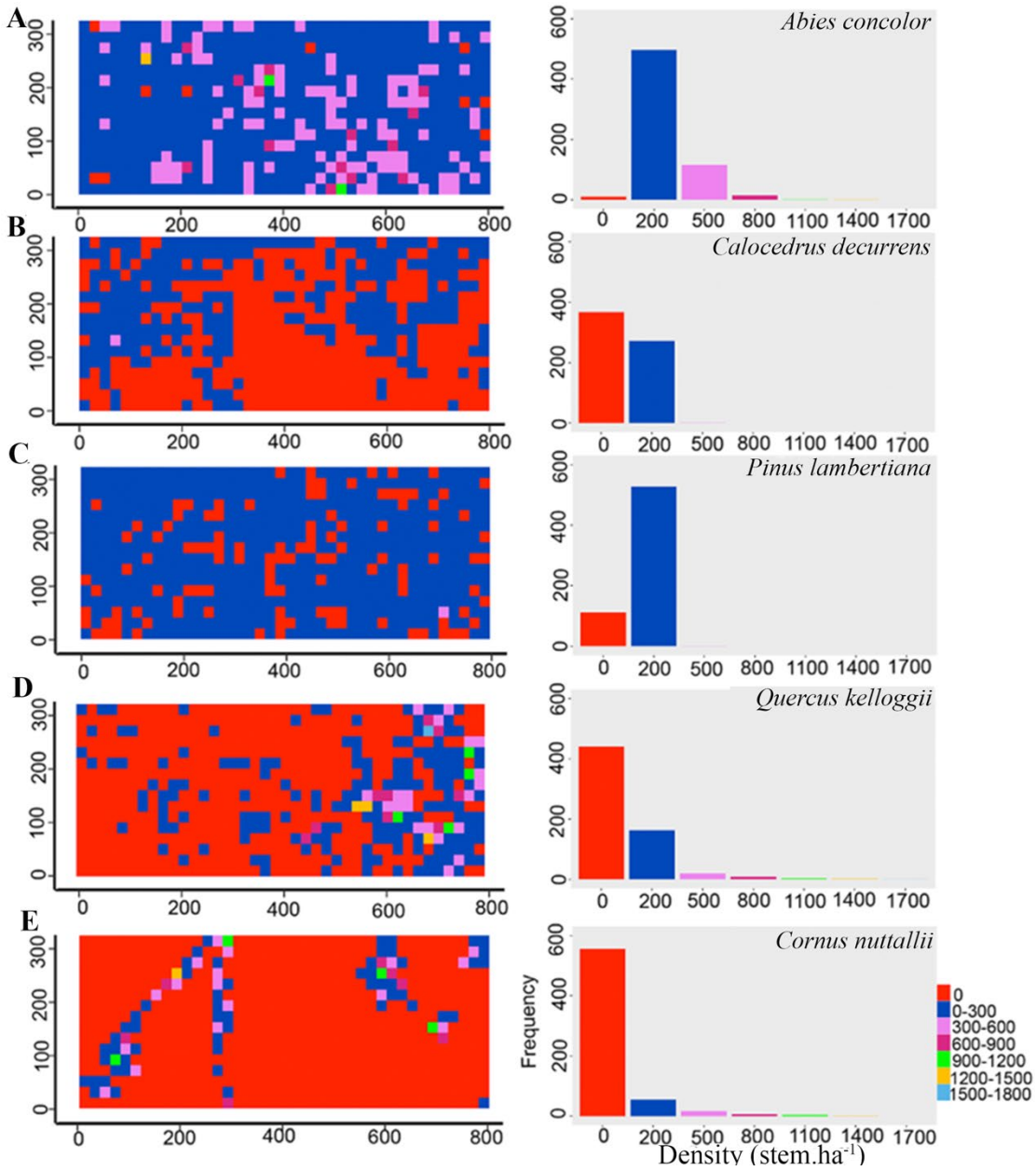

Fig A.1. Distribution and stems per hectare and distribution of the five most abundant species in the Yosemite Forest Dynamics Plot in 2019, including: *Abies concolor* (A), *Calocedrus decurrens* (B), *Pinus lambertiana* (C), *Quercus kelloggii* (D), and *Cornus nuttallii* (E).

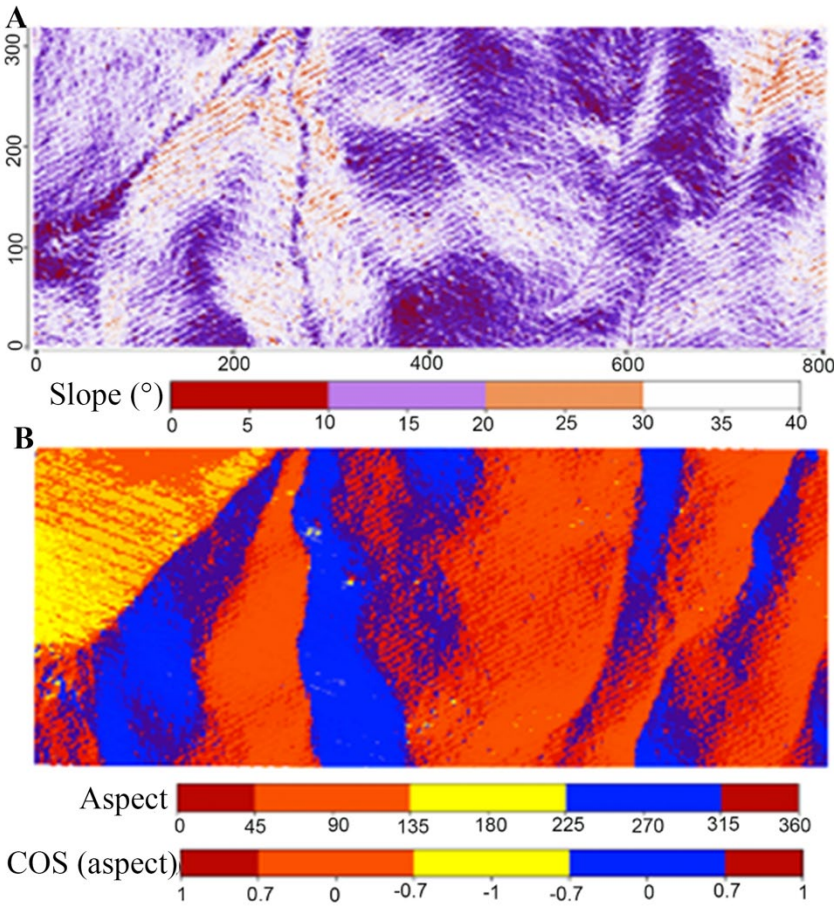

Fig A.2. Slope (A) and aspect (B) at the scale of 1 m × 1 m DEM in the Yosemite Forest Dynamics Plot (25.6 ha) in the Yosemite National Park, California, USA.

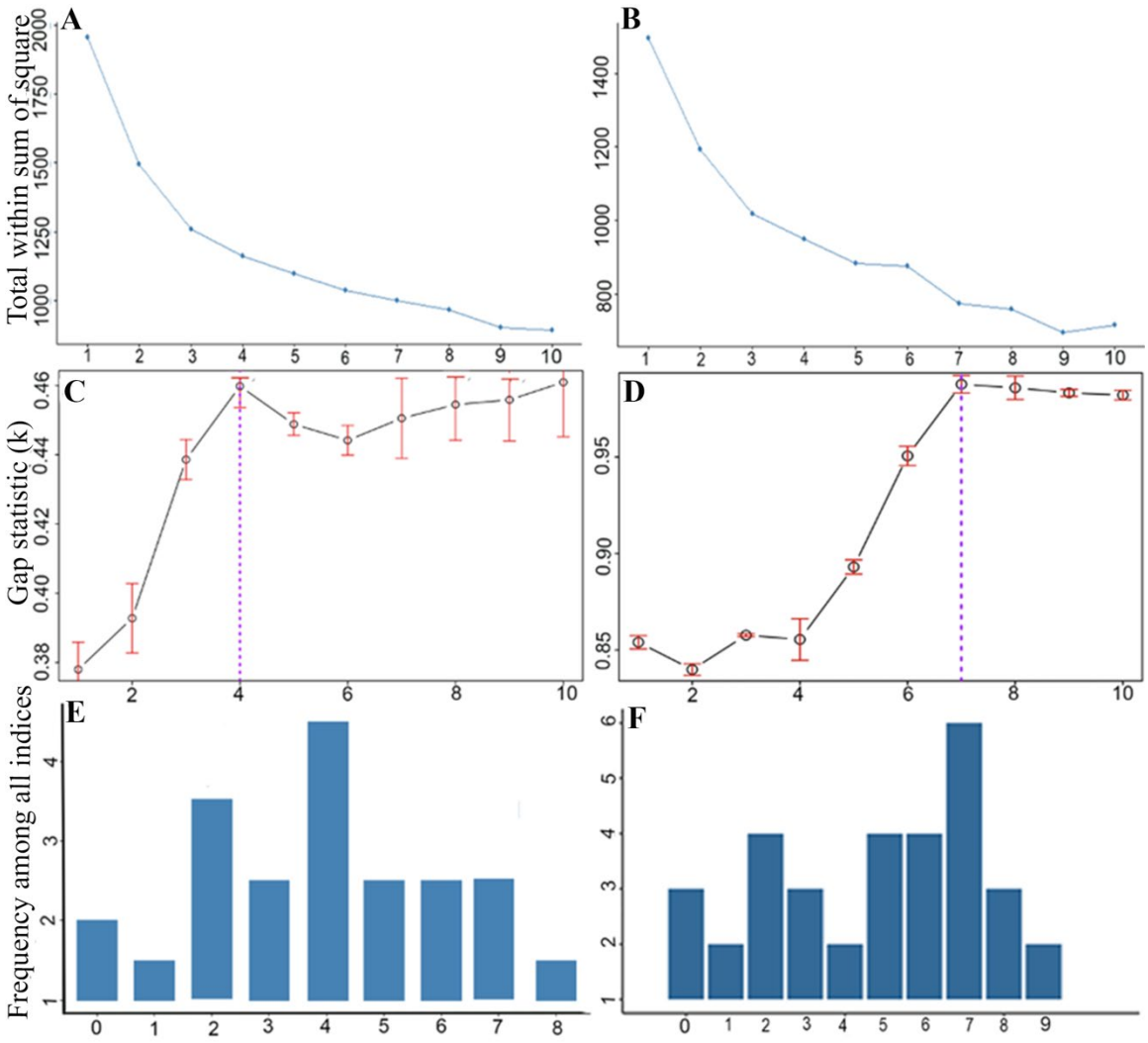

Fig A.3. Computation of the optimal numbers of habitats based on topographic (left panels) and soil variables (right panels). Elbow (A, B), Gap statistics (C, D), NbClust package (E, F) were used to compute optimal numbers of habitat types.

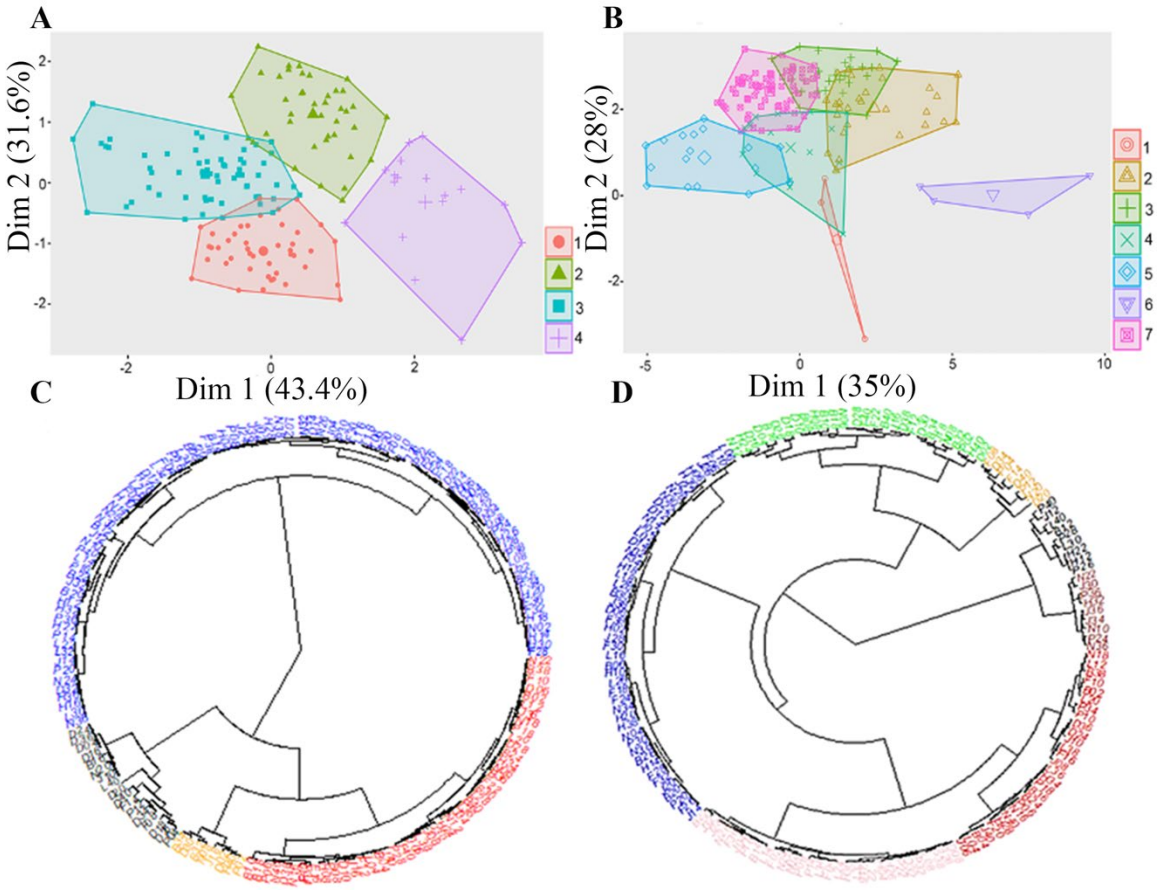

Fig A.4. The results of K-Means clustering results from topographic variables (A) and edaphic variables (B) which group data based on the minimum distance to centroids. Hierarchical clustering for classifying quadrats into four habitats (based on topographic variables) (C) and seven habitats (based on the edaphic factors) (D) within the Yosemite Forest Dynamics Plot.

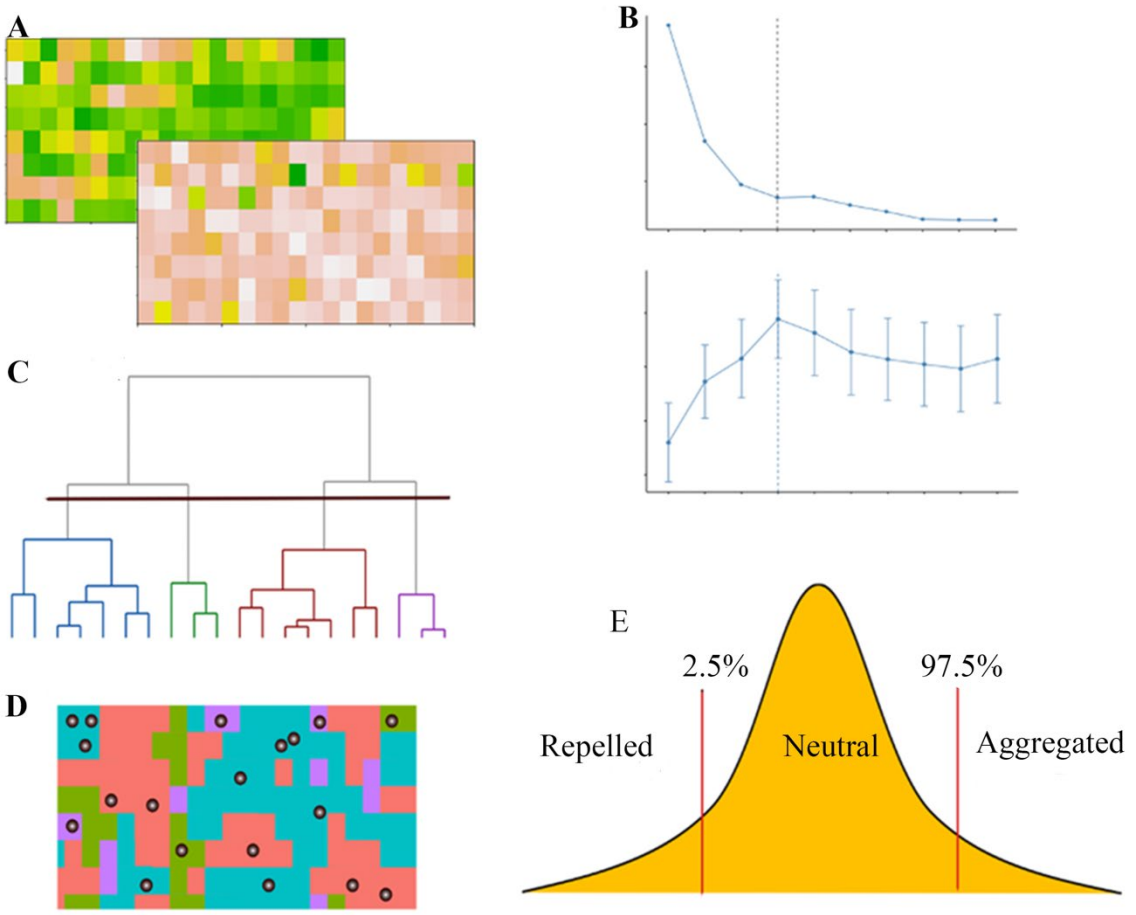

Fig A.5. Data flow used to quantify species-habitat association in Yosemite Forest Dynamics Plot. The procedures included: A) environmental variables calculated at 20 m × 20 m quadrat resolution, B) optimal number of habitats determined by elbow, gap statistic, and NbClust package methods, C) hierarchical clustering used to generate dendrogram from environmental variables and selective cut (brown line which was determined by optimal number of habitats) and defining habitats, D) torus translation test was conducted to quantify observed abundance of each species in each habitat type and compare this observed value to abundance value calculated for simulated habitat maps (Simulated maps were generated by shifting the actual habitat map in four directions by 20-m increments while the location of the stems did not change), E) determination of species which were significantly positively (aggregated) or negatively (repelled) associated with a specific habitat type (at $\alpha = 0.05$) (observed abundance was higher (lower) than at least 97.5 % (or 2.5%) of the simulated abundance in simulated maps).

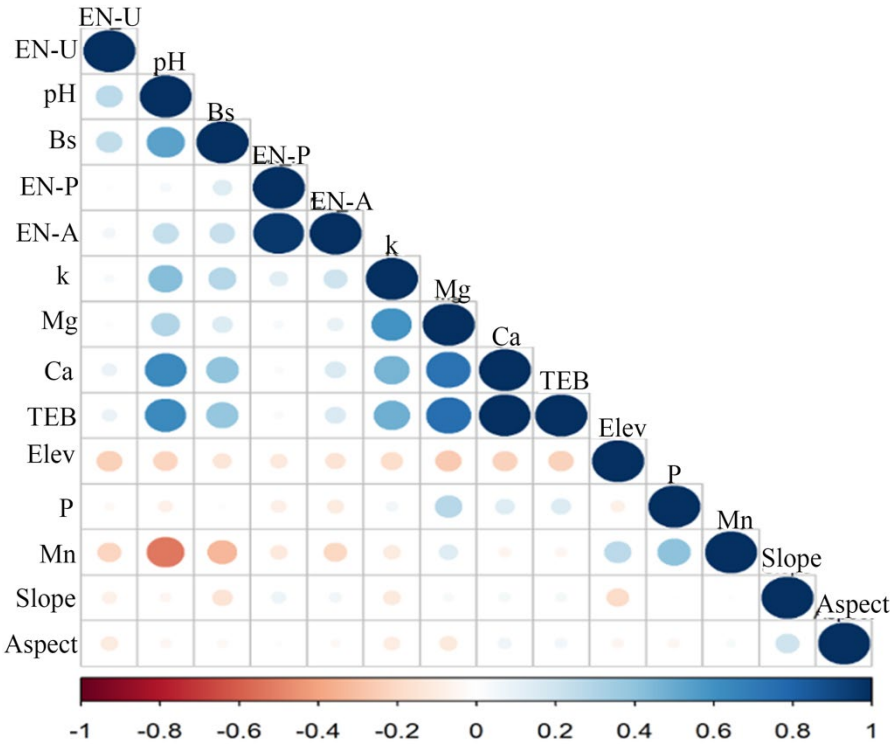

Fig A.6. Correlation between environmental variables in each quadrat. Positive correlations are displayed in blue and negative correlations in red. Color intensity and the size of the circle are proportional to the correlation coefficients. In the right side of the correlogram, colors show the correlation coefficients. Environmental variables include: slope, phosphorus (P), base-cation saturation (BS), elevation (Elev), phosphatase enzyme (EN-P), urease enzyme (EN-U), alkaline phosphatase enzyme (EN-A), total exchangeable bases (TEB), manganese (Mn), magnesium (Mg).

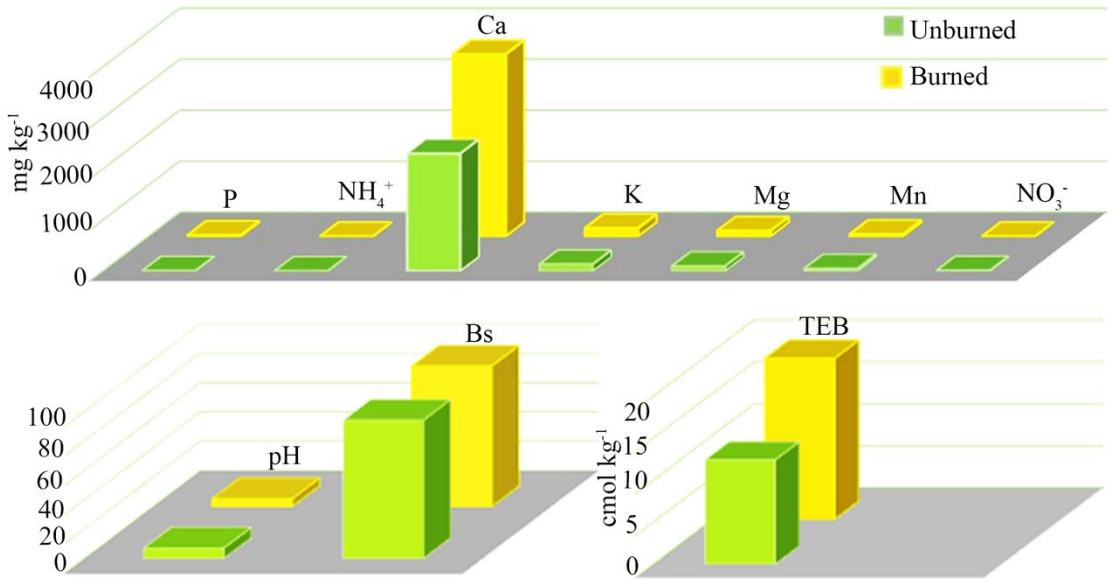

Fig A.7. Mean values of soil chemical properties in burned and unburned patches within the Yosemite Forest Dynamics Plot.

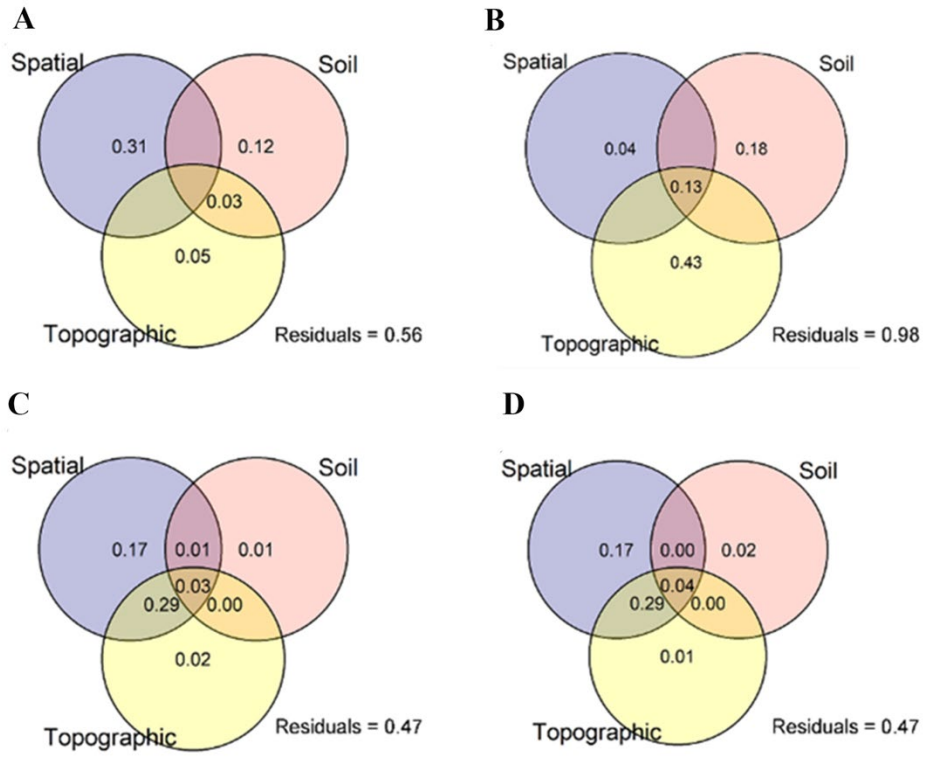

Fig A.8. Variation partitioning of 11 live species with ≥ 25 stems in the Yosemite Forest Dynamics Plot. The numbers showed the explained proportion of variation in species abundances in 2019 (A), basal area change in species between (2014 to 2019) (B), numbers of mortality (between 2014 to 2019) (C), and number of recruitment (between 2014 to 2019) (D) by spatial, edaphic (including chemical properties, acid and alkaline phosphatases and urease enzymes), and topographic variables. Negative values of explained variation were not shown in the figures (unlabeled regions).

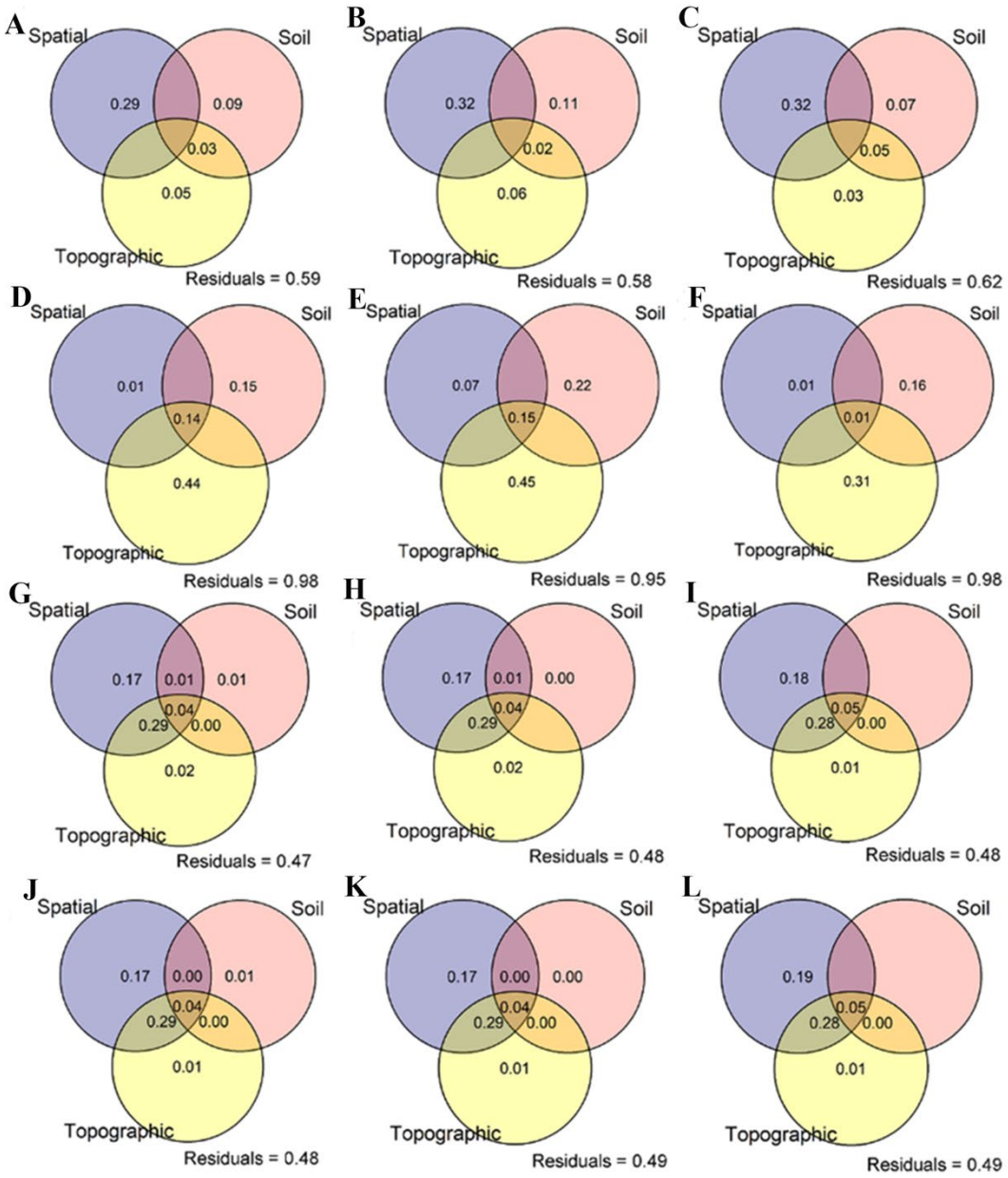

Fig A.9. Variation partitioning of 11 live species with ≥ 25 stems in the Yosemite Forest Dynamics Plot. Numbers show the proportion of variation in species abundances in 2019 (A, B, C), species basal area change (between 2014 to 2019) (D, E, F), numbers of mortality (between 2014 to 2019) (G, H, I), and number of recruitment (between 2014 to 2019) (J, K, L) with considering the hydraulic conductivity in edaphic component. The number of enzymes contribution in soil component changed from the first column to the third column which include alkaline phosphatase + urease + acid phosphatase / urease + acid phosphatase / without enzymes respectively. Negative values of explained variation were not shown in the figures (unlabeled regions).

APPENDIX B: Chapter 3 Supplemental Tables and Figures

Table B.1. Stem numbers of juveniles and adults in species in 2019 in the Yosemite Forest Dynamics Plot.

Year	Species	Family	Stems <5 cm dbh	Stems ≥20 cm dbh
2019	*Abies concolor*	Pinaceae	284	3508
	Pinus lambertiana	Pinaceae	45	326
	Calocedrus decurrens	Cupressaceae	36	1306
	Quercus kelloggii	Fagaceae	1041	279

Table B.2. Live juveniles (1 cm ≤ dbh < 5 cm) of *Abies concolor* and *Quercus kelloggii* in 2013, 2016, and 2019 in the Yosemite Forest Dynamics Plot.

Year	Species	Family	Stems <5 cm dbh
2013	*Abies concolor*	Pinaceae	8695
	Quercus kelloggii	Fagaceae	271
2016	*Abies concolor*	Pinaceae	251
	Quercus kelloggii	Fagaceae	81
2019	*Abies concolor*	Pinaceae	182
	Quercus kelloggii	Fagaceae	1033

Table B.3. Relative importance of best model in most abundant species including *Abies. concolor*, *Calocedrus. decurrens*, and *Pinus. lambertiana* in 2019 in the Yosemite Forest Dynamics Plot.

Best model	< 2 m	2-5 m	5-10 m	10-20 m	20-40 m	40-60 m
Homogeneous Poisson process	0%	0%	0%	0%	0%	0%
Inhomogeneous Poisson process	0%	0%	67%	100%	100%	100%
Homogeneous Thomas process	100%	100%	33%	0%	0%	0%

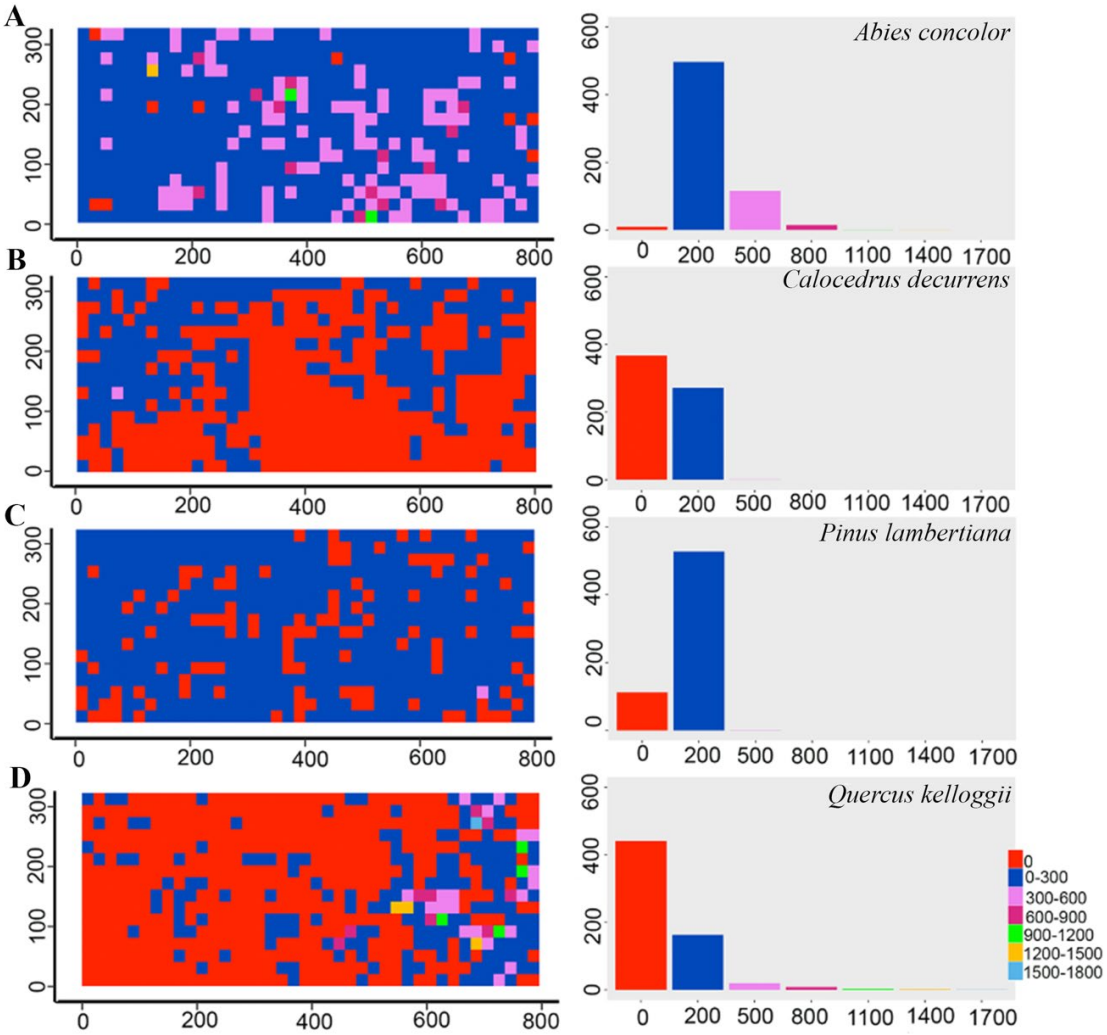

Fig B.1. Distribution and abundance of four most abundant species in the Yosemite Forest Dynamics Plot in 2019, including *Abies concolor* (A), *Pinus lambertiana* (B), *Calocedrus decurrens* (C), *Quercus kelloggii* (D).

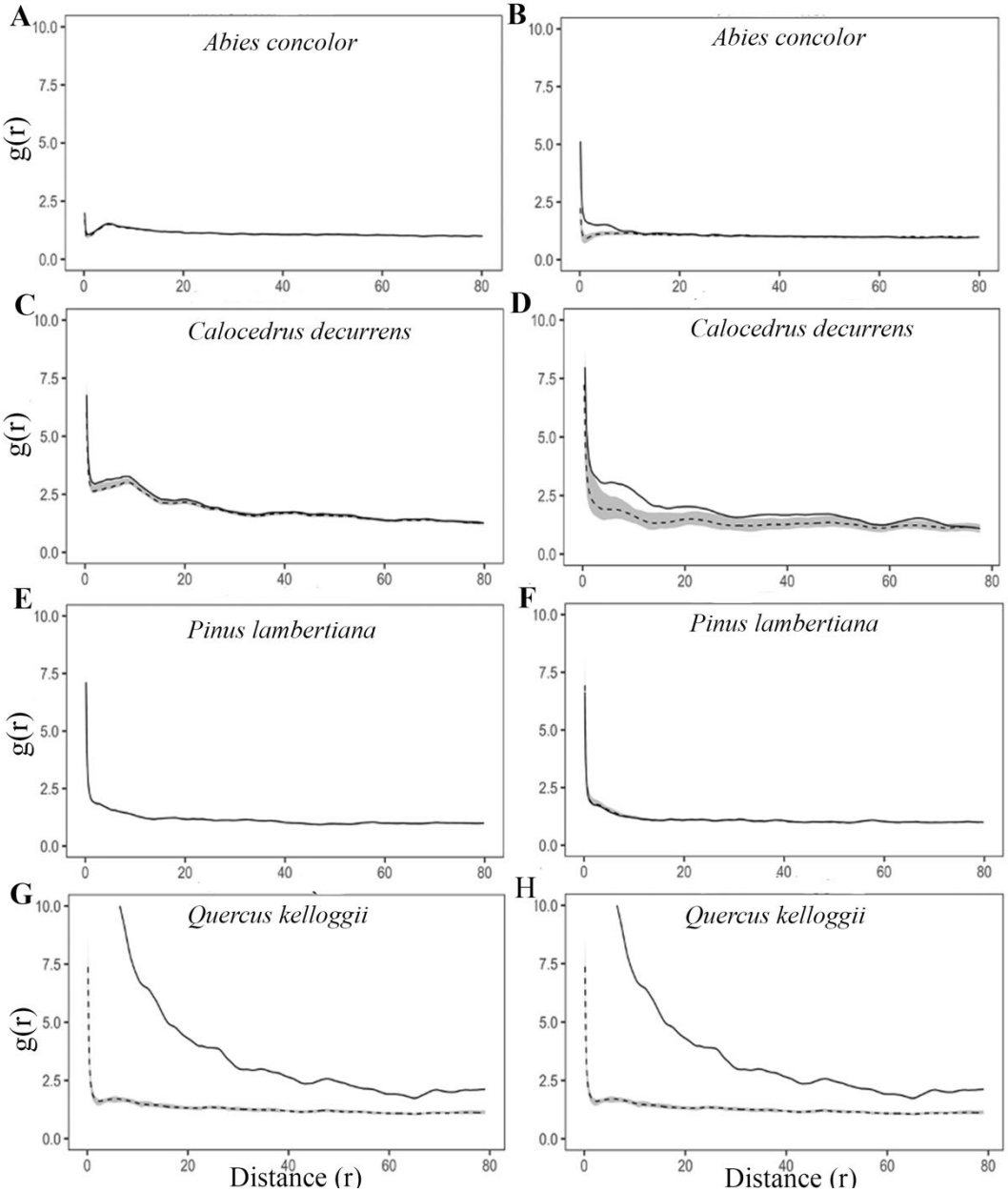

Fig B.2. Results of the sensitivity analysis for diameter cutoff values chosen for the grouping of adult and juvenile stems in 2019 in the Yosemite Forest Dynamics Plot. Bivariate null model between juveniles and adults was generated for a ±50% range of diameter thresholds (<5 cm and ≥20 cm). The values were changed from 2.5 cm and ≥10 cm dbh for juveniles and adults respectively (A, C, E, G) to 7.5 cm and ≥30 cm for juveniles and adults (B, D, F, H). Black lines show the observed g function and gray areas indicate the simulation envelopes generated from 999 Monte Carlo simulation.

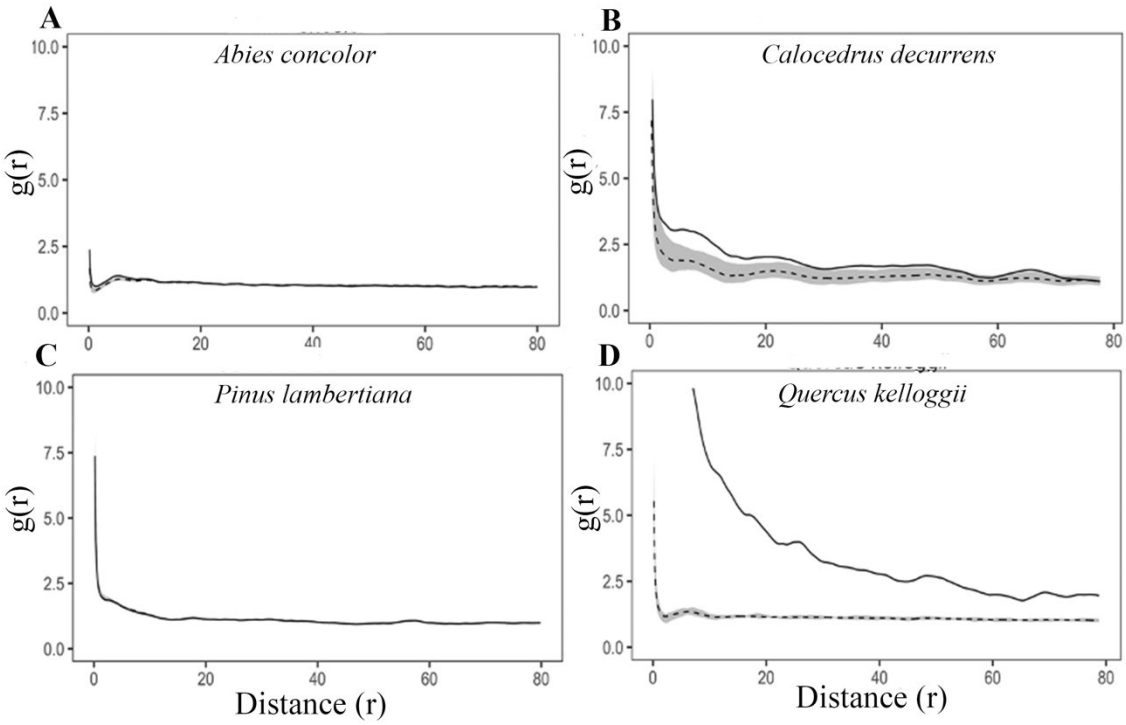

Fig B.3. Results of the sensitivity analysis for diameter cutoff values chosen for the grouping of adult and juvenile stems in 2019 in the Yosemite Forest Dynamics Plot. Bivariate null model between juveniles and adults was generated for 5 cm and ≥20 cm dbh for juveniles and adults respectively. Black lines show the observed g function and gray areas indicate the simulation envelopes generated from 999 Monte Carlo simulation.

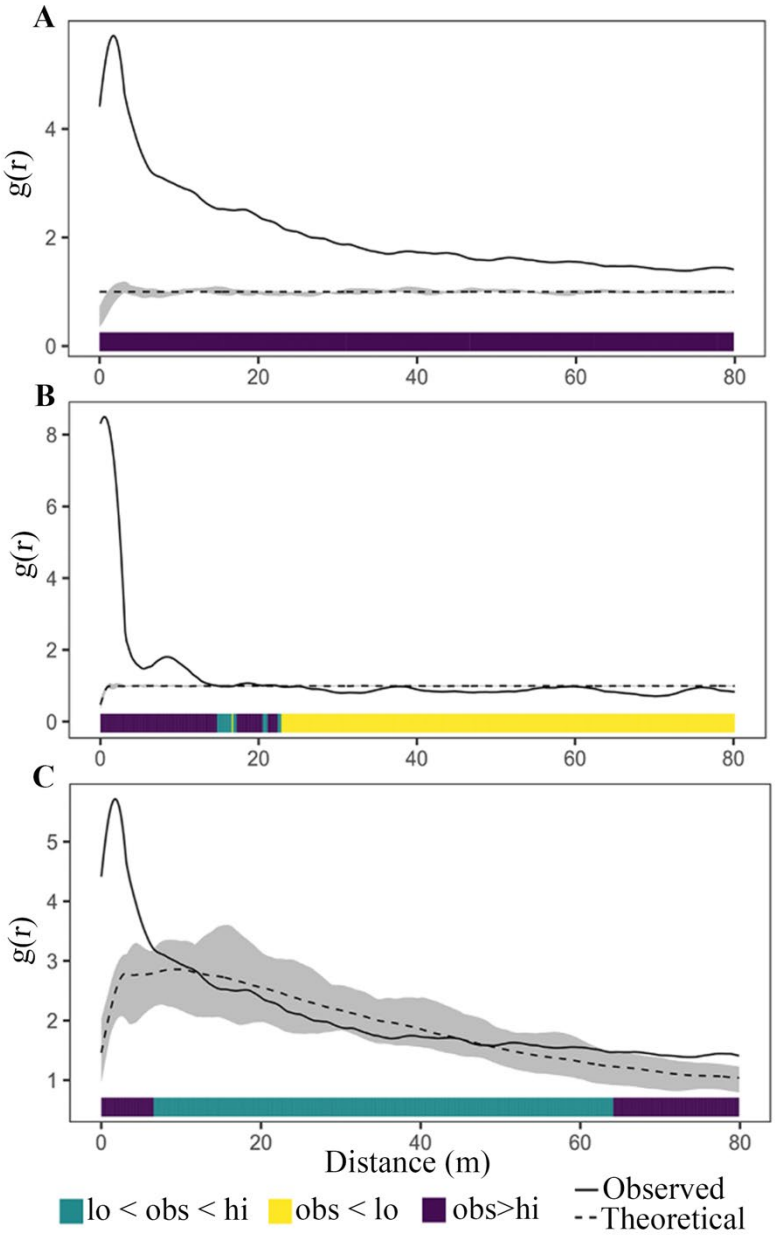

Fig B.4. Panels display the results of different point process models of *Calocedrus decurrens* in the Yosemite Forest Dynamics Plot in 2019. The gray regions indicate the boundaries of the 999 Monte Carlo simulation envelopes under the homogeneous Poisson process (A), heterogeneous Poisson process (B), and homogeneous Thomas process (C). The bold black lines show the calculated g function from observed data and the black dashed lines indicate the mean of simulated values. Green, yellow, and violet colors show randomness, segregation, and clustering respectively.

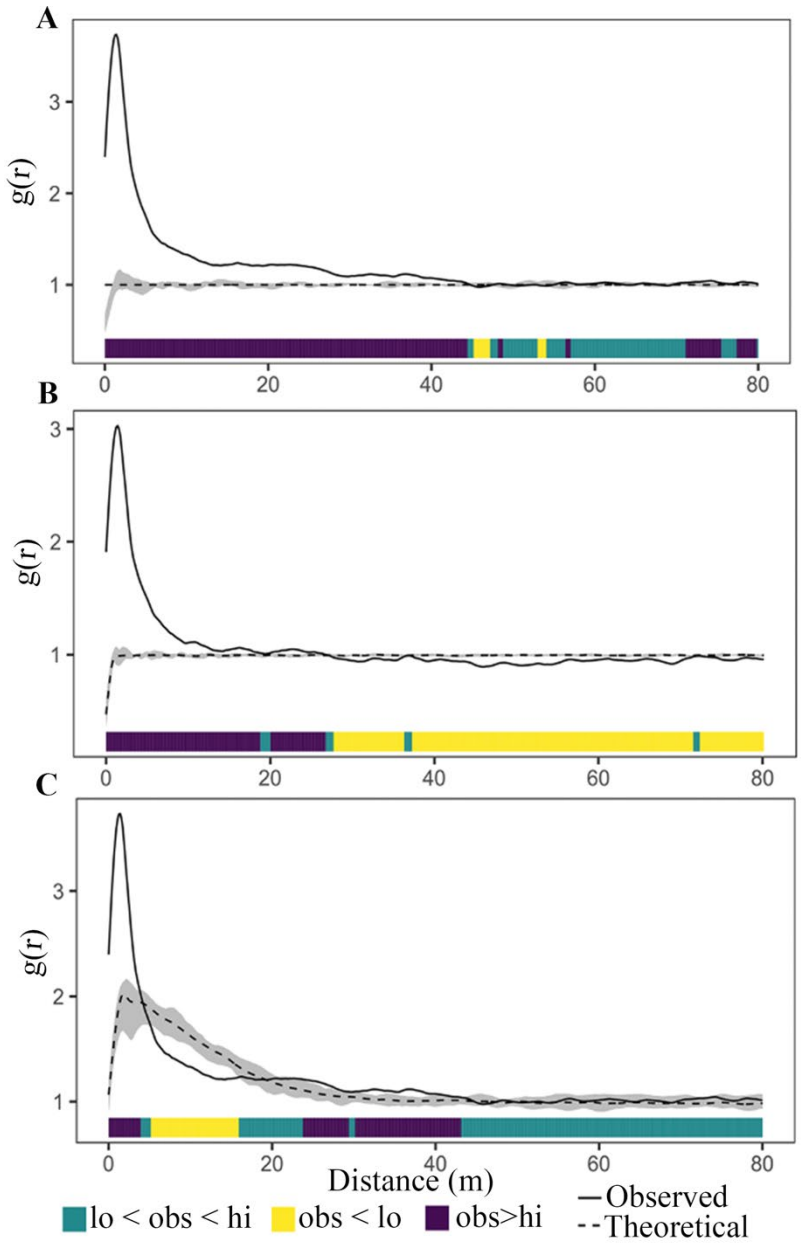

Fig B.5. Panels display the results of different point process models of *Pinus lambertiana* in the Yosemite Forest Dynamics Plot in 2019. The gray regions indicate the boundaries of the 999 Monte Carlo simulation envelopes under the homogeneous Poisson process (A), heterogeneous Poisson process (B), and homogeneous Thomas process (C). The bold black lines show the calculated g function from observed data and the black dashed lines indicate the mean of simulated values. Green, yellow, and violet colors show randomness, segregation, and clustering respectively.

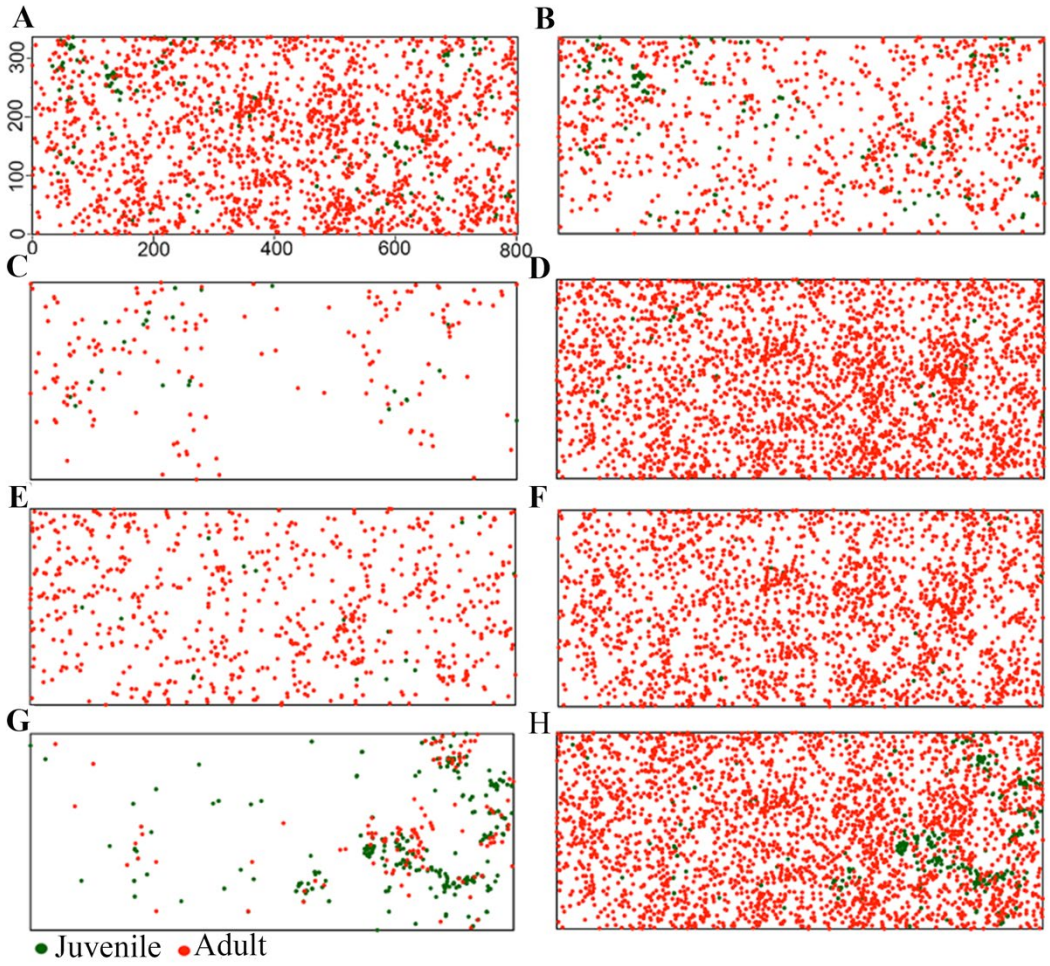

Fig B.6. Left panels display the distribution of juvenile (1 cm ≤ dbh < 5 cm) and conspecific adults (dbh ≥ 20 cm) in *Abies concolor* (A), *Calocedrus decurrens* (C), *Pinus lambertiana* (E), and *Quercus kelloggii* (F) in the Yosemite Forest Dynamics Plot in 2019. The right panels show the distribution of juvenile of *Abies concolor* (B), *Calocedrus decurrens* (D), *Pinus lambertiana* (F), and *Quercus kelloggii* (H) and adult of other species in the Yosemite Forest Dynamics Plot in 2019.

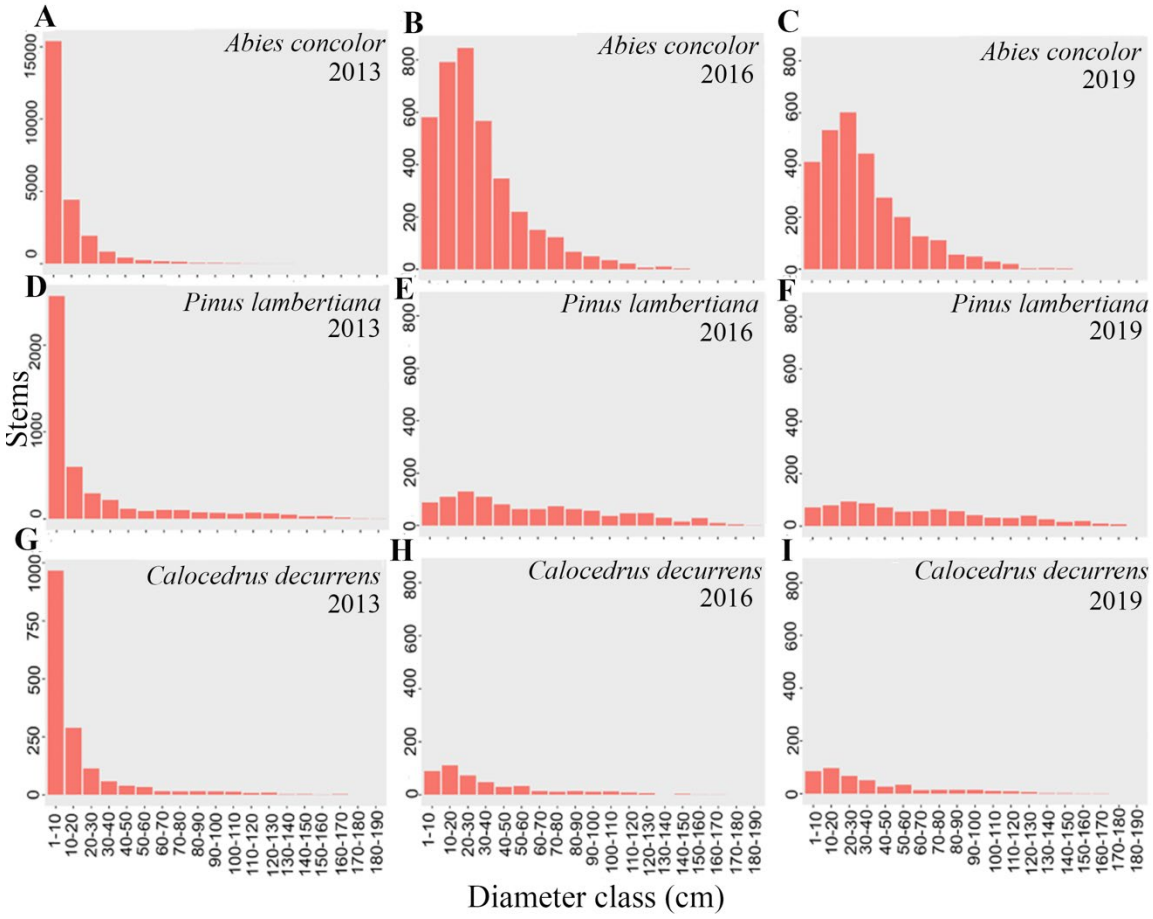

Fig. B.7. Diameter distributions of living three species in 2013 (pre-fire), 2016 (little post-fire), and 2019 in the 25.6 ha Yosemite Forest Dynamics Plot.

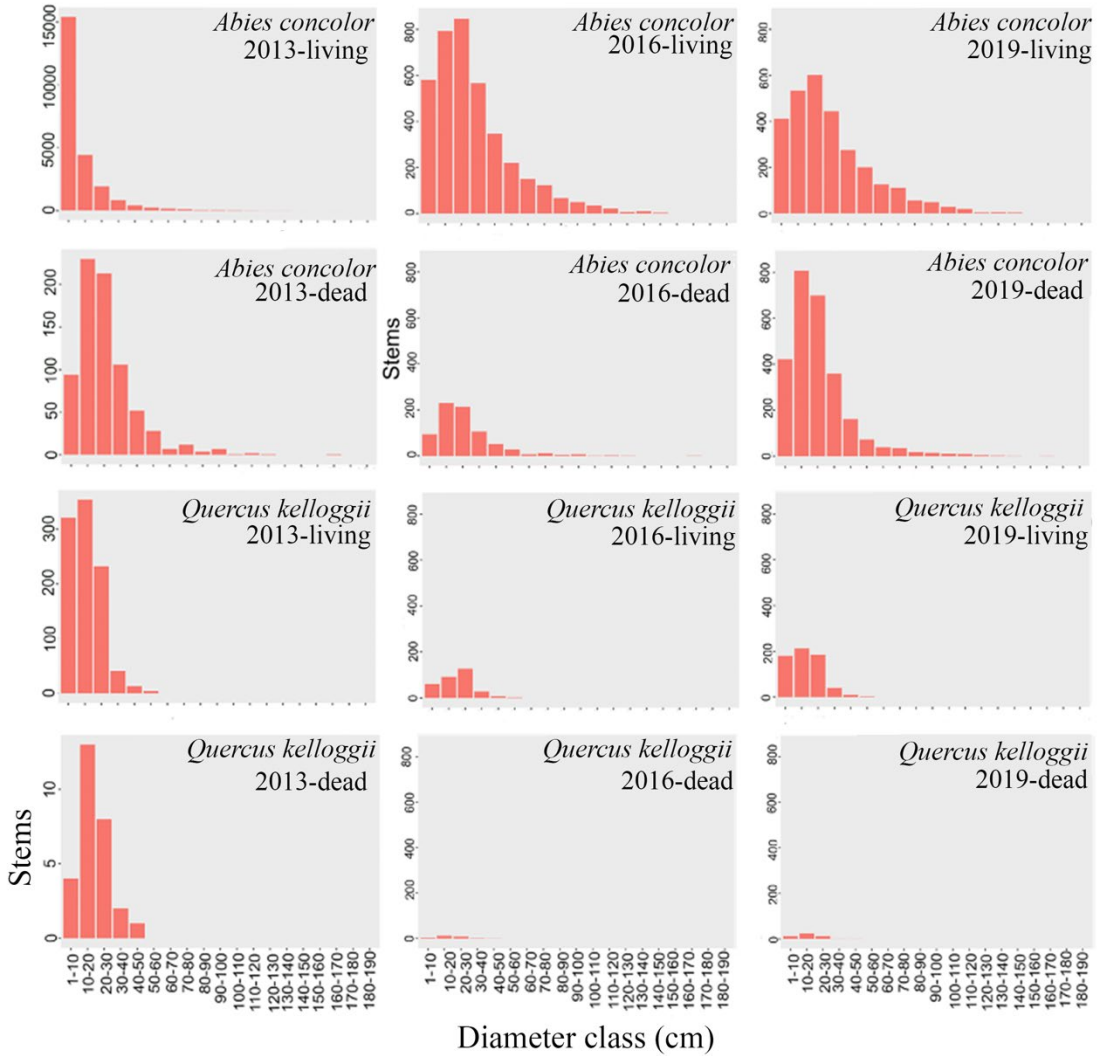

Fig. B.8. Diameter distributions of live stems (panels in first and third rows) and dead stems (panels in second and forth rows) for species in 2013, 2016, 2019 in the 25.6 ha Yosemite Forest Dynamics Plot.

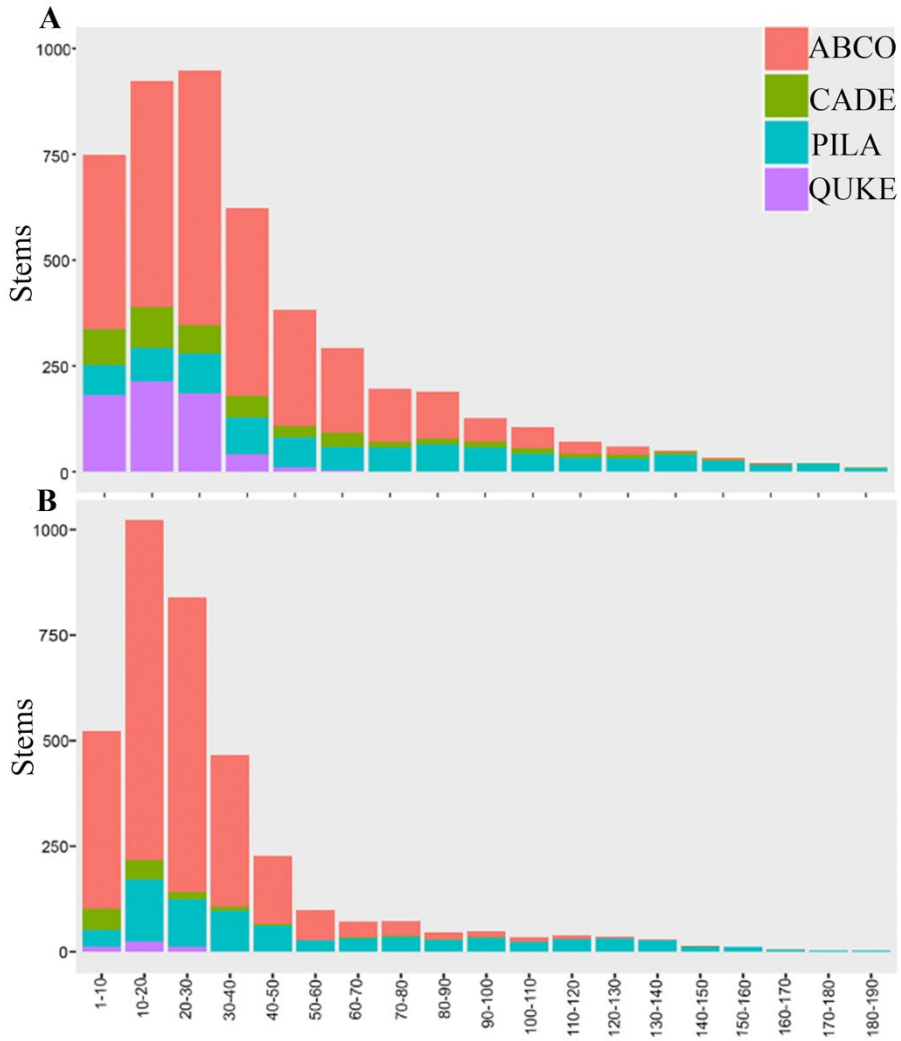

Fig B.9. Diameter distributions of living (A) and dead (B) for *Abies concolor* (ABCO), *Calocedrus decurrens* (CADE), *Pinus lambertiana* (PILA), and *Quercus kelloggii* (QUKE) trees in 2019 in the 25.6 ha Yosemite Forest Dynamics Plot.

APPENDIX C: Soil Enzymes Measurements

Urease Enzyme

We placed 5 g of soil into each of three 50 ml plastic bottles. Two bottles were treated with 2.5 ml of Urea solution and 20 ml of borate buffer and one bottle treated just with 20 ml of borate buffer and one bottle just with 20 ml of borate buffer (as a control). All bottles were incubated at 37 °C for two hours. Then, 2.5 ml of Urea solution were added just in control samples. All bottles were shaken for 30 minutes in a shaker. Soil suspension filtered using folded filters and 1 ml of filtrate poured into new bottle. 9 ml of water and 5 ml of sodium salicylate solution were added to all new bottles. All extracts were treated with 2 ml of sodium dichloroisocyanurate and swirled at room temperature for 30 minutes. All extracts measured with spectrophotometer to measure the urease content.

Standard curve

0, 1, 1.5, 2, 2.5 ml of the ammonium chloride poured in 100 ml plastic bottle and hydroxide solution and brought them up to 100 ml with KCl (2M) -HCl (0.01 M).1 ml of prepared solution pipetted into new plastic bottles and 9 ml water were added. All standards were mixed with 5 ml Sodium salicylate-sodium hydroxide solution and 2 ml of sodium dichloroisocyanurate solution. All standards were swirled for 30 minutes and urease activities were measured with spectrophotometer.

Solutions

1) Borate buffer: 57.2 g of disodium tetraborate were dissolved in 1500 ml warm water. The solution was titrated by adding 3M NaOH to 10 and content were brought to 2000 ml with water.
2) Urea solution: 21.6 g of Urea were dissolved in water and brought up to 500 ml with water.
3) Potassium chloride (2M) -hydrochloric acid (0.01M) solution: 149.2 g of KCl dissolved in the water and 10 ml of 1 M HCl were added into solution. The solution was brought up to 1000 ml with water.
4) Sodium hydroxide solution (0.3 M): 12 g of NaOH were dissolved with 500 ml of water and brought it up to 1000 ml with water.
5) Sodium salicylate solution: 17 g of sodium salicylate and 120 mg of sodium nitroprusside were dissolved in the water and brought up the solution 100 ml with water.
6) Sodium salicylate-sodium hydroxide solution: 100 ml of sodium hydroxide solution and 100 ml of sodium salicylate solution with 100 ml of water.
7) Sodium dichloroisocyanurate solution: 0.1 g of dichloroisocyanurate were dissolved in the water and brought up to the 100 ml with water.
8) Ammonium chloride for standard curve: 3.8207 g of ammonium chloride were dissolved in water and brought to 1000 ml with water.

Acid and Alkaline phosphatase enzymes

1 g of soil were placed into a plastic bottle and 0.2 of toluene and 4 ml of modified buffer were added to soil. The pH for Modified buffer were considered equal to

6.5 for acid phosphatase and 11 for alkaline phosphatase. 1 ml of p-Nitrophenyl solution were added to bottles and swirled bottles for a few seconds. Then, kept all samples into an incubator at 37° C for one hour. 1 ml of 0.5 M $CaCl_2$ and 4 ml of 0.5 M NaOH were added to all samples. All bottles swirled for a few minutes and filtered the soil solution through the filter papers. The enzyme activities measured with spectrophotometer between 400 nm and 410 nm.

Standard curve:

1 ml of standard p-Nitrophenyl solution were diluted with water to 100 ml. 0, 1, 2, 3, 4, 5 ml of diluted standards were pipetted into 6 plastic bottles and the volume were adjusted to 5 ml by water. 0.5 ml of 0.5 M $CaCl_2$ and 4 ml of 0.5 M NaOH were added and the intensity of solution measured with spectrophotometer.

Solutions:

1) Modified buffer: 12.1 g of hydroxymethyl aminomethane, 11.6 g of maleic acid, 14 g of citric acid, and 6.3 g of boric acid were dissolved in 488 ml of 1 N sodium hydroxide and the solution diluted to 1000 ml with water. 200 ml of modified buffer solution placed into a 500 ml beaker and the beaker placed on the magnetic stirrer with magnetic stirring bar. The solution titrated to pH 6.5 with 0.1 M hydrochloric acid for measuring acid phosphatase enzyme and the volume adjusted to 1000 ml with water. Also, another 200 ml of modified buffer solution placed into another 500 ml beaker and titrated the pH of solution to 11 by adding the 0.1 M NaOH and the volume adjusted to 1000 ml with water.

2) P-Nitrophenyl phosphate solution: 0.840 g of disodium p-nitrophenyl phosphate tetrahydrate dissolved in a 40 ml of modified buffer and the solution diluted to 50 ml by the modified buffer.
3) Calcium chloride 0.5 M: 73.5 g of $CaCL_2 2\ H_2O$ were dissolved in a 700 ml of water and diluted to 1000 ml with water.
4) Sodium hydroxide 0.5 M: 20 g of NaOH were dissolved in 700 ml water and diluted to 1000 ml with water.
5) Standard p-Nitrophenyl: 1 g of p-nitrophenyl were dissolved in a 700 ml of water and diluted to 1000 ml with water.